DECLARATION

I, Susanna Maria du Preez, hereby declare that the dissertation entitled:

The influence of minerals on the moisture adsorption and desorption properties of South African fine coal.

Submitted to the North-West University in completion of the requirements set for the degree *Masters in Engineering in Chemical Engineering* is my own original work, except where acknowledged in the text and has not previously been submitted to any institution.

Signed at Potchefstroom

_____

S.M du Preez.

ACKNOWLEDGEMENTS

I hereby wish to thank all the people and institutions who contributed to the completion of this research project. Your assistance and valuable inputs are deeply appreciated. The following persons deserve special thanks:

- Our heavenly Father for giving me courage to pursue my dreams and the conviction that anything is possible.
- Professor Quentin Campbell for his guidance and willingness to help. Without his evaluations and suggestions this dissertation would not have been a reality.
- Coaltech for their financial support.
- The Coal research group at the North-West University for many insightful discussions.
- Johan de Korte for his assistance and willingness to answer all my questions.
- Chris van Alphen for the QEMSCAN analysis.
- My family for their words of encouragement and unwavering support in everything I do.
- George van der Merwe for being the love and light of my life.

ABSTRACT

Five coal samples from the Witbank, Free State and Limpopo provinces in South Africa were studied to determine and understand the influence of minerals and other coal properties on the moisture adsorption and desorption behaviour. All the experiments were conducted in a climate chamber at isothermal conditions. The climate chamber controlled the relative humidity and temperature to which the coal particles were exposed during each experiment. The climate chamber was also equipped with a mass balance to record the increase (adsorption) and decrease (desorption) in mass, where a constant mass reading denoted equilibrium conditions. The coal samples were characterised in terms of proximate analysis, ultimate analysis, petrographic analysis, CO_2 and N_2 BET sorption analysis. The mineral characterisation of each coal was performed with XRF and QEMSCAN analysis, where the QEMSCAN analysis allowed for the quantitative evaluation of the minerals present in each of them. A constant particle size of +1mm -2mm was used to evaluate the adsorption/desorption characteristics for this investigation.

The characterisation results indicated higher moisture- and oxygen contents for the lower ranked bituminous coal samples compared to the higher ranked bituminous coal sample. Adsorption results also indicated that the lower ranked coals samples adsorbed the most moisture whereas the higher ranked coal sample adsorbed the least moisture. The oxygen content is an indication of the oxygen containing functional groups present on the coal surface which facilitates moisture adsorption. It was therefore expected that the lower ranked coals would absorb more moisture than the higher ranked ones.

QEMSCAN analysis revealed that the predominant mineral present in all the coals samples were the clay mineral kaolinite followed by quartz. The influence of kaolinite on the adsorption properties was investigated and no significant relationship was found. The kaolinite, however contributed more to the moisture adsorbed by the higher ranked bituminous coal in comparison to the lower ranked bituminous coals. This could most likely be attributed to the fact that the water uptake by the organic material of higher ranked coal is less than that for lower ranked coals. The amount of moisture adsorbed by the kaolinite seems to be less for lower ranked coal containing more oxygen and more for higher rank coal containing less oxygen. It can thus be said that the amount of moisture adsorbed in the different coal samples were influenced by kaolinite but to a lesser extent for the lower ranked coals. QEMSCAN analysis also displayed increased levels of calcite and pyrite present in the lower ranked coal samples and increased levels of illite and muscovite present in the higher ranked coal samples.

A positive relationship was observed when comparing the amount of moisture adsorbed and illite content for coals similar in rank. Increased levels of illite corresponded to increased levels of moisture adsorbed for the lower ranked bituminous coals. There was a significant amount of illite present in the higher ranked bituminous coal but no significant increase in the amount of moisture adsorbed was observed.

Lower water adsorption surface areas were observed in comparison to CO_2 surface areas. It was also found that the mineral matter present in the coal samples inhibited the CO_2 adsorption surface areas.

Modelling of the experimental data indicated that the monolayer adsorption capacity, estimated by the BET model, correlated very well with the surface oxygen content of each coal sample. This is an indication that moisture is first adsorbed at the surface oxygen groups. The modified BET model described the moisture adsorption mechanism very well for each coal at the relative pressure range applicable to this study. From the modified BET model the contribution of water adsorbed due to primary and secondary sites could also be estimated. Energies for the primary sites, ranging between 44 kJ/mol and 50 kJ/mol, were higher than those for the secondary sites, varying between 42 kJ/mol and 43 kJ/mol. This indicated that the water-coal interactions in the monolayer were weaker than those interactions in subsequent layers. The parameters estimated from both models correlated very well with the values presented in the literature.

TABLE OF CONTENTS

LIST OF FIGURES

LIST OF TABLES

LIST OF SYMBOLS

Symbol	Description	Unit
A	Antoine coefficient	(-)
a_m	Molecular area of water molecule	$A^2.molecule^{-1}$
$A_{specific}$	Specific micropore area	$m^2.g^{-1}$
B	Antoine coefficient	(-)
C	Antoine coefficient	(-)
E	Energy of adsorption	$kJ.mol^{-1}$
E_L	Heat of water liquefaction	$kJ.mol^{-1}$
h	Langmuir constant	kPa^{-1}
n_1^{exp}	Gas adsorbed at primary sites	$mmol.g^{-1}$
n_2^{exp}	Gas adsorbed at secondary sites	$mmol.g^{-1}$
N_A	Avogadro's number	$molecules.mol^{-1}$
n_o'	Monolayer adsorption capacity	$mmol.g^{-1}$
P	Partial pressure	bar or kPa
P_S	Saturation pressure	bar or kPa
R	Molar gas constant	$J.mol^{-1}.K^{-1}$
S	Surface area	$m^2.g^{-1}$
T	Temperature	$^{\circ}C$ or K

ABBREVIATIONS

Abbreviation	Description
ACT	Advanced Coal Technology
ASTM	American Society for Testing Materials
BDDT	Brunauer-Deming-Deming-Teller
BET	Brunauer- Emmitt -Teller
BJH	Barret-Joyner-Halenda
BP	British Petroleum
d.a.f	Dry, ash free basis
d.b	Dry basis
DME	Department of Minerals and Energy
D-R	Dubinin-Radushkevich
Eskom	South African Electricity Supply Commission
IEA	International Energy Agency
ISO	International Organisation for Standardisation
m.m.b	Mineral matter basis
m.m.f.b	Mineral matter free basis
QEMSCAN	Quantitative Evaluation of Minerals by Scanning Electron Microscopy
RH	Relative humidity
SABS	South African Bureau of Standards
Sasol	South African Coal, Oil and Gas
SEM	Scanning Electron Microscope
WCA	World Coal Association
XRD	X-Ray diffraction
XRF	X-Ray fluorescence

CHAPTER 1:
GENERAL INTRODUCTION

With a 5.6% increase in the global demand for energy in 2010 and a decrease in high quality coal resources, a better understanding of the factors influencing the behaviour of coal during utilisation is needed, not only to benefit the global economy, but also to satisfy public demands for clean coal technologies (BP, 2011). This study focuses on the influence of minerals and other intrinsic coal properties of the moisture adsorption and desorption properties of South African coal. In this introductory chapter some background as well as the motivation for this study is given in Section 1.1. The objectives for this investigation are described in Section 1.2 and finally the scope and outline for this dissertation is presented in Section 1.3.

1.1 Background and motivation

The industrial revolution in the 18th and 19th centuries utilised mechanical energy to produce valuable materials. The initial source of energy to maintain these processes was thermal energy stored in coal. With the development of electricity in the 19th century the future of coal was closely linked to electricity generation. However, rapid progress was made in the transportation sector and petroleum soon replaced coal as a primary source of energy to sustain the fast growing human population's demands. Ironically the oil crises of the 1970's shifted the limelight back to coal and it became yet again the dominant fuel for power stations. Over the past decades coal has been the leading supplier of energy for electricity generation. Coal consumption grew by 7.6% in 2010, its fastest growth since 2003 and currently accounts for 29.6% of global energy consumption, the highest in 31 years (BP, 2011).

The future of coal in this century will be largely influenced by new energy technologies where a good and constant fuel quality will be imperative for their optimal operation. In the past the cost of coal was mainly influenced by its calorific value but, in future, taking environmental legislation into account, factors including ash and sulphur content will play a more important role. The increase in environmental concern over fossil fuel utilisation will shift the focus to alternative energies such as nuclear and bio-fuels. However, energy from fossil fuels will continue to dominate as long as there is public and political resistance against the

development of nuclear energy. It is estimated that over the next 30 years the energy demand will increase by 60%, where two-thirds of this energy demand will be from developing countries including South Africa (WCI, 2009). Coal dominates as the fuel source for power generation and is currently responsible for approximately 42% of the global electricity supply; furthermore approximately 60% of steel produced worldwide comes from iron made in blast furnaces fired by coal (WCA, 2010). Oil remains the world's primary fuel, at 33.6% of global energy consumption as depicted in Figure 1.1 (BP, 2011).

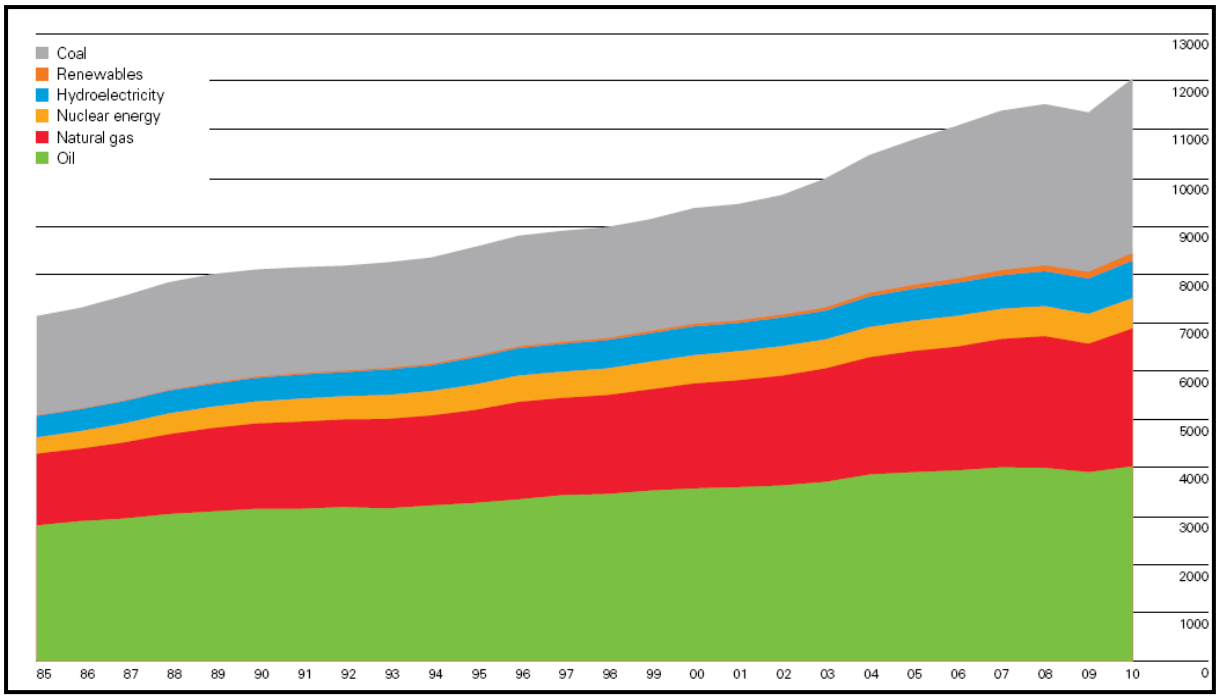

Figure 1.1: World energy consumption (BP, 2011).

Growth was above average for oil, natural gas, coal, nuclear, hydroelectricity as well as for renewable in power generation. The contribution of coal to the total energy consumption continuous to grow and the share of natural gas was the highest on record (BP, 2011).

Table 1.1 displays the top five countries in terms of global hard coal production. The Peoples Republic of China produces the largest amount of hard coal annually, followed by the United Stated of America and India producing 932 Mt/yr and 538 Mt/yr respectively (WCA, 2010). South Africa is currently ranked fifth in the global production rating of hard coal and produces 255 Mt/yr.

Table 1.1: Leading global hard coal producers (WCA, 2010).

Country	Production (Mt/year)
PR China	3162
USA	932
India	538
Australia	353
South-Africa	255

At current production rates global coal reserves can be approximated to last for the next 118 years, while oil and gas reserves are estimated to last around 46 and 59 years respectively (WCA, 2010). South Africa's economically recoverable reserves are estimated at between 15 and 55 billion tonnes at current production rates (BP, 2011). These coal reserves are predominantly mineral rich with 96 % of the reserves consisting of bituminous coals.

South Africa is one of the world's largest coal consumers as well as producers, ranked as the fifth largest exporter of coal with an annual export rate of 70Mt, as shown in Table 1.2 (WCA, 2010).

Table 1.2: Top coal export countries (WCA, 2010).

Country	Total of *which is exported (Mt)*	Steam (Mt)	Coking (Mt)
Australia	298	143	155
Indonesia	162	160	2
Russia	109	95	14
USA	74	23	51
South Africa	70	68	2
Colombia	68	67	1
Canada	31	4	27

South Africa is heavily dependent on coal for power generation and it is estimated that coal is responsible for 93% of the energy needed to generate electricity (WCA, 2010). The country will remain dependent on coal for the foreseeable future due to the availability of extensive coal reserves together with the expected continuous increase in oil and natural gas prices.

The majority of the coal mines in South Africa are located in the Central Basin which includes the Highveld, Ermelo and Witbank coalfields. Production in these coalfields is likely to peak in the next decade (Eberhard, 2011; Jeffrey 2005).

According to reports from the Department of Minerals and Energy (DME, 2007), 21% of South African coal is used locally (excluding coal used for electricity generation), 21% is exported, while the remainder is distributed to different local industries as summarised in Table 1.3.

Table 1.3: Distribution of South African coal to local industries (DME, 2007).

Coal use in South Africa	Contribution (%)
Electricity generation	62
Synthetic fuel production	23
General industry	8
Metallurgical industry	4
Merchants and domestic	3

The major driver for future growth in the domestic market will undoubtedly be Eskom's investment in new coal fired plants to satisfy the ever increasing energy demand for consistent and reliable power generation in the country. In 2008, Eskom estimated that it would require 200 Mt/a of coal by 2018 and that South Africa will need an additional 40 coal mines to meet requirements (Eberhard, 2011).

An estimated 45 % of coal worldwide is either high in moisture or mineral rich, which can either cause difficulties during coal beneficiation or result in inefficiencies in power plants. Elevated levels of moisture present in coal relates to low calorific values, increased cost of transportation and materials handling. Therefore a strong need for new and improved drying technologies exists and progress is being made by Germany, the United States and Australia, however, efforts must be made to integrate these technologies on a large scale (IEA, 2011).

At present large quantities of fine and ultra-fine coal are being discarded in South Africa due to the quality of the coal, more specific the heat value of the coal, it is too low to be included in the export product. In the past South Africa's export coal was mined from the No. 2 Seam where the fine coal fraction was relatively easy to beneficiate. In the future a large portion of coal will be produced from the No. 4 Seam where the fine coal fraction is difficult to beneficiate and low quality fines will be produced that cannot be included in the final export

product (de Korte, 2002). If wet fine coal is added to the coarse coal product the heat value of the combined product decreases. To compensate for this, the coarse coal product must be produced at a higher heat value which in turn decreases the yield of the coarse product. Generally, the yield loss from the coarse coal is more than the gain by adding the fine coal, and it is therefore more economical to discard the fine coal (de Korte & Mangena, 2004). Thermal drying can reduce the moisture content to acceptable levels but there is a concern that fine coal can pick up moisture during transportation and stockpiling.

The influence of varying environmental conditions can become particularly prominent when large quantities of coal are stored or transported over great distances. Conventional evaporative drying processes are only effective if the dried coal is utilised immediately, which is not always possible. If the dried coal is not used immediately, handling and transportation may induce moisture re-adsorption (IEA, 2011).

The response of coal in regard to changing moisture levels is influenced by factors such as clay content and percentage fines. Coal containing a significant amount of clay will become sticky as it tends to hold moisture. This is particularly important as the mineral matter found in South African coals are predominantly clay minerals, largely in the form of kaolinite and illite, which can cause problems in varying climatic conditions (Pinetown & Boer, 2006). It is therefore essential to fully understand the influence of clay minerals on the moisture adsorption properties of South African coal, as well as their response to varying environmental conditions during transportation.

For this study, it was important to determine and fully comprehend the influence of minerals on the moisture adsorption and desorption properties of South African coals. A better understanding concerning this relationship will provide valuable information that may benefit and improve the coal beneficiation and utilisation processes of South African coal.

1.2 Objectives of the study

Different coal properties influence the moisture adsorption and desorption behaviour of coals under different environmental conditions. Coal properties that are most likely to influence the adsorption and desorption characteristics of a specific coal are clay minerals and-, coal rank as well as the subsequent properties associated with coal rank, such as surface properties and porosity (Mahajan & Walker, 1971; Unsworth et al., 1988; and McCutcheon & Barton, 1999). This dissertation presents results from a detailed investigation into the moisture adsorption and desorption properties of South African coal along with the coal

characteristics and environmental conditions influencing it. In order to achieve the above mentioned objectives the study was divided into the following integrated parts:

- To determine the chemical and structural properties for each of the coal samples used in this investigation.
- To characterise the minerals present in each coal qualitatively with the use of QEMSCAN analysis.
- To evaluate the adsorption and desorption behaviour of the selected coals under varying environmental conditions as a function of relative pressure under isothermal conditions.
- To determine whether the clay minerals present in each coal sample will influence the moisture adsorption and desorption behaviour.
- To investigate if the moisture adsorption and desorption behaviour can be linked to other coal properties such as coal rank, as well as coal petrology.
- Also to determine the effect of temperature on the moisture adsorption and desorption behaviour as a function of relative pressure under non isothermal conditions.
- Evaluate an appropriate model to describe the moisture adsorption mechanism present for each coal sample and to assess the relevant parameters obtained from these models.

1.3 Scope of the dissertation

The scope of this dissertation has been constructed to illustrate and answer the respective research questions outlined in the in the objectives of this study. It is schematically presented in Figure 1.2.

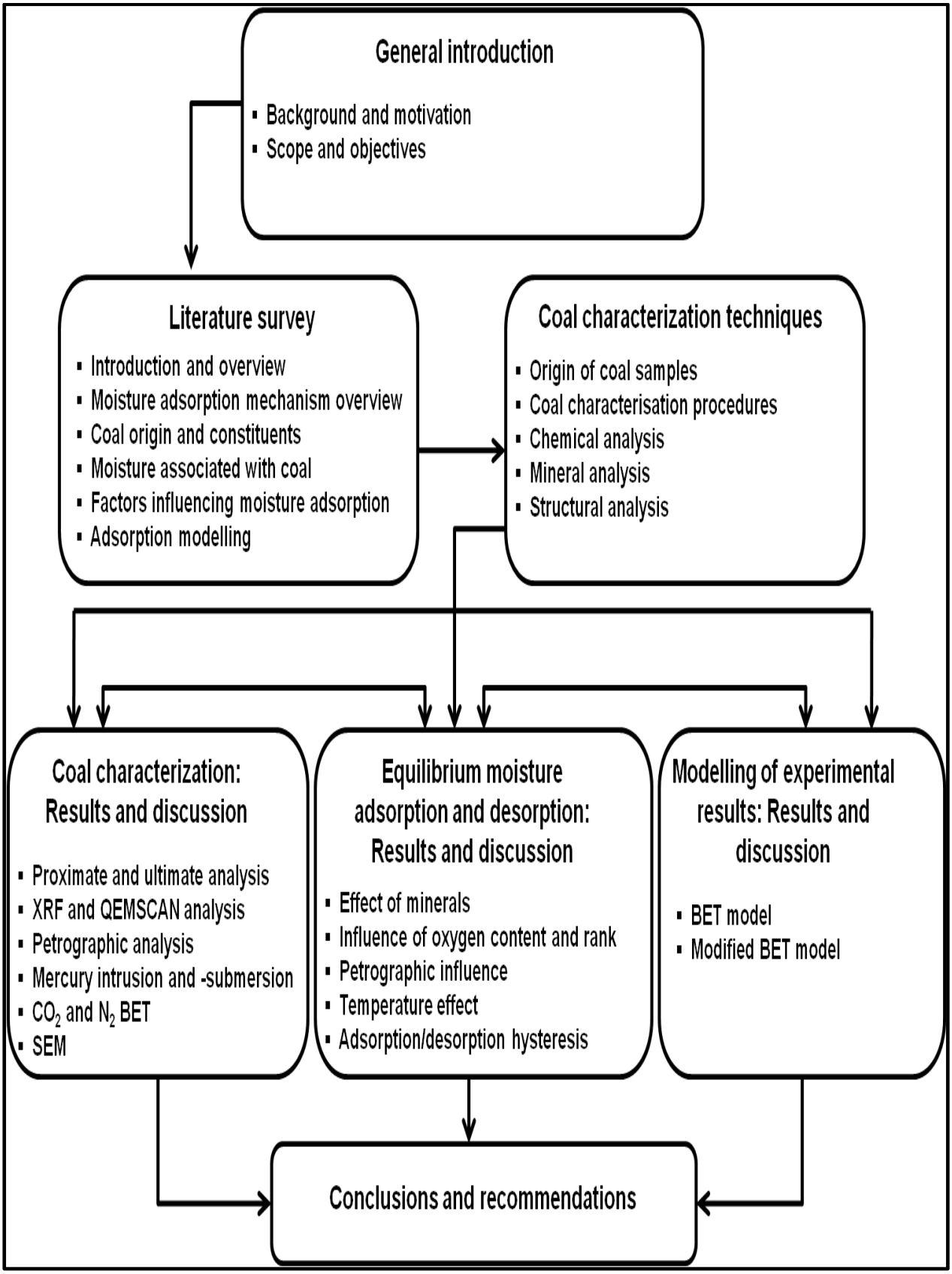

Figure 1.2: Scope of investigation.

Chapter 1 furnishes a general introduction regarding the background information of this study as well as a motivation that corroborates the arguments made in support of this investigation concerning the moisture adsorption and desorption properties of South African coal and the coal properties influencing them. The chapter concludes with a section detailing the aims and objectives of this study in order to ensure that all the necessary outcomes can be obtained from this investigation. Chapter 2 presents the literature survey that was conducted, which will provide the necessary information to better understand the origin of coal and its main constituents. It further presents information regarding the parameters and characteristics that will influence the moisture adsorption and desorption properties of South African coal. The literature survey also briefly discusses the relevant models associated with water adsorption. Chapter 3 discusses the characterisation techniques and apparatus used to determine the chemical-, mineralogical,- and structural analysis as well as the origin of the selected coal samples. Chapter 4 reports the characterisation results, discusses the information and presents the conclusions that could be drawn from these results. Chapter 5 examines the moisture adsorption and desorption behaviour of the five South African coal samples used in this study. It subsequently reports the influence of minerals on the moisture adsorption/desorption behaviour. This chapter also presents the moisture adsorption/desorption behaviour based on properties such as coal rank, coal petrology and varying temperature. At the end of this chapter the adsorption/desorption hysteresis effect is also investigated. The modelling results are portrayed in Chapter 6 together with the relevant calculated parameters. Some of the model parameters are also be correlated with coal properties determined in Chapter 4 and adsorption properties presented in Chapter 5. This illustrates the interchangeable relationship between Chapters 4, 5 and 6. Finally, Chapter 7 discusses the conclusions that could be drawn regarding the outcomes of this study in detail, and makes some recommendations for future research.

CHAPTER 2:
LITERATURE REVIEW

2.1 Introduction

Chapter 2 contains the necessary information to understand the research conducted in this study, beginning with a general overview of the adsorption/desorption mechanisms involved during moisture adsorption on coal, as presented in Section 2.2. It was also essential to investigate and understand the differences between the wealth of coal types found globally, the different conditions present during their formation as well as their diverse constituents. This will provide a proper basis for determining and understanding their suitability for different utilisation processes and, more importantly, their behaviour during the moisture adsorption/desorption process. Coal formation and the coalfields of South Africa are discussed in Sections 2.3 and 2.4 respectively. The types of moisture associated with coal are reviewed in Section 2.6 followed by a detailed assessment of the factors influencing moisture adsorption on coal in Section 2.7. The occurrence of hysteresis during the adsorption/desorption of moisture in coal as well as the adsorption and desorption behaviour of clay minerals in the presence of water are discussed in Section 2.8. Finally, Section 2.9 presents the different models describing the mechanisms present during adsorption and desorption.

2.2 Moisture adsorption and desorption on coal: general process overview

In general, adsorption isotherms illustrate the relationship between the amount of gas/vapour adsorbed and the relative pressure at a constant temperature. The majority of isotherms found in literature can conveniently be grouped into five classes according to the classification system developed by Brunauer, Deming, Deming and Teller (BDDT) (Brunauer et al., 1938). The different isotherms are illustrated in Figure 2.1.

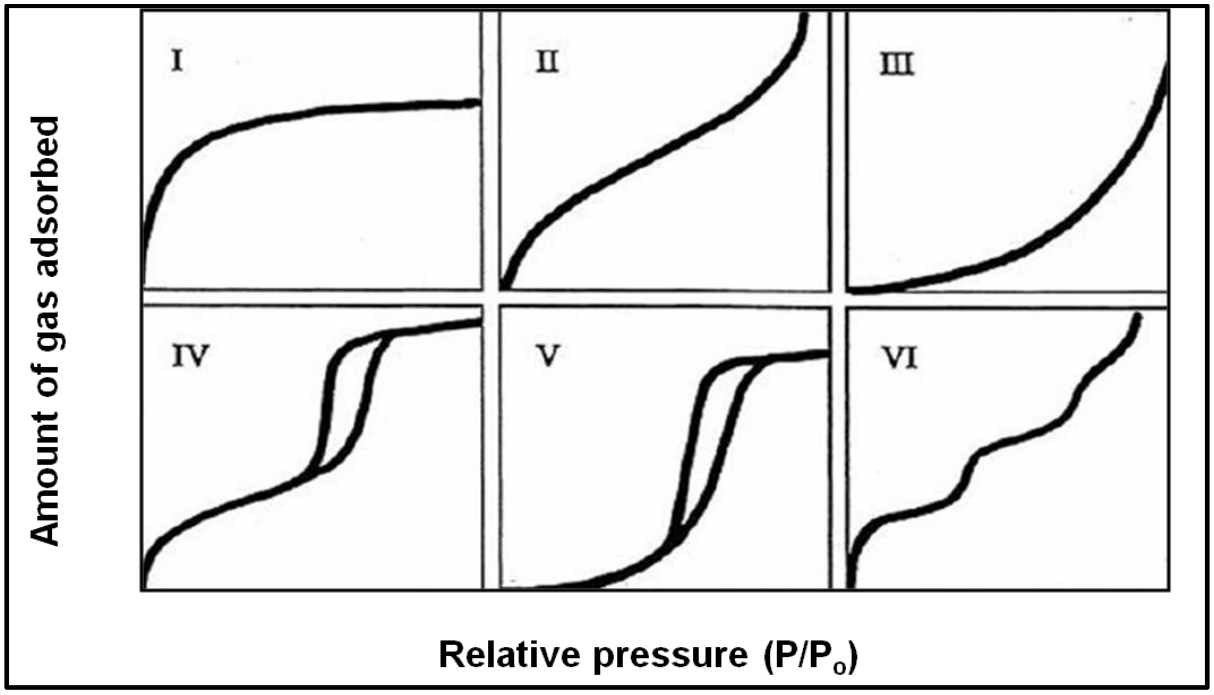

Figure 2.1: The five main isotherms (I-VI) according to the BDDT classification system (Gregg and Sing, 1982).

The adsorption of a gas/vapour by a solid can provide valuable information regarding the surface area as well as the pore structure of a particular solid. Type I isotherms are characteristic of microporous solids with monolayer adsorption mechanisms; whereas, Type II isotherms are observed when the initial adsorption takes place in the monolayer followed by multilayer adsorption (Do, 1998). Mesoporous solids usually resemble Type IV isotherms while Type III and V isotherms are characteristic of systems where the interaction between the surface and the adsorbed molecules are weak (Gregg & Sing, 1982, Do, 1998). Type IV and V isotherms are associated with hysteresis, where the adsorption and desorption isotherms do not follow the same path (Gregg & Sing, 1982; Ruthven, 1984). Type VI behavior occurs for materials with relatively strong fluid-wall forces with temperatures close to the melting point for the adsorbed gas.

Moisture adsorption on coal is quite different from other gasses such as CO_2, N_2 and CH_4 essentially due to weak interactions between the water molecules and the coal surface accompanied by strong interactions between the water molecules themselves. Figure 2.2 gives a visual representation of the water adsorption process as a function of relative pressure.

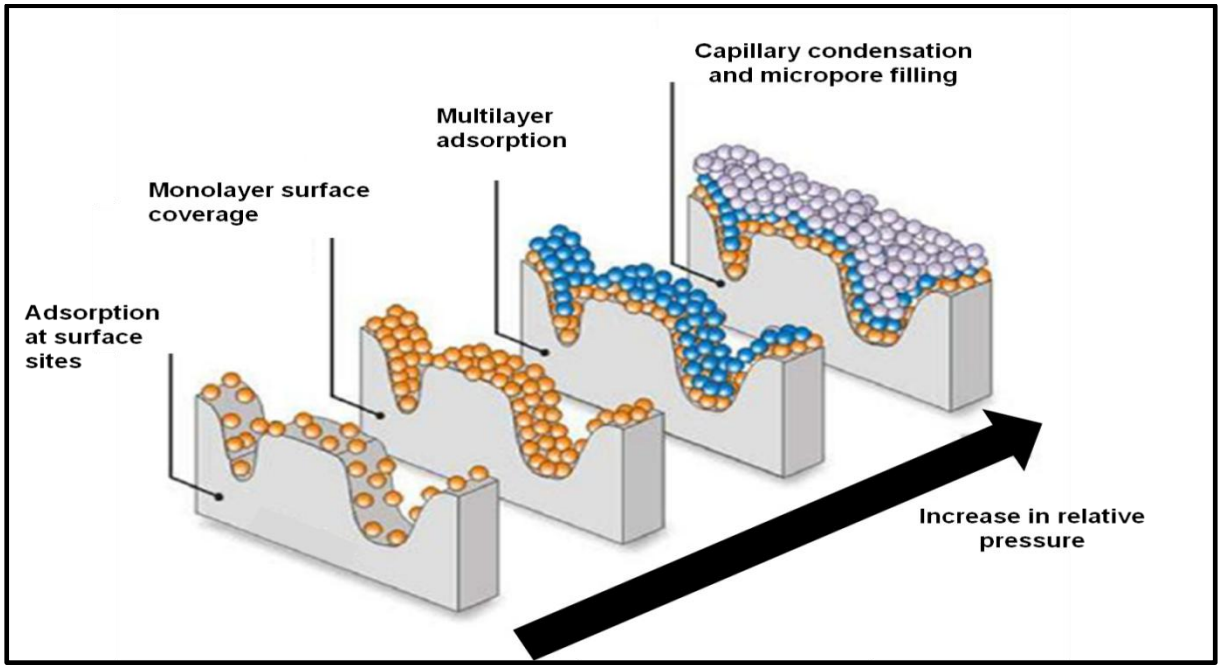

Figure 2.2: Moisture adsorption process as a function of relative pressure (Jasińska, 2011).

At low relative pressures the uptake of water at the coal surface will be small due to the weak interaction between the coal surface and the water molecules. The polar nature of the water molecule will allow it to bond to oxygenated surface functional groups (Gregg & Sing 1982; Rutherford & Coons, 2004). Once a molecule is adsorbed on the coal surface it will promote the adsorption of further molecules through hydrogen bonding and consequently, a monolayer will form on the coal surface. As the relative pressure increases multi layer formation takes place followed by cluster formation and ultimately capillary condensation or micropore filling (Kaji et al., 1986; Charrière & Behra, 2010; Švábová et al., 2011).

2.3 Coal origin and formation

From a simplistic point of view, according to Ward (2002), coal can be considered as consisting of organic components (macerals) on the one hand, and a range of mineral components and other inorganic elements, on the other hand.

Arnold (1989) defined coal as a heterogeneous mixture of plant debris and minerals that underwent physical and chemical transformations over an extended period of time. The mechanisms and conditions under which coal formation took place greatly influenced coal properties resulting in different coal processing technologies. A thorough understanding of the total coal structure and its properties would greatly aid the development and improvement of various coal utilisation techniques.

From a global point of view it is important to differentiate between coal originating from the Southern Hemisphere, often called Permian coal and coal from the Northern Hemisphere, also referred to as Carboniferous coal. Differences in the characteristics of Northern- and Southern hemisphere coals can be attributed to the conditions reigning at the time of coal formation and the subsequent history of the geological events in each region (Falcon & Ham, 1988). Warm moist conditions in the Northern Hemisphere ensured the rapid growth of vegetation, resulting in a massive accumulation of organic material whereas, even, low-lying terrain surrounding the swamps ensured minimal transportation of mineral matter via rivers and streams into the decaying vegetation (Kershaw & Taylor, 1992).

The swamps in the South developed under cool increasing to warm conditions associated with the decline of a massive ice age (Falcon & Ham, 1988). The rivers flowing into the swamps were glacier fed and mineral matter content was introduced into the swamps abraded from the path of the glacier. A portion of the mineral matter was also carried into the swamps via rain and wind. The topographic and sedimentary environments varied to a great extent, resulting in different levels of decay in plant matter. These combined conditions gave rise to mineral rich peat forming swamps, which developed into wide spread shallow coal seams over an extended period (Falcon & Ham, 1988). Therefore, South African coal and coal from other Gondwanaland regions are distinctively rich in mineral matter, relatively difficult to beneficiate and particularly variable in rank and maceral composition (Falcon & Ham, 1988).

2.3.1 Coalification process

Over extended periods of time ongoing changes in temperature and pressure allowed accumulated vegetation in peat swamps to increase in maturity, this progressive transformation in organic material via the steps of lignite, sub-bituminous, bituminous, anthracite and graphite is known as coalification. Another requirement for coal formation is enough water to restrict the oxygen supply to the organic material to prevent its breakdown. The degree to which the vegetation varies in maturation is referred to as coal rank or as the extent of metamorphism (Falcon & Snyman, 1986). The main chemical changes that occur during the coalification process are summarised in Table 2.1.

Table 2.1: The main chemical changes in coalification (Falcon, 1977).

Rank	C (%)	H (%)	O (%)	N (%)
Wood	50	6	43	0.5
Peat	59	5	33	2.5
Lignite	70	5.5	23	1
Bituminous coal	82	5	10	2
Anthracite	93	3	2.5	1
Graphite	100	0	0	0

The coalification process consists of an initial biochemical phase followed by a geochemical or metamorphic phase. The biochemical phase includes the processes that take place in the peat swamp following deposition. Intense biochemical changes take place at shallow depths mainly in the form of bacteriological activity (Thomas, 2002). Microbiological activity can only continue if fungi and bacteria participate in the decomposition process which is limited to a certain burial depth since fungi does not occur beyond a depth of about 40cm. The Carbon- rich components and volatile content are only slightly affected during the biochemical stage but with an increase in the burial depth and compaction of the peat, the moisture content decreases and the calorific value increases. The proportions of organic constituents which are formed during biochemical degradation at the peat stage are the predecessors of macerals, which are the building blocks of coal and therefore play an important role in determining coal type (Falcon & Snyman, 1986).

In the metamorphic phase conversion to the final coal type occurs. Temperature, pressure and time play a key role in this phase. Metamorphic change determines the degree of coalification and thus also the rank of the coal (Thomas, 2002). During either of the two phases, the progressive changes that occur within the coal are an increase in carbon content and a decrease in the hydrogen and oxygen content, resulting in a loss of volatiles as illustrated in Table 2.1.

2.4 Coalfields of South Africa

Coal plays a key role in the South African economy and is a commodity responsible for approximately 93% of the energy needed to generate electricity (WCA, 2010). The reliance on coal for energy is not likely to change in the near future due to a lack of suitable alternatives to coal as an energy source and the favourable costs at which coal can be mined. Future coal production will come mainly from the Witbank coalfield (de Korte, 2000).

South Africa has large, although not unlimited, reserves of coal situated in 19 coalfields in widely separated provinces. Important coal mining areas are the Witbank-Middelburg, Ermelo, Standerton- Secunda areas of Mpumalanga and the Sasolburg-Vereeniging area in the Free State (Jeffrey, 2005). Within this extensive west-east band of coal occurrences, there is a progressive increase in coal rank from high to low volatile bituminous coal (Kershaw & Taylor, 1992).

The coal samples used for this investigation originate from the Free State, Witbank and Soutpansberg coalfields. Coal quality varies considerably across the various coalfields with for instance some very low quality coal in the Free State that can be used only for power generation in places where boilers are specifically designed to cope with such feedstock (Peatfield, 2003). Anthracite is produced in Natal and soft coking coal is primarily mined in the northern parts of South Africa.

2.5 Coal composition

The inherent constituents of coal can be classified according to its most fundamental components or building blocks, namely the organic constituents that are mainly fossilised plant material and the inorganic fraction made up of a variety of primary and secondary minerals. The organic elements and mineral matter, intimately associated with a specific coal, are fundamental in characterising the nature of coal as well as determining its significance in different utilisation processes (Falcon & Snyman, 1986). The inorganic fraction of coal is the minerals that are not combustible and ash is often erroneously referred to as a component of coal, whereas ash is the mineral residue left after the combustion of coal. The inorganic fraction is viewed as a diluent that leaves an ash residue after combustion and is viewed as a source of unwanted abrasion, stickiness and corrosion associated with coal handling (Ward, 2002). Minerals are also considered to be inhibitors of gas adsorption and retention, consequently reducing its gas storage capacity (Rodrigues et al., 2008). The benefits derived from coal including the energy gained from combustion

processes, its potential as an alternative hydro-carbon source and its capacity for methane storage can mostly be attributed to its maceral constituents.

2.5.1 Petrographic constituents

The organic matter in coal consists of the fragmented and decomposed remains of the original vegetation found in the swamps where the process of coal formation started. These discrete organic components can be observed microscopically and are termed macerals (Falcon & Ham, 1988). Three main groups of macerals can be distinguished namely vitrinite, liptinite and inertinite.

The vitrinite group originated from cell wall material or woody plant tissue at various stages of decomposition and it is usually rich in oxygen in comparison to other macerals. Vitrinite is formed as a result of the anaerobic decay of ligno-cellulosic materials in swamps (ICCP, 1998). It is the main component of bright coal and is more frequently found in Carboniferous than Gondwana coal.

Liptinites are from waxy, resin parts of plants, and contributes to about 2-8% of South African coal. The liptinite maceral group is characterised by a higher hydrogen concentration and a high proportion of volatile matter (ICCP, 1998).

Inertinites are composed of plant material that has been strongly altered and degraded in the peat stage of coalification and are characterised by a higher carbon content and lower hydrogen and oxygen content compared to other macerals in coal from the same rank (Osborne, 1988). The inertinite group derives its name from the fact that these macerals are inert or semi-inert during normal carbonisation processes in which they act as diluents (ICCP, 2001). Macerals of the inertinite group includes fusinite, semifusinite and secretinite. When inspected microscopically, the reflectance of the inertinite macerals in low- and medium ranked coal is higher in comparison with the reflectance observed in the vitrinite and liptinite groups (ICCP, 2001).

2.5.2 Mineral matter constituents

Coal is notoriously heterogeneous, consisting of a combination of combustible plant remains and inorganic components that vary both in physical and chemical composition. The variance in original vegetation and the degree of coalification are the main causes for the variation in physical properties in coal. Mineral matter in coal is heterogeneous in distribution, composition and is intimately associated with coal macerals (van Alphen, 2005).

Inorganic matter includes minerals and other non- mineral inorganic constituents either in, or associated with coal. The mineral matter can consist of discrete crystalline mineral particles, inorganic elements or compounds that are integrated in the organic molecules of the coal as well as dissolved salts in the pore or surface water of the coal (Ward, 2002). The combined effect of moisture expulsion and chemical changes in the organic matter observed with the increase of coal rank supports the removal of non-mineral inorganics from the coal. Non-mineral inorganics are therefore usually only associated with lower ranked coal (Ward, 2002)

Ragland and Baker (1987) further discussed the occurrence of mineral matter in coal and concluded that the mineral constituents in coal can occur as discrete grains, flakes or aggregates. The physical forms in which they transpire in coal include the following:

- Microscopic inclusions within maceral;
- As layers of partings, where in finely distributed clay minerals predominate;
- As spherical nodules;
- As fissures in fractures or void fillings; and
- As rock fragments found within the coal bed.

Minerals are divided into different classes according to their origin, time of emplacement and relative abundance. There are two ways in which mineral matter is captured within coal; the terms extrinsic (extraneous) and intrinsic best describe the origin and formation of the minerals (van Alphen, 2005). Intrinsic mineral matter is closely entwined with coal and cannot be removed by preparation techniques. Minerals present in the original vegetation in which the coal formation took place as well as finely divided clays are the main constituents for this type of mineral matter. South-African coal consists of varying quantities of such minerals, which include finely dispersed clays, quarts, carbonate, and pyrite group minerals (Ward, 2002). Extraneous/extrinsic mineral matter is either introduced into the mined product from the floor and roof of the seam, or during peat accumulation and can be removed by coal preparation techniques. During peat accumulation minerals are introduced into the swamps through wind action, the process of precipitation or fluvial action (van Alphen, 2005). Most of this mineral matter consists of dirt bands in the seam, shales, sandstones and intermediate rocks. The majority of shales associated with South- African coal are black and carbonaceous with a higher density than coal. These minerals can easily be separated via flotation or density separation (Stach et al., 1982).

Various clay minerals (kaolinite/illite), quartz, carbonates (calcite, dolomite), sulphides and oxides (pyrite) together with imbedded sedimentary rock such as shale and sandstone are associated with South African coal (Falcon & Snyman, 1986). According to Gaigher (1980)

South African coal consists essentially of clay minerals (kaolinite, illite) and quartz, and to a lesser extent, carbonate minerals (calcite, dolomite and siderite). Gaigher (1980) also found a strong correlation between clay minerals and inertinite, but a negative association between clay minerals and vitrinite. The average clay composition of South African coal was estimated using XRD analysis and was found to be 54.1% kaolinite, 29.2% illite and 16.7% expandable clays.

2.5.2.1 Clays

Clay minerals or aluminosilicates are finely distributed in the coal matrix with illite, kaolinite and montmorillonite being the most plentiful (Speight, 1994). The types of minerals present are greatly influenced by the type of environment in which the coal formation took place. Kaolinite is frequently found in an acidic fresh water depositional environment, while illite is more readily found in an alkaline or marine depositional environment. Therefore, higher illite concentrations are found in the Natal coalfields than in coal from the Highveld, Witbank and Orange Free State coalfields (Snyman et al, 1983).

Clay minerals are found in very small grains within the coal (1-2µm), and can occur as small lenses or microscopically visible bands. They can account for 50% or more of the total mineral content in a specific coal and are the most abundant mineral occurring in coal (Falcon & Snyman, 1986). Clay minerals contain a substantial amount of water in their lattices and carry an economical penalty as it lowers the calorific value of the coal and elevates the cost involved in ash handling and ash disposal (Spears, 2000). Clay minerals especially from the montmorillonite group possess prominent swelling properties. Swelling is usually accompanied by a substantial reduction in strength and can lead to complete disintegration when coal containing this type of swelling clay encounters water. In coal processing plants swelling clays tend to form high quantities of slimes that result in difficulties during dewatering.

2.5.2.2 Quartz

Silica in the form of quartz can account for up to 20% of the total minerals in coal and are therefore the next most abundant after clay minerals (Matjie and van Alpen, 2008). The occurrence of quartz in coal particles can be attributed either to the action of wind and water carrying the minerals into the swamps or it could be an intrinsic part of the plant material (van Alphen, 2005).

2.5.2.3 Carbonates

Carbonates generally occur as nodules in the form of siderite and as veins and cell fillings of calcite, dolomite and ankerite (Falcon & Snyman, 1986). According to van Alphen (2005), the deposition of carbonates in the stress fractures and cleats of the coal seam is the result of ionic rich groundwater percolating through the established coal seams over an extended period.

2.5.2.4 Sulphides

During coal formation, the presence of sulphur reducing bacteria in an alkaline, sulphate rich environment will favour the formation of pyrite and marcasite while an acidic fresh water environment deficient in sulphate will favour siderite formation. Consequently, siderite is more frequently found in Australian coal, whereas pyrite is the more common iron bearing phase present in South African coal (van Alphen, 2005). Pyrite in South African coal is typically associated with lower ranked coal and can occur as fine to coarsely distributed grains and nodules in vitrinite or inertinite maceral varying from 0.1 to hundreds of microns in size (Yinghui, 2004; van Alphen, 2005; Wagner and Hlatshwayo, 2005).

Sulfides account for less than 5 % of the total minerals found in coal, nevertheless, a lot of attention is afforded to this group of minerals despite the relatively low concentration in comparison to other minerals and this is mainly due to environmental concerns.

When emitted into the environment SO_2 and SO_3 formed during combustion can contribute significantly to air pollution and acid rain (van Alpen, 2007).

2.6 Moisture in coal

Due to the organic and hygroscopic nature of coal, it usually contains a certain quantity of inherent moisture held by capillary force within its porous structure. The original environmental conditions under which coal formation took place had a substantial amount of water associated with it. As the coalification process progresses the coal becomes more hydrophobic and inherent moisture is repelled by the internal structure of the coal. The water associated with coal plays a key role in the economics of coal utilisation as it significantly affects the cost of transportation and the efficiency of coal burning facilities such as boilers (Kaji et al, 1986). Moisture also has a direct effect on reactivity, drying, pyrolysis and the ignition point of coal.

In the past, three main types of water were associated with coal; chemically bound water, water adsorbed by physicochemical forces and free water linked to coal via mechanical forces (Monazam et al., 1998). However, recent studies introduced a different approach to classifying the moisture residing in coal particles. This more detailed classification defined four main types of water content in coal, that is, bulk (free moisture), capillary (equilibrium moisture), multilayer and monolayer water (chemically bound water) (Wang, 2007). Water residing at the external surfaces of coal particles or in the large voids inside the particles are denoted surface, free or bulk water. Water condensed into the coal-pore matrix as clusters are termed capillary water and can also be referred to as equilibrium moisture or the moisture holding capacity of coal. This type of moisture cannot be removed by mechanical means and is contained within the coal in equilibrium with an atmosphere saturated with water vapour (Wang, 2007). Multi layer water is found in thin layers on the surface of the coal pore, literally only a few molecular diameters in depth. This water is weakly associated with hydrogen atoms, while monolayer water is strongly bonded to oxygen containing functional groups at the pore surface (Wang, 2007). The equilibrium moisture content present in a coal sample can be determined according to ASTM D-1412 (ISO 1018) at 96 to 97% relative humidity and 30°C (Speight, 2005).

2.6.1 Economic impact of moisture associated with coal

The handling of coal and the operation efficiency of handling equipment is significantly influenced by the amount of water present, as the surface moisture increases, so does the difficulty in handling. Water associated with coal is usually introduced during the beneficiation step or it can be a direct result of water present in the coal seams, bearing in mind that South Africa's entire mined coal seams are situated below the water table (Campbell, 2006). Water present in the coal seam may be regarded as inherent moisture that cannot be removed by mechanical means. This moisture, with the exception of that combined with the mineral matter, can be eliminated by heating the coal for a short period at 105 °C. Water introduced during beneficiation or during transportation can be largely eliminated by air-drying.

Open-air stockpiles exposed to heavy rainfall and other climatic conditions can experience an increase in moisture content, which can result in extensive handling problems, the plugging of belt conveyors or even moisture contract penalties.

The response of coal in relation to changing moisture levels may be influenced by factors such as clay content and percentage fines. Coal containing a significant amount of clay will become sticky, as these minerals are better at retaining moisture. The mineral matter found

in South African coal is predominantly clay minerals, largely in the form of kaolinite and illite, thus, posing a problem in varying climatic conditions (Pinetown et al., 2007).

Specifications from coal consumers, in particular coal-burning power plants, contain requirements for a maximum moisture content to prevent coal handling problems and to minimise evaporative losses in boilers. Therefore, to prevent water-based problems, dewatering and sometimes thermal drying is required to meet moisture specifications. However, a fact that must not be over looked is the re-adsorption of moisture as transport and handling processes may expose the dried coal to the atmosphere (Karthikeyan & Mujumdar, 2007).

2.7 Factors influencing moisture adsorption and desorption on coals

Various publications were found in the literature concerning the subject of water adsorption on coal as a function of vapour pressure (Mahajan & Walker, 1971; Unsworth et al., 1988; and McCutcheon & Barton, 1999). Due to the heterogeneous nature of coal, it follows that several individual coal properties will influence the adsorption/desorption behaviour of coal. The authors found that the extent of moisture adsorption is influenced to a large extent by coal rank and mineral matter content, and that the specific adsorption sites are determined by oxygen functional groups. Other factors influencing moisture adsorption on coal include porosity, surface area, temperature and, to a lesser extent, particle size and petrographic constituents.

2.7.1 Influence of mineral matter

A study of the influence of minerals on the gas adsorption behavior of three bituminous coals, similar in rank, from South Africa revealed that minerals are non porous and cannot store gas and that they occupy space that could otherwise be occupied by other gas or fluids (Rodrigues et al., 2008).

It is widely recognised that the amount of minerals (predominantly clay minerals) contained in coal influences the amount of water adsorbed by the specific coal (McCutcheon & Barton, 1999). The differences in water uptake for coal samples obtained from the same seam could be accounted for completely by the mineral matter content. At relative pressures of 0.9 the water uptake by the mineral components were found to be 2.3-2.8 times the uptake as a result of the organic material. It was also found that the mineral matter containing the swelling type clay, montmorillonite had more than twice the water up-take than the mineral

matter that was richer in kaolinite (McCutcheon & Barton, 1999). This consequently implies that the extent to which higher ranked bituminous coal interacts with water, increases with an increase in mineral matter content. This fact is clearly illustrated in Figure 2.3.

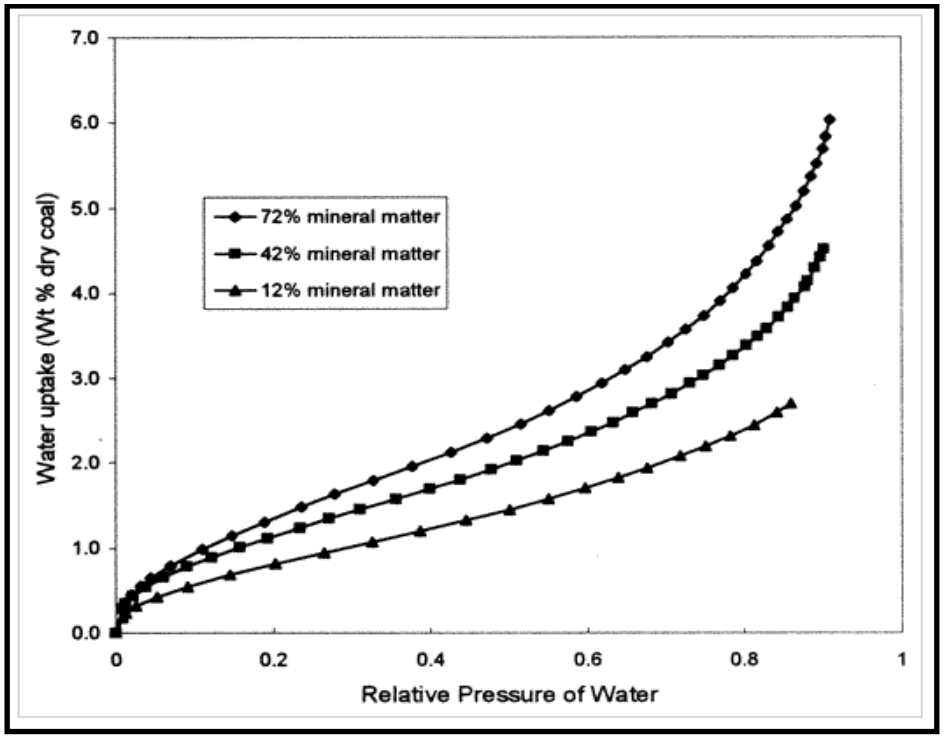

Figure 2.3: Influence of mineral matter on water uptake of bituminous coals (McCutcheon & Barton, 1999).

The interaction of water with lower ranked coal becomes less notable since the water uptake by the organic components is substantially greater than for higher ranked coal, as a result the influence of mineral matter contained in this type of coal is less significant for lower ranked coal.

2.7.2 Effect of coal rank and surface oxygen

The degree of water adsorption on coal greatly depends on coal rank; bituminous coal adsorbs more moisture at relatively low pressures than anthracite (Mahajan & Walker, 1970). Falcon (1986[b]) also stated that low rank coal is characterised by high moisture content as well as comprising the highest molecular porosity and total internal surface area. The high porosity of inertinite, which is widely associated with low rank coal, provides for better passage and storage of gasses/vapours.

Mahajan & Walker (1971) investigated water adsorption on six coal samples of varying rank and suggested that water adsorption depends on coal rank. Bituminous coal proved to

adsorb more water at relatively lower vapour pressures than anthracite. However, it was observed from the data that for a given coal rank, moisture sorption does not necessarily vary in the same proportion as the volatile matter content. The authors suggested that this occurrence could be either due to the influence of impurities (mineral content) or the role of oxygen functional groups present in the coal sample.

A further study conducted by McCutcheon et al., (2003), investigating the effect of coal rank on water adsorption at a relative pressure of 0.9, confirmed a trend between coal rank and water uptake. However, some scatter was also observed, which could be attributed to the presence of mineral matter in the coal samples. It was observed by others investigating water adsorption on coal varying in rank, that adsorbed water is attached to the coal surface by means of oxygen containing functional groups, resulting in the formation of hydrogen bonds with the adsorbed water molecules (Allardice & Evans, 1971; Kaji et al*.,* 1986).

2.7.3 Petrographic influence

According to a study carried out by McCutcheon and Barton (1999) on bituminous coal, it was found that a large difference in maceral composition between two samples of the same rank had little or no effect on their moisture holding capacity. No clear dependence of inherent moisture content and maceral type seems to exist, according to Unsworth et al. (1989), thus inertinite-rich and vitrinite– rich coal of the same rank contains more or less the same amount of pore held moisture. For higher ranked bituminous coal in particular, there seems to be no sensitivity towards maceral composition but the interaction of water with this type of coal can be significantly enhanced by inherent clay minerals (Bourgeois et al., 2000). Faiz *et al.,* (1992) also reported that there is no clear correlation between gas adsorption capacity and maceral composition, in fact, the strong dependence of adsorption on coal rank overshadows the influence of maceral composition on gas adsorption to a large extent.

2.7.4 Influence of porosity

Conceptually coal porosity can be viewed as the volume fraction of coal occupied by empty spaces or else as the fraction of coal occupied by a particular fluid, which varies from fluid to fluid. Coal rank and porosity are closely related (Osborne, 1988; Gan et al., 1972). It has been shown that coal rank significantly affects moisture adsorption and, therefore, porosity may influence moisture adsorption. Porosity is an influencing factor that plays a key role in the chemical reactivity of solids as well as the physical interaction between solids and gasses (Rouquerol *et al*., 1994).

In general, coal can be associated with a range of pore sizes. Macropores (>50nm) are generally associated with lower ranked coal, transitional or mesopores (2-50nm) and micropores (<2nm) are associated with higher ranked coal (Sing et al., 1985). Higher ranked coal also tends to have fewer pores due to a greater degree of orientation in its layers whereas lower ranked coal is more randomly orientated with many cross-links which result in a highly porous structure (Osborne, 1988; Gan et al., 1972). Faiz *et al.,* (1992) acknowledged that the occurrence of mineral matter for a specific coal contributes mainly to its macro pore volume; consequently, an increase in mineral matter can lead to a decrease in micro- and meso-porosity.

When describing a porous structure some confusion can arise between the different pore types present and care should be exercised in the choice of terminology in order to avoid ambiguity. Figure 2.4 provides a clear illustration of the different pores present in a coal particle according to their availability to external fluid.

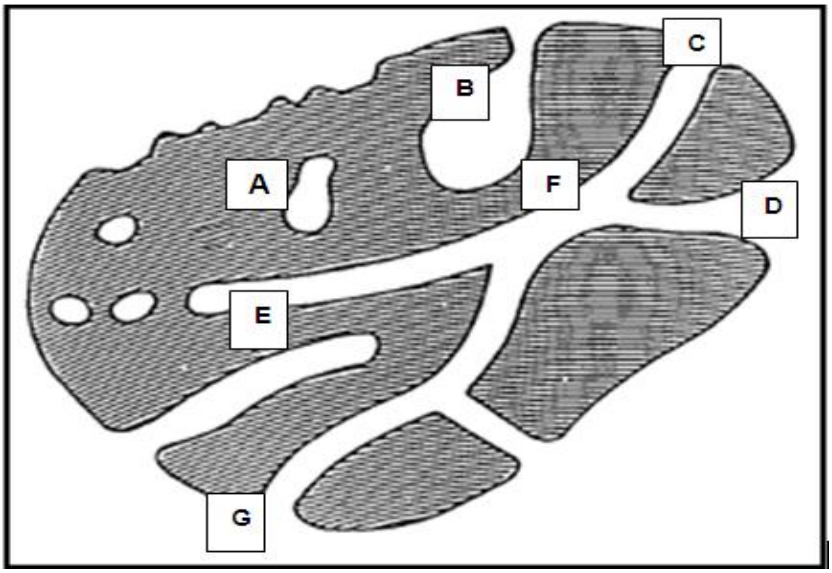

Figure 2.4: Schematic representation of a porous solid (Rouquerol *et al*., 1994).

Pores that are inaccessible and isolated from neighbouring pores are often described as closed pores and can be seen in region A of Figure 2.4. This type of pores influence macroscopic properties such as bulk density but are inactive in the adsorption of gasses. On the other end of the spectrum, pores which have continuous contact with the outside surface of the particle can be found and are appropriately called open pores (B, C, D, E, F, G). Some pores for example B and E are characterised as blind pores and are only exposed to the outside surface of the particle at one end (Rouquerol et al., 1994). Pores can also be grouped according to their individual shapes. They can be cylindrical (E, G), inkbottle shaped (B), funnel shaped (D) or slit-shaped. Coal consists of intrinsic pore networks

intermeshing with a continuous coal structure, and Ruthven (1984) found that rates of adsorption and desorption in porous materials are governed by transport in the pore network, rather than by the intrinsic kinetics of sorption at the surface. It should be further noted that for a given mass of coal sample smaller particles possess a greater surface area compared to larger particles thus enhancing the rate of adsorption. However, as a consequence of porosity, the coal's significant internal surface of porosity dominates so much that particle size becomes negligible, having no effect on the final adsorption capacity of the coal (Azmi et al., 2006).

Various techniques exist to estimate the porosity and pore volumes of a specific coal. Generally, mercury porosimetry, carbon dioxide and nitrogen gas adsorption methods can be used to determine certain parameters that offer a better understanding of the coal pore structure (Gan et al., 1972; Gregg & Sing, 1982; Rodrigues & de Sousa, 2002).

2.8 Adsorption desorption hysteresis

Adsorption and desorption isotherms with hysteresis yield qualitative information regarding the type of pores present as well as the solid surface chemistry (Charrière & Behra, 2010). The combined adsorption and desorption isotherms for a specific solid produces a hysteresis loop where the desorption isotherm is greater than the adsorption isotherm for a definite relative pressure range (McCutcheon et al., 2003). Adsorption/desorption hysteresis for two bituminous coal types are demonstrated in Figure 2.5.

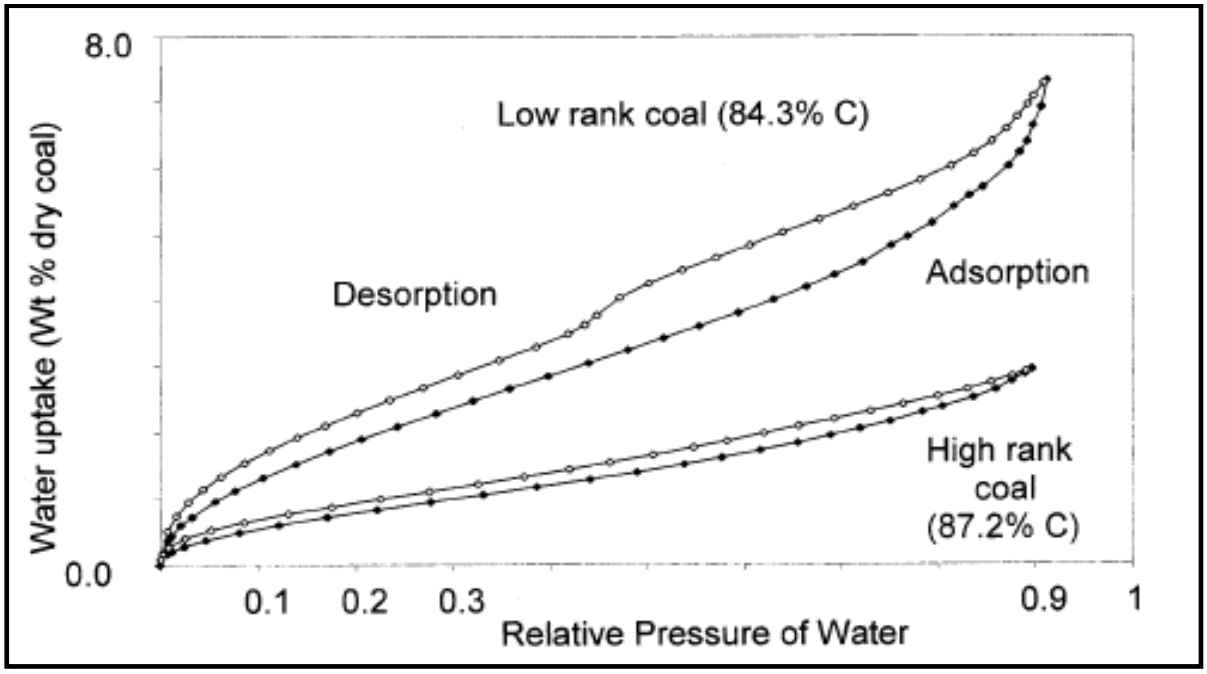

Figure 2.5: Adsorption/desorption isotherms for two coal samples of different rank (McCutcheon *et al*., 2001).

The figure above illustrates the equilibrium isothermal adsorption and desorption of water for a high rank bituminous coal (C6 87.2 wt.% C) and a low rank bituminous coal (C2, 81.5 wt.% C). The adsorption and desorption isotherms were recorded within the pressure range of 0-0.9 (P/P_0) and a temperature of 26°C. The isotherms show typical type II behavior according to the BDDT classification system discussed in Section 2.2 (Gregg and Sing, 1982). The adsorption and desorption isotherms do not follow the same path which can be referred to as hysteresis. This pathway shift is much greater for the low rank bituminous coal than for the high rank bituminous coal (McCutcheon *et al*., 2001).

The moisture adsorption and desorption results reported by McCutcheon et al., (2003) indicated that lower ranked bituminous coal displayed a significant amount of hysteresis when compared to higher ranked bituminous coal. Low pressure- as well as high pressure hysteresis was observed for lowered rank bituminous coal, where the change in type of hysteresis is clearly evident in Figure 2.5 above at relative pressures above 0.45. Low pressure hysteresis is usually associated with the swelling and shrinking of water clusters penetrating the coal structure. During the desorption process this process is not fully reversed. Water molecules will desorb in order of increasing bond strength where the weakest bound molecules will desorb first and the water molecules strongly attached to the internal surface of the coal structure will desorb last. This will delay the collapse of the structure resulting in low pressure hysteresis well into the monolayer region (Allardice & Evans, 1971). The degree of water clusters is related to the number of oxygen containing

functional groups present on the coal surface which are in turn related to coal rank. It is therefore expected that lower ranked coal will swell to a greater extent (McCutcheon et al., 2003). High pressure hysteresis in lower ranked bituminous coal can be attributed to the ink- bottle effect. This only occurs when pores present in the coal structure are not fully open at the neck. Water can enter the pore easily but difficulty is experienced during desorption due to capillary blockage. This occurrence is not present in higher ranked coal due to the closing of fine pores and apertures during the coalification process, thereby forming closed pores which are inaccessible to water (McCutcheon et al., 2003).

Clay minerals consist of negatively charged aluminosilicate layers bound by cations. A distinct feature of clay minerals is their ability to adsorb interlayer water, resulting in strong repulsive forces and clay expansion (Hensen & Smith, 2002). The adsorption and desorption behaviour of clay minerals in the presence of water is illustrated in Figure 2.6.

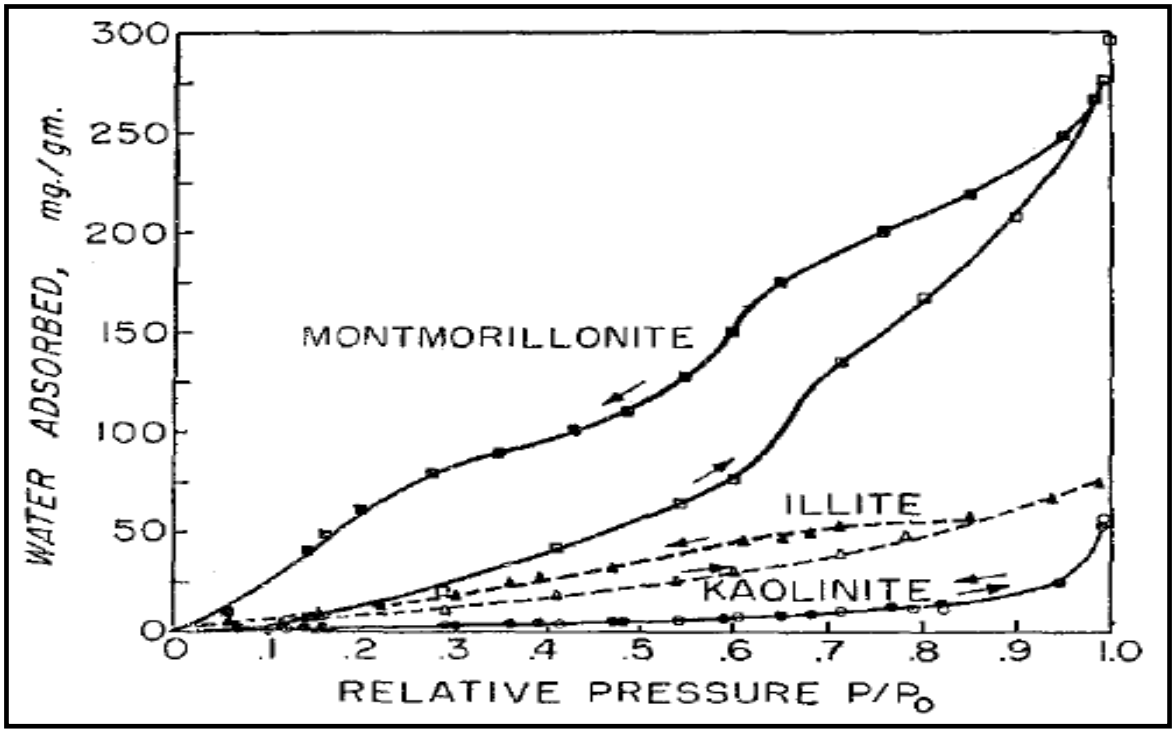

Figure 2.6: Adsorption and desorption isotherms for different clay minerals (Johansen & Dunning, 1957).

The adsorption desorption isotherms for montmorillonite, kaolinite and illite is distinctive of their behaviour in the presence of water and can be an aid in indentifying these minerals. Montmorillonite adsorbs the most moisture and also demonstrates a distinct amount of hysteresis, kaolinite adsorbs the least amount of moisture accompanied by very little hysteresis and illite is intermediate between the kaolinite and montmorillonite isotherms (Johansen & Dunning, 1957). This distinctive behaviour of clay minerals in the presence of

water will play an important role in predicting the moisture adsorption and desorption behaviour of coal containing significant amounts of a specific clay mineral.

2.9 Moisture adsorption models

Adsorption information plays an important role in understanding the adsorption process and is essential in identifying how much of a component, in this case moisture, can be accommodated by a porous adsorbent (Do, 1998). Section 2.9 aims to investigate the models used in the literature for adsorption on solids in order of progression, beginning with the basic Langmuir model depicting monolayer surface adsorption, followed by the slightly more refined BET and modified BET models illustrating multilayer surface adsorption and concluding with the Dubinin Radushkevich model that is based on the theory of micropore-filling.

2.9.1 Langmuir model

The celebrated Langmuir model is the cornerstone of all the theories related to adsorption and it is therefore appropriate to start with this model. The Langmuir theory conveys the fundamental equilibrium adsorption of pure components and allows for better insight into monolayer adsorption on ideal surfaces (Do, 1998). The Langmuir theory assumes a homogeneous surface where the adsorption energies are constant for all sites and where each site can only accommodate one molecule (Gregg & Sing, 1982; Do, 1998). The Langmuir isotherm is depicted in Equation 2.1.

$$\mathbf{n^{exp} = \frac{n_0' hP}{1 + hP}} \qquad (2.1)$$

The parameter h is commonly referred to as the Langmuir constant and is a measure of how strong a molecule is attracted to the surface (Do, 1998).

2.9.2 BET model

Various models have been developed to describe the adsorption of gases on solids where molecules are first adsorbed onto the solid surface at low relative pressures followed by multi-layer formation at higher relative pressures. Brunauer, Emmett and Teller first

developed a very well-known theory to describe multilayer adsorption in 1938. This theory assumes that infinite layers can be accommodated on a flat adsorption surface with no interaction between the adsorbed molecules and that the energy does not vary with the progress of adsorption in the same layer (Do, 1998). Molecules already adsorbed on the surface provide adsorption sites for additional molecules, ensuring the formation of at least a second layer. The interaction energy between the water molecules are set equivalent to the heat of liquefaction, approximated as 43.99KJ/mol at 298K (Koretsky, 2003). Equation 2.2 describes the well-known BET model where the amount of adsorbed gas is related to the saturation pressure.

$$\frac{n^{exp}}{n_o'} = \frac{K\frac{P}{P_s}}{\left(1-\frac{P}{P_s}\right)\left(1+K\frac{P}{P_s}-\frac{P}{P_s}\right)} \qquad (2.2)$$

The above mentioned model's range of validity is very narrow ($0.05<P/P_S<0.35$); above these relative pressures the amount of moisture is usually less than predicted by the model. However, it remains widely used and is a very important method in characterising mesoporous solids largely due to its simplicity (Gregg & Sing 1982; Do 1998).

2.9.3 Modified BET model

Recognising the narrow pressure range where the BET model is applicable and the fact that the amount adsorbed is less than predicted by the BET model at higher relative pressures, Anderson (1946) proposed new theories to extend this range. He proposed that the heat of adsorption for the second layer is less than the heat of liquefaction and that the nature of the structure allows only for a finite amount of layers to form. Various authors have since implemented the modified BET model to predict the amount of gas/vapour adsorbed as a function of relative pressure (Švábová et al., 2011; Charrière & Behra, 2010). This model allows for the extension of the range of applicability to $P/P_s=0.8$ as opposed to the narrow range of applicability of the conventional BET model described in the previous section (Do, 1998). Water vapour is assumed to adsorb at two types of surface sites, the primary sites located at the coal surface and the sites provided by other water molecules already adsorbed at the surface serving as secondary adsorption sites. However, it must be kept in mind that any multilayer theory has a maximum pressure limit where the capillary condensation phenomenon will take over. The characteristic equation for the isotherm of the modified BET model, describing the amount of adsorbed gas/vapour in the presence of two sorption sites as a function of relative pressure, is shown below (Do, 1998);

$$\frac{n^{exp}}{n_o'} = \frac{K_1 \frac{P}{P_s}}{\left(1 - K_2 \frac{P}{P_s}\right)\left(1 + K_1 \frac{P}{P_s} - K_2 \frac{P}{P_s}\right)} \quad (2.3)$$

Water adsorbed due to primary and secondary sites can be described by the following two equations respectively (Charrière & Behra, 2010);

$$\frac{n_1^{exp}}{n_o'} = \frac{K_1 \frac{P}{P_s}}{\left(1 + K_1 \frac{P}{P_s} - K_2 \frac{P}{P_s}\right)} \quad (2.4)$$

$$\frac{n_2^{exp}}{n_o'} = \frac{K_1 K_2 \left(\frac{P}{P_s}\right)^2}{\left(1 + K_1 \frac{P}{P_s} - K_2 \frac{P}{P_s}\right)\left(1 - K_2 \frac{P}{P_s}\right)} \quad (2.5)$$

where n_1^{exp} and n_2^{exp} are the adsorption capacities of the primary and secondary sites, correspondingly. The constants K_1 and K_2 are related to the adsorption energies at the primary and secondary sites. Primary sites such as carboxyl and hydroxyl groups exhibit high binding energies, whereas secondary sites display lower binding energies (Švábová et al., 2011).

2.9.4 Dubinin Radushkevich

The Dubinin Radushkevich (D-R) model describes the physical adsorption of gasses on microporous solids and is based on a micropore-filling mechanism rather than a surface adsorption mechanism as proposed by the previous models (Gil & Grange, 1996). This theory forms the basis for many other equations which are currently used to describe adsorption equilibrium in microporous solids (Do, 1998). Micropore adsorption is completely different from adsorption on the surface of large pores mainly due to the comparable difference between the pore dimension and the dimension of the adsorbate molecule. The Dubinin Radushkevich model is illustrated by Equation 2.6 (Do, 1998);

$$n^{exp} = n_0' \exp\left\{-\left[K \ln\left(\frac{P_s}{P}\right)\right]^n\right\} \quad (2.6)$$

where K is an affinity coefficient between the adsorbate and the adsorbent and n is an exponent related to the heterogeneity of the solid adsorbent. For this particular model n'_o represents the micropore capacity.

2.10 Summary

This chapter reviewed the most recent published literature concerning the field of moisture adsorption and desorption on coal as well as the most relevant properties influencing the behaviour of moisture associated with coal. Chapter 2 concluded with an investigation into the appropriate models that could be used to describe the moisture adsorption mechanism on coal. It was evident from this extensive literature survey that moisture adsorption and desorption on a diverse amount of coal types have been studied in detail over the past decades. However, no literature could be found regarding the effect of clay minerals, more specifically kaolinite, on the moisture adsorption and desorption behaviour of South African coal. In addition, little information could be found reporting the effects of different coal properties and temperature on the moisture adsorption and desorption behaviour of South African coal. The objectives stated in Chapter 1 will aim to address these shortcomings.

CHAPTER 3:

COAL CHARACTERISATION TECHNIQUES AND APPARATUS

3.1 Introduction

Coal is highly heterogeneous in nature and to better understand and relate the moisture adsorption and desorption properties to fundamental coal characteristics, a detailed characterisation was conducted. This chapter covers a description of the origin of the coal samples as well as the methods and techniques used for the coal characterisation. Section 3.2 furnishes a short description regarding the origin of the coal samples. Section 3.3 begins with a summary of all the characterisation techniques used in this study, followed by an overview of each of the techniques and the relevant apparatus implemented.

3.2 Origin of coal samples

Five coal samples from three different collieries in the major coalfields of South Africa were chosen for this study. According to the literature the major coalfields were identified as the Waterberg, Witbank-Middelburg, Free State (Sasolburg-Vereeniging) and Limpopo regions (Jeffrey, 2005).

The Sasolburg-Vereeniging coalfield in the Free State province is an important supplier of coal necessary for power generation. Free Sate coal is generally of poor quality associated with high levels of inherent moisture and ash content (Peatfield, 2003). Coal C originated from the Free State coalfield.

Coal samples (B1 export, B2 middlings, B2 discard) from the Witbank colliery were taken from three different sampling points, that is, the middlings, export and discard sections so as to ensure a variation in ash content while keeping the coal rank constant, since the literature reviewed in Section 2.7.2 recognises that coal rank is expected to have a major influence on the moisture adsorption properties of a specific coal (Mahajan & Walker, 1971; McCutcheon et al*.,* 2003). Analyses of the export sample will furthermore yield better insight into the moisture adsorption properties of coal that will be transported for more than 500 kilometres to the Richards Bay coal terminal. The middlings produced by the plant is sent to the nearby

Kendal power station for power generation. This plant in particular is also becoming one of the largest throughput capacity plants in the Witbank coalfield (Cresswell, 2006).

Coal A originated from the Limpopo province, from a colliery situated 140km east of Musina which produces premium hard coking coal for Mittal Steel works in Vanderbijlpark. It must be noted that coal A is ROM, and consequently will contain a high amount of minerals. After further beneficiation coal A will be more suitable to use as a coking coal however in this dissertation the influence of minerals on moisture adsorption was the focus therefore the choice to use the coal before beneficiation (ROM) to highlight the influence of minerals.

All the coal samples selected cover a broad spectrum of South African coal and will provide interesting and valuable insight into the moisture adsorption and desorption properties of typical South African coal utilised in several different utilisation processes.

3.3 Coal characterisation analysis

A summary of the all the different analyses conducted on the five coal samples is presented in Table 3.1 together with the laboratories that were responsible for the analysis.

Table 3.1: Characterisation analyses performed on the five coal samples.

Analyses	Property	Laboratory responsible
Chemical	Proximate	Advanced Coal Technology
	Ultimate	Advanced Coal Technology
	Total sulphur	Advanced Coal Technology
Mineralogical	XRF (Ash analysis)	Advanced Coal Technology
	QEMSCAN	ESKOM
Petrographic	Maceral	Advanced Coal Technology
	Vitrinite reflectance	Advanced Coal Technology
Structural	Mercury intrusion	North-West University
	Mercury density(submersion)	North-West University
	BET (CO_2, N_2)	North-West University

3.3.1 Chemical analyses

The chemical analyses conducted on the coal samples were outsourced to Advanced Coal Technology (Pty) Ltd. Table 3.2 gives a summary of all the chemical analyses, including the type of analyses and relevant ISO standards used.

Table 3.2: Chemical analyses methods.

Analysis	ISO standard
Proximate	
Moisture content	SANS 5925: 2007
Volatile matter	SABS ISO 562 ; 1998
Ash content	SABS ISO 1171: 1997
Fixed carbon	By difference
Ultimate	
Carbon/hydrogen/nitrogen	ISO 12902
Total sulphur	ISO 19579
Oxygen	By difference

In the proximate analysis four constituents were established, that is, moisture, ash, volatile matter and fixed carbon content. The moisture determined in the proximate analysis is the air dried moisture; the ash is the inorganic residue remaining after combustion; the volatile matter is the part of the coal that can be driven off as gases and condensable liquids on heating to a high temperature; and fixed carbon is the non- volatile part of the coal remaining after the determination of moisture, volatile matter and ash. Fixed-carbon values, corrected to a dry, mineral matter free basis, are used as parameters in the coal classification system (ASTM D-388). The moisture, ash and volatile matter are determined analytically whereas the fixed carbon is then determined by difference (Speight, 2005).

The ash calculated in the proximate analysis should not be confused with mineral matter, which is composed of unaltered inorganic minerals in coal. The amount of ash calculated can be more than, equal to, or less than the amount of minerals in the coal, depending on the nature of the minerals in the coal and the chemical changes that took place during the incineration. Some of the changes that occur include loss of water from silicate minerals, loss of carbon dioxide from carbonate minerals, oxidation of iron pyrite to iron oxide and fixation of oxides of sulphur by bases such as calcium and magnesium (Speight, 2005).

The Ultimate analysis of coal involves the determination of the weight percent carbon, hydrogen, nitrogen, sulphur and oxygen contained in the coal (usually determined by difference). The carbon determination includes carbon present as organic carbon occurring in the coal substance and any carbon present as mineral carbonate (Speight, 2005). All of

the nitrogen is assumed to occur within the organic matrix of the coal. The hydrogen determined in the ultimate analysis includes hydrogen present in the organic materials as well as hydrogen in the water associated with the coal. Sulphur occurs as organic sulphur compounds, as organic sulphides or inorganic sulphides. The sulphur value presented in the ultimate analysis may include, depending on prior methods of cleaning, organic and inorganic sulphur (Speight, 2005).

Oxygen occurs both in the organic and inorganic portions of the coal. Oxygen is present in the organic fraction of the coal as hydroxyl groups, phenol groups, carboxyl groups, methoxyl groups and carbonyl groups. The inorganic fraction containing oxygen includes various forms of moisture, silicates, carbonates, oxides and sulphates. Oxygen in the ultimate analysis is calculated by deducting from 100.0 the sum of the percentages of moisture, ash, carbon, hydrogen, nitrogen and sulphur. The result of this method for calculating oxygen is the accumulation of all the experimental errors involved in determining the constituents forming part of this calculation (Speight, 2005).

3.3.2 Mineral analysis

The mode of occurrence and concentration of mineral matter varies considerably for different coals; consequently the determination of the mineral matter content and elemental analysis provide important parameters for the assessment of a specific coal. The mineral analysis for this study comprised of QEMSCAN and X-ray fluorescence (XRF). QEMSCAN is an advanced analytical technique that provides an accurate method to determine the mineral and organic matter association quantitatively on a particle by particle basis (Liu et al, 2005). XRF analysis, in accordance with the ASTM D4326 standard, was used to determine the elemental composition of the coal ash samples.

The Parr formula is regularly used to assess the proportion of mineral matter in coal using data from ashing techniques. In the Parr formula, the mineral matter content is derived from the expression:

$$\text{Mineral matter (\% w/w)} = 1.08A + 0.55S \quad (3.1)$$

where A is the percentage ash in the coal an S the total sulphur in the coal (Speight, 2005). The first term in the formula is a correction for the loss in weight due to the elimination of water in the decomposition of clay minerals at elevated temperatures. The second term in the formula is a correction for the loss in weight when pyrite burns to ferric oxide.

3.3.2.1 XRF

The XRF analysis for all five of the coal samples were carried out by the laboratories of Advanced Coal Technology (ACT). Initially the coal samples were pulverised and mixed thoroughly to ensure a homogeneous mixture. The samples were then ignited at 815°C for one hour after which one gram of oxidising agent (ammonium nitrate) was added to one gram of sample. The sample was then transferred into a platinum crucible and fused in a semi-automated fusion machine at approximately 1000°C, after which the molten sample was poured into a platinum mould where the cooled sample formed a glass bead. Finally, the glass bead was subjected to testing with Thermo Fisher instruments, calibrated for approximately 15 elements using various certified standards. The XRF analysis was conducted in accordance with the ASTM D4326 standard.

3.3.2.2 QEMSCAN

The coal samples for the QEMSCAN analysis were outsourced to the Research and Development department of Eskom. Samples were prepared by mixing the coal with molten carnauba wax and placing it in a 30 mm mould allowing the mixture to cure. This solid block was then polished to expose the individual particles in a cross section. A scanning electron microscope electron beam was positioned at predefined points across a particle and at each point a 7 millisecond 1000 count X-ray spectrum was acquired. The elemental proportions were then used to identify the mineral/amorphous phases present at each point. Mineral proportions were determined by dividing the number of analytical points for each phase by the total number of analysed points.

3.3.3 Petrographic analyses

The main field of coal petrology is coal microscopy, (Stach et al., 1982). Microscopic analysis provides valuable information regarding the organic and inorganic constituents in coal as well as the degree of metamorphism of these constituents.

Maceral analyses define the relative reactive and inert constituents of coal. For the maceral analysis a representative sample was used to prepare a polished block of coal. The block was then microscopically examined under reflective light where the maceral groups were identified in an immersion medium according to their relative reflectance, colour, size and morphology. The ISO standard 7404-3 (1994) technique of point counting was used, creating transverses across a polished block. By inspecting the petrographic block under

binocular reflected light microscopes, the type of maceral lying at the interception of the crossed lines could then be identified.

Vitrinite reflectance is the property normally used to determine coal rank independent of the maceral composition. Vitrinite reflectance is used as a parameter of coal rank since it is the most abundant maceral in most coal types and is principally responsible for many technological processes. The occurrence of these macerals is more abundant in coal particles as opposed to other macerals and it also increases with increasing rank (Pusz, 2002). Vitrinite random reflectance measurements were conducted in accordance to the ISO standard 7404-5 (1994) to determine coal rank. Table 3.3 illustrates the criteria to classify different coals according to vitrinite reflectance (Falcon & Snyman, 1986).

Table 3.3: Coal classification using vitrinite reflection.

Coal rank			Vitrinite reflectance		Vitrinite Color
			% RoV Random	*% RoV* max	
Low	Peat		0-0.3	1.7	Dark grey
	Lignite		0.3-0.4	1.7	Dark grey
	Sub-Bituminous		0.4-0.5	1.7	Dark to medium grey
Medium	Bituminous	HVB	0.5-1.1	1.7	Dark to medium grey
		MVB	1.1-1.6	1.7	Medium grey
		LVB	1.6-2	1.7-2.2	Pale grey
High	Anthracite	Semi-Anthracite	2-2.5	2.2-2.8	White
		Anthracite	2.5-3.5	2.8-4	White
		Meta-Anthracite	>3.5	4-10	Whiter than inertinite
	Graphite		>3.5	10-18	Crystallised

The %RoVis defined as the random percentage reflectance of vitrinite and the %RoV maximum is defined as the maximum percentage reflectance of vitrinite (Falcon & Snyman, 1986).

The rank classification of South African coals, based on vitrinite reflectance and reactives content in accordance with ISO 11760, 2005 can be seen in Table 3.4 (ISO 11760, 2005 and Falcon, 1986[a]).

Table 3.4: Rank classification of South African coals.

Rank	$\%R_0V_{Mr}$	% Total Reactives	Description
Lignite	X<0.4		Lowest rank of coal
Sub-Bituminous	0.4<X<0.5	20<Y<100	High volatile bituminous coal
Bituminous	0.5<X<2	20<Y<100	Medium to low volatile bituminous coal
Anthracite	2<X<4.6	20<Y<100	Highest rank coal

The amount of light reflected from the surface of vitrinite is directly related to the changes in carbon and volatile matter content with rank- the higher the reflectance, the higher the carbon content. Therefore, the rank of a specific coal can be directly determined by measuring the reflectance of vitrinite (Falcon & Snyman, 1986).

The total mineral matter may be point counted or calculated from ash and sulfur contents in accordance to test methods ASTM D3174 and ASTM D3177. The percent of mineral matter calculated from the Parr formula (1.08 ash % + 0.55 sulfur %, dry basis) on a weight basis can be converted to a volume basis using a density of 2.8 g/cm^3 for mineral matter and 1.35 g/cm^3 for organic components, unless more specific information regarding density is available (ASTM 3177). The following formula can be used to calculate the mineral matter (vol. %);

$$\boldsymbol{MM = \frac{100\left[\frac{(1.08A + 0.55S)}{2}.8\right]}{\frac{[100 - (1.08A + 0.55S)]}{1.35} + \frac{(1.08A + 0.55S)}{2}.8}} \qquad (3.2)$$

3.3.4 Structural analyses

Numerous techniques exist to better understand and distinguish between the different pore sizes that define the intricate pore network of a coal structure (Toda et al., 1971; Thomas & Damberger, 1976; Clarkson & Bustin, 1999). A clear understanding of the pore network for

each coal sample will give valuable insight into the moisture adsorption mechanisms involved in this study.

Some of the techniques applied in this study to characterise structural coal composition include mercury porosimetry, mercury submersion, CO_2 as well as N_2 BET. These methods are explained in the following paragraphs.

3.3.4.1 Mercury porosimetry

Mercury porosimetry is a useful and convenient characterisation technique for porous materials, especially coal (Clarkson & Bustin, 1999). This technique is based on the principle of a non-reactive liquid, which does not wet the surface of the coal particle or penetrate its pores until a specific pressure is applied to force the liquid into the pores (Thomas & Damberger, 1976). The ratio between the applied pressure and the pore sizes are defined by the Washburn equation, the higher the pressure the smaller are the pores into which the liquid can intrude. It provides a wide range of information including pore size distribution, skeletal and apparent density, porosity and the specific area of a sample.

The apparatus used for the mercury porosimetry is the AutoPore IV 9500 system which is depicted in Figure 3.1.

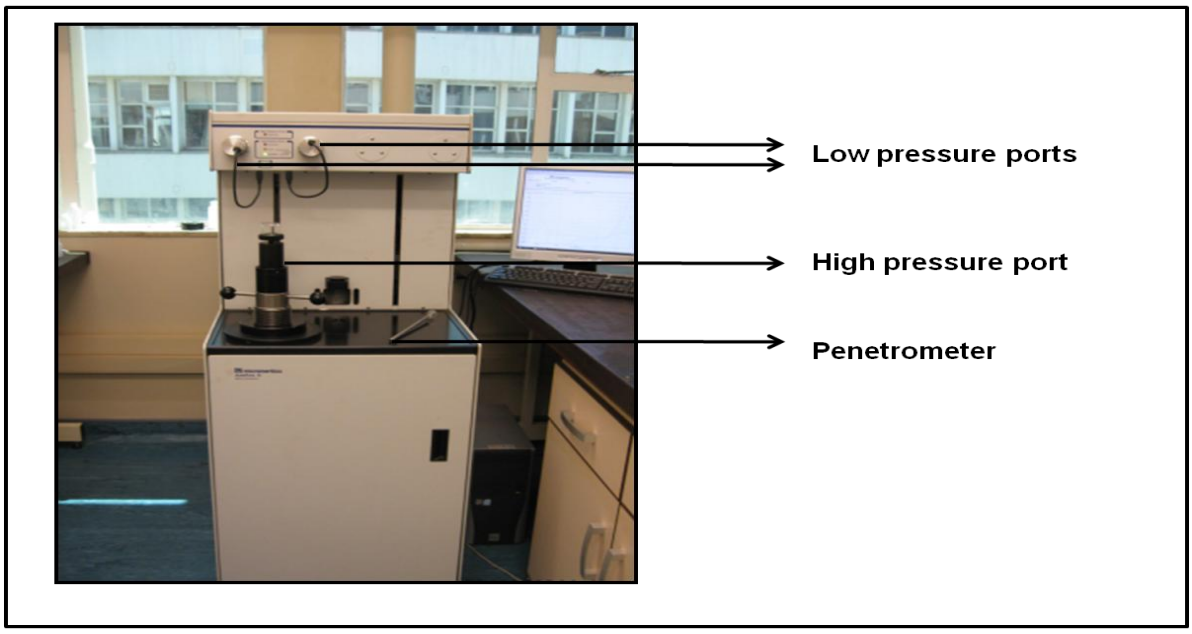

Figure 3.1: Micromeritics AuotoPore IV analyser.

Coal particles of a mean particle size of 5 mm were used. The coal particles were dried over night at 100°C to remove any excess moisture from the external surface and pores of the coal particles. A penetrometer with a stem volume of 0.392 cm3 was used for all the

intrusion measurements. The samples were loaded to obtain a used stem volume of between 60 and 90% under high pressure intrusion. Mercury was intruded at a contact angle of 130° while a surface tension of 0.0485 kPa.cm was used.

The low pressure part of the experiment is to determine the bulk (true) density of the specific coal. The penetrometer, containing the sample, was connected to the low pressure port where it was evacuated to a pressure of 50 µmHg for 5 minutes where after the mercury was introduced to a filling pressure of 3.59 kPa. The mercury filled penetrometer was then placed in the high pressure section of the machine where the mercury was intruded at pressures ranging from 0.69 kPa and 413.7 MPa. The amount of mercury filling the pores at each pressure could then be determined very accurately and related to the structural parameters of the coal such as total porosity and skeletal density.

.

3.3.4.2 Mercury submersion density measurements

The bulk densities calculated for each sample plays an important role in estimating the porosities of the micro- and meso-pore ranges determined by the CO_2 and N_2 BET adsorption analysis respectively. Due to this important fact it was decided to use an additional experimental method to determine the bulk densities of the coal samples. It was also interesting to see how the bulk densities calculated from mercury porosimetry (intrusive method) and mercury submersion (non-intrusive method) experiments correlated.

A mercury density method was used to determine the bulk density of a specific particle. The advantage of this method above the mercury porosimetry for determining bulk density is that individual particles can be tested without destroying or damaging the particles. A specific particle can then be used for further characterisation, thus ensuring that there is as little as possible variations in the results obtained between methods used to characterise the coal particles. Particles of up to 60 mm can be individually tested with the mercury density method. A diagram of the apparatus can be seen in Figure 3.2.

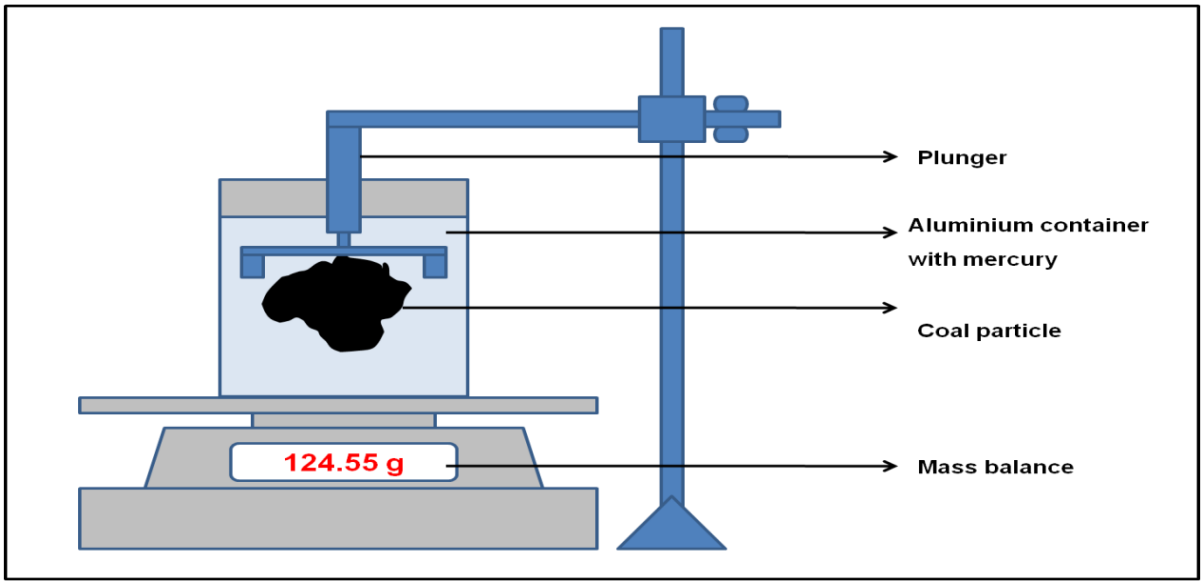

Figure 3.2: Mercury submersion apparatus.

3.3.4.3 BET

A Micromeritics ASAP 2010 analyser was used to perform the N_2 and CO_2 gas adsorption analyses on all five coal samples. The apparatus can be viewed in Figure 3.3.

Figure 3.3: Micromeritics ASAP BET unit.

A 0.2 gram sample with a mean particle size of 212 µm was prepared and placed overnight in a vacuum oven at 105 °C to remove excess moisture and placed in a sample tube in the degas port. A funnel was used to ensure that the particles did adhere to the sides of the sample tube. The sample was then degassed for 48 hours at 25˚C and 4µmmHg. After

degassing, the sample was placed in the analysis port to start the adsorption analysis. A specific cooling medium, ice water and liquid nitrogen, was used for the CO_2 and N_2 analysis correspondingly to control the temperatures at 273.15K and 77.35K.

3.3.4.4 SEM

Scanning Electron Microscope (SEM) analysis was done on all five coal samples using a FEI Quanta 200 ESEM microscope with an integrated Inca 400 EDS system. The SEM is equipped with an Energy Dispersive Spectrometer (EDS). The samples were prepared by grinding the raw coal to a particle size of 125 µm. A sample casing was prepared by applying two sided carbon tape to it. The sample casing was then pressed onto the finely ground coal sample resulting in a single layer of coal particles adhering to the sample casing. The prepared sample casing containing the single layer of coal particles was then mounted on a microscope plate where an appropriate degree of magnification was chosen. A Backscattered Electron Image (BSI) was then obtained which allowed for the evaluation of the elemental composition of the coal by means of image processing procedures. Image regions containing elements of high average atomic numbers will appear bright relative to regions containing elements with lower atomic numbers.

3.4 Summary

Chapter 3 covers all the equipment used and procedures followed to characterise the coal samples investigated in this study. The characterisation results obtained by applying the methods and equipment discussed in this chapter are presented in Chapter 4.

CHAPTER 4:

RESULTS AND DISCUSSION: COAL CHARACTERSATION

4.1 Introduction

In this chapter all the coal characterisation results are reviewed and discussed. In Section 4.2, the results obtained from the chemical analyses are presented followed by the mineral analysis and petrographic analysis in Sections 4.3 and 4.4 respectively. The structural analysis conducted on the five coal samples is evaluated in Section 4.5. Section 4.6 concludes with an overall summary of the characterisation results.

4.2 Chemical analyses

Results obtained for the proximate and ultimate analyses conducted on all five coal samples are presented in Sections 4.2.1 and 4.2.2 respectively.

4.2.1 Proximate analysis

The proximate analysis of coal evaluates the moisture, ash, volatile matter and fixed carbon content according to the series of standard test methods listed in Section 3.3.1. The results obtained from the proximate analysis can be seen in Table 4.1.

Table 4.1: Proximate analysis.

	A	B1	B2	B3	C
Moisture %	0.60	2.60	2.20	1.20	3.90
Ash content %	50.10	14.90	31.60	63.5	34.10
Volatile matter %	13.80	26.20	20.60	18.20	20.60
Fixed carbon %	35.50	56.30	45.60	17.10	41.40

*Air dried basis, percentages reported as wt. %

According to the characterisation results in Table 4.1 all the coal samples excluding coal B1, which is beneficiated specifically for the export market, can be regarded as high ash coals. The very high level of ash (63.5%) along with the low fixed carbon content (17%) in coal B3 is expected as it is not further utilised and is sent to the discard heaps. Due to the high ash content in coal B3, it represents more a coaly shale than coal in other words, it is no more a coal *per se*.

Unsworth *et al.,* (1989) included a South African coal their study and the values obtained in the proximate analysis for this coal revealed an ash content of 15.5% (d.b) which closely resembles the ash content (14.9% d.b) of coal B1. Coal C contained a distinctly higher amount of moisture when compared to the other four coal samples and correlated very well with results found by Waanders et al., (2003), who conducted a study on this specific coal. A clear variation in the ash contents of coals B1 (14.9%), B2 (31.6%) and B3 (63.5%) can be observed from the results in Table 4.1. This variance in ash content suggests a variance in mineral matter and therefore supports the aim of this investigation regarding the influence of mineral matter on the moisture adsorption properties of these coal samples. The variance in ash content also validates further investigation into the mineral matter properties with advanced characterisation techniques. It should be noted that the ash percentage is not a direct measure of the total mineral matter content of the coal.

4.2.2 Ultimate analysis

The ultimate analysis data is presented in Table 4.2. The carbon, hydrogen oxygen and total sulphur content for each coal sample is reported in this table.

Table 4.2: Ultimate analysis.

	A	B1	B2	B3	C
Carbon content %	87.36	83.85	80.80	62.46	78.53
Hydrogen content %	5.62	4.82	4.95	5.47	5.16
Nitrogen content %	2.02	1.94	1.83	1.59	2.05
Oxygen content % *(By difference)	4.14	8.98	11.68	10.68	14.03
Total sulphur %	0.85	0.4	0.73	19.83	0.23

*Dry, ash free basis, percentages reported as wt. %

From Table 4.2 a great difference in the oxygen content can be observed. Coals B and C contained a significant amount of oxygen compared to coal A, but it must be kept in mind that the oxygen was calculated by difference. Oxygen content is an important indicator of the availability of primary sites for moisture adsorption (McCutcheon et al., 2003). The oxygen containing functional groups on the coal surface may be considered to be the most likely place for moisture adsorption to take place compared to other groups (Nishino, 2000). Coal B1 was rich in carbon, 83.85% (d.a.f), and low in sulphur, 0.4%, making it ideal for the export market where it can be used for coal conversion processes. The values reported in the ultimate analysis for coal B1 correlated very well with values obtained by Unsworth et al., (1989). They reported a carbon content of 83.8% (d.a.f), hydrogen content of 4.6% (d.a.f) and oxygen content by difference of 9.2% (d.a.f).

The carbon content decreased from coal A to coal B1 to coal B2 to coal C to coal B3.

4.3 Mineral analysis

The mineral analysis performed on all five coal samples investigated in this study included XRF and QEMSCAN analysis. The results obtained from this analysis are included in Sections 4.3.1 and 4.3.2.

4.3.1 XRF

The ash composition analysis results can be viewed In Table 4.3 for coal A, B1, B2, B3 as well as coal C.

Table 4.3: Ash composition (XRF) analysis of coal samples.

Inorganic species	A	B1	B2	B3	C
Al_2O_3 %	24.61	28.93	30.35	21.36	32.19
SiO_2 %	66.65	49.46	56.65	42.58	51.50
CaO %	0.97	8.86	3.55	4.49	7.87
Fe_2O_3 %	2.71	1.81	2.61	22.38	2.37
K_2O %	2.45	0.49	0.54	0.70	0.48
MgO %	0.53	1.32	0.75	1.44	0.71
Na_2O %	0.32	0.04	0.04	0.05	0.38
V_2O_5 %	0.16	1.61	0.28	0.22	0.1
TiO_2 %	0.95	2.02	2.13	1.18	1.80
SO_3 %	0.68	4.21	2.89	6.04	1.85
Other %	0.25	1.25	0.27	0.36	0.39
Total	100	100	100	100	100

*(All percentages are reported as wt. %)

The results in Table 4.3 indicate that the ash composition was rich in Al_2O_3 and SiO_2, which corresponded to the presence ofhigh levels of quartz and kaolinite in the coal. It can be observed that the bulk of the ash for each of the five coal samples consisted of SiO_2 which is derived from quarts and clay minerals, such as kaolinite, K-bearing aluminosilicates and montmorillonite (Saikia & Ninomiya, 2011; Van Dyk & Keyser, 2005; Spears, 2000). The second largest contributor to the ash was Al_2O_3 which corresponded to the presence of elevated amounts of clay minerals (Saikia & Ninomiya, 2011). Fe_2O_3 can be related to the pyrite present in the coal samples. A significant fraction of the ash also contained SO_3 indicating the presence of sulphur bearing species (Saikia & Ninomiya, 2011).

4.3.2 QEMSCAN

QEMSCAN analysis provides valuable and accurate information regarding the amount of minerals present in coal samples, more so than XRF analysis, making it more applicable to determine the amount of moisture adsorbed for a specific mineral on a qualitative basis. The QEMSCAN analysis performed on all five coal samples is summarised in Table 4.4.

Table 4.4: Mineral composition of the coal samples according to QEMSCAN analysis

Mineral	A	B1	B2	B3	C
Gibbsite	-	0.53	0.26	0.51	0.26
Pyrite	2.5	0.53	2.32	28.17	0.52
Siderite	5.34	1.60	3.35	9.26	1.04
Calcite	3.51	13.83	10.31	3.42	23.38
Dolomite	2.00	12.23	6.44	4.18	3.64
Apatite	0.17	4.79	1.29	0.25	0.26
Kaolinite	46	46.8	48.2	34.26	54.29
Quartz	17.7	15.43	22.68	13.32	12.47
Illite	7.18	1.06	1.29	1.27	0.78
Muscovite	8.51	1.06	1.29	1.52	1.04
Microcline	6.34	-	0.77	1.90	0.52
Rutile	0.33	1.06	0.77	0.38	1.04
Other	0.5	1.06	1.03	1.65	1.01
Total	100	100	100	100	100

*(All percentages are reported as wt. %, mineral matter basis)

In Table 4.4 it is evident that the main contribution to the minerals in the coal samples stemmed from kaolinite and quartz, varying from 47.46% wt. for coal B3 to 70.88% wt. for coal B2, which is in line with the results obtained from the XRF analysis presented in Table 4.3. Kaolinite found in the coal samples varied between 54% wt. and 34% wt. and quartz between 22 wt. % and 12 wt. %. Muscovite, also a clay mineral, was present in relatively low concentrations in coals B and C, varying between 1% wt. and 1.5% wt. but was more noticeably present in coal A which contained 8.5% wt. According to Pinetown & Boer

(2006), the Witbank coalfield clay mineral composition is on average similar to Australian coal, but with less expandable clays like illite-smectite and montmorillonite. This was also observed for the coal samples originating from the Witbank coalfield (B1, B2 and B3) investigated in this study, with illite only present in small amounts, varying from 1.06 wt. % to 1.29 wt. % and also, with no observance of montmorillonite. Gaigher (1980) found a correlation that suggested that higher ranked coal contains more illite and less kaolinite compared to lower ranked coal (carbon content<82% d.a.f.). The same correlation could be seen from the QEMSCAN data with higher ranked coal A (87.36% C, d.a.f.), consisting of more illite and less kaolinite than the lower ranked coal C (78.53% C, d.a.f.). The high levels of pyrite present in coal B3 discard also fell in line with the results from the XRF analysis.

The QEMSCAN predicted ash % was based on determining the total mineral matter content in the coal. The mineral derived volatiles were calculated and subtracted from the total mineral matter content. The predicted ash content can be seen in Table 4.5.

Table 4.5: Mineral matter-ash reconciliation

	A	B1	B2	B3	C
Mineral matter	59.9	18.8	38.8	78.0	38.5
Mineral volatiles	8.2	3.7	6.7	21.5	7.8
Predicted Ash %	51.7	15.1	32.1	57.3	30.6

*(All percentages are reported as wt. %)

The predicted QEMSCAN ash% presented in Table 4.5 showed that coal B3 contained the highest amount of predicted ash (57.3%), followed by coal A (51.7%), B2 (32.1%) and C (30.6%). Coal B1 contained the least amount of predicted ash (15.1%).

A comparison of the ash content results obtained from the proximate analysis presented in Table 4.1, the QEMSCAN predicted ash content presented in Table 4.5 and the minerals content calculated by Parr's formula (Section 3.3.2) is illustrated in Table 4.6.

Table 4.6: Comparison of Ash content for all five coal samples as determined by different methods.

	A	B1	B2	B3	C
Ash % from Proximate analysis	50.1	14.9	31.6	63.5	34.1
QEMSCAN predicted Ash %	51.7	15.1	32.1	57.3	30.6
Minerals % Parr's formula	54.3	16.3	34.4	72.4	36.9

*(All percentages are reported as wt. %)

When comparing the results obtained for the ash content in each coal it can be seen that the values calculated in the proximate analysis and the values calculated by QEMSCAN are closely related. The results obtained from Parr's formula were also in line with the results from the proximate and QEMSCAN analysis. The minerals % calculated by Parr's formula was slightly higher than the values calculated by the proximate analysis for all five coal samples. This was expected since the formula indicated that the total sulphur is added to the ash calculated in the proximate analysis. When comparing the minerals % obtained from QEMSCAN analysis presented in Table 4.5 and the minerals % obtained from Parr's formula Table 4.6 it can be seen that the values from QEMSCAN was higher that the values for Parr's formula which was expected due to the different techniques of analysis. Parr's formula was only an approximation based on the ash content and the total sulphur in the coal whereas; QEMSCAN analysis determined the amount of minerals present in the coal qualitatively. The lower values observed for minerals% for Parr's formula in comparison to QEMSCAN analysis could also be due to chemical changes that took place during incineration as discussed in Section 3.3.1 for the proximate analysis.

The fact that these values were closely related shows that the analyses methods used can be compared and that the analyses conducted were reliable. QEMSCAN analysis was also chosen to qualitatively determine the amount of minerals present in each of the five coals studied in this dissertation.

4.4 Petrographic analyses

The petrographic analysis of all five coal samples are summarised in Table 4.7 and include the volume percentages for vitrinite, liptinite (exinite), inertinite and visible minerals present

in each coal. The minerals% reported in Table 4.7 were calculated from Parr's formula as discussed in Section 3.3.3. The inertinite reported in the table below consists of reactive semifusinite, inert-semifusinite, fusinite, secretinite and micrinite.

Table 4.7: Petrographic analysis of the coal macerals.

Maceral composition	A	B1	B2	B3	C
Vitrinite %	45.3	20.3	8.8	12.2	14.5
Liptinite %	0	4	1.2	0.2	1.5
Inertinite %	27.4	67.3	72.4	50.9	64.8
Minerals %	27.3	8.4	17.6	36.7	19.2

*(All percentages are reported as vol. %, m.m.b)

The maceral analysis results determined by point count analysis in Table 4.7 clearly indicated that coals B and C were inertinite rich, which is distinctive of South African coal originating from the Free State and Witbank coalfields (Mangena & de Korte, 2004). The inertinite contents of these samples were well over 50% (m.m.b). Coal A was rich in vitrinite, containing 45% vitrinite (m.m.b). The inertinite rich coal samples contained the highest amounts of oxygen, ranging between 8 and 14%, whereas the vitrinite rich coal A only contained 4% oxygen. All of the coal samples also contained a substantial amount of visible minerals, with coal B1 containing the least. The minerals% results presented in the table above were calculated in accordance to Parr's formula based on vol. % (ASTM 3177).

A mean random reflectance analysis was done according to the SABS ISO 7404 (1994) classification and can be viewed in Table 4.8.

Table 4.8: Coal vitrinite random reflectance data.

Vitrinite reflectance	A	B1	C
Rv_{max} %	1.36	0.71	0.79

*(All percentages are reported as vol. %)

The mean random reflectance results for coal A was the highest at 1.36, followed by coal B1 and C having reflectance values of 0.71 and 0.79 respectively. Coal A could be characterised as medium bituminous rank B and coals B and C as medium bituminous rank C. The mean random reflectance analysis was only done for three coal samples as coals B1, B2 and B3 were sampled from the same colliery at the same time, only from different sampling points. Therefore, it could be assumed that they were of the same rank and consequently the analysis was only conducted for sample B1. Mangena et al., (2004) obtained very similar petrographic results for coal originating from the Witbank coalfield.

4.5 Structural analyses

The structural analyses conducted on all five coal samples were mercury porosimetry, mercury submersion, CO_2 and N_2 BET. Information regarding the pore structure and densities of the coal samples could be obtained from these analyses. Characterising the coal pore structure with different gasses was very complex and the size of the gas molecules as well as their relationship with the coal structure had to be taken in consideration (Rodrigues & de Sousa, 2002).

4.5.1 Mercury porosimetry

Mercury porosimetry analysis was performed on all five coal samples to assess coal properties such as bulk- and skeletal densities as well as porosity. Macropore properties such as total macropore volume could also be estimated. The results are displayed in Table 4.9.

Table 4.9: Mercury porosimetry.

	A	B1	B2	B3	C
Total macro pore volume (cm^3/g)	0.039 ±0.002	0.041± 0.004	0.032 ± 0.01	0.023 ± 0.01	0.065 ± 0.02
Pore area (m^2/g)	15.41 ± 1.16	17.73 ± 2.45	12.61 ± 1.29	6.31 ± 2.31	23.20 ± 5.11
Average pore diameter (nm)	11.90 ± 0.35	9.30 ± 0.53	10.30 ± 1.62	13.50 ± 3.2	11.50 ± 0.95
Bulk density (kg/m^3)	1366 ± 12.47	1430 ± 54.10	1639 ± 72.02	1992 ± 230	1624 ± 220
Skeletal density (kg/m^3)	1456 ± 15.72	1519 ± 55.43	1731 ± 55.6	2091 ± 212	1817 ± 214
Porosity %	6.20 ± 0.26	5.90 ± 0.38	5.40 ± 1.10	3.90 ± 0.70	10.70 ± 1.75

It is apparent from the results obtained by mercury porosimetry that coal C had the largest macro-pore volume, pore area and porosity in comparison with the other four coals. The % porosity of coal C is 10.70 and is significantly higher than for coal A with a % porosity of 6.20. The % porosity of coal A (6.20), B1 (5.90) and B2 (5.40) did not vary significantly. Coal A contained more vitrinite (45.3 vol. %) than coal B1 (20.3 vol. %) and B2 (8.8 vol. %). According to Gan et al., (1972), porosity was related to maceral composition. Vitrinite predominantly contains microporous contents, while inertinite mainly contains meso- and macroporous contents. It was therefore expected that the macro-porosity of coal A will be lower due to its high vitrinite content. This was, however, not the case and it could most likely be attributed to the high amount of impurities present in coal A (50 wt. %), which diluted the presence of vitrinite and therefore, the % macro-porosity of these coal samples (A, B1, B2) did not vary considerably. There was also no significant difference in total macro-pore volume for coals A, B1 and B2.

When comparing the bulk densities of coals B1, B2 and B3, a clear trend was evident in the data, in particular, when comparing these to the pyrite content obtained from the XRF as well as the QEMSCAN analysis. Coal B3 possessed the highest bulk density (2091 kg/m^3) as well as the highest pyrite concentration, whereas coal B1 had the lowest bulk density (1430

kg/m^3) and also the lowest amount of pyrite. Coal B2 had an intermediate bulk density of 1639 kg/m^3 and an intermediate amount of pyrite. This difference in densities could be ascribed to the variation in mineral matter content due to the different beneficiation steps the samples were subjected to on the plant. The heavier minerals, for example pyrite, therefore concentrated in the middlings and discard fractions and to a lesser extent in the lighter export fraction. This was however not applicable to all the minerals present in the coal samples since pyrite, for example, is extrinsic and is better beneficiated according to different densities whereas kaolinite, for instance, is far more difficult to beneficiate according to density as these minerals are intrinsically associated with coal.

It is interesting to note that coal A had both the lowest bulk density (1366 kg/m^3) as well as the lowest skeletal density (1456 kg/m^3); this could be due to the fact that this particular coal was more vitrinite rich in comparison to the other four coal samples. According to Borrego et al., (1980), the density of maceral groups may vary, with inertinite concentrating in the denser fractions and vitrinite concentrating in the lighter fractions.

4.5.2 Mercury submersion density measurements

The bulk densities determined from the mercury submersion method can be viewed in Table 4.10.

Table 4.10: Bulk densities: mercury submersion.

	A	B1	B2	B3	C
Bulk density (kg/m^3)	1450 ± 20	1486 ± 57	1626 ± 68	2211 ±200	1580 ± 220

According to the bulk density results in Table 4.10 coal B3 had the highest bulk density followed by B2 and B1. The bulk densities of coal C and A were 1580kg/m^3 and 1450 kg/m^3 respectively. There seems to be a good correlation between the bulk density results obtained from the mercury porosimetry analysis method and submersion method. Discrepancies observed in the results from both methods could be due to the different state of the samples for each individual method. Solid coal particles were used in the mercury submersion methods whereas crushed coal samples were used in the mercury porosimetry analysis method. It can therefore be used as a cheaper, more readily available method to characterise bulk densities of coal particles.

4.5.3 CO_2 and N_2 BET

Low pressure adsorption of CO_2 and N_2 gasses plays a crucial role in determining the physical properties of a specific coal. Micro and meso-pore volumes can readily be determined implementing these adsorption/ desorption techniques, (Prinz & Littke, 2005; Clarkson & Bustin, 1999; Faiz et al, 1992; Unsworth et al., 1989). CO_2 adsorption occurs in the micropore range, while N_2 adsorption measurements are usually confined to the meso-pore range. The micropore surface area and monolayer capacity was calculated with the Dubinin-Radushkevich equation. The BET and Langmuir surface areas were determined as well. The CO_2 BET results are summarized in Table 4.11.

Table 4.11: CO_2 BET.

	A	B1	B2	B3	C
Micropore surface area (m^2/g) (D-R)	87.34	48.09	120.26	73.89	155.56
Monolayer capacity (cm^3/g) (D-R)	19.13	32.41	23.32	16.17	34.05
BET surface area (m^2/g)	68.95	97.45	80.18	50.98	96.18
Langmuir surface area (m^2/g)	79.34	106.24	85.66	55.79	103.35
% Porosity (Pores <5Å)	2.06	4.20	4.04	2.93	5.01

The error associated with the determination of the different surface areas was +/-5m^2/g which indicated a good approximation of the different values. The analysis of the data presented in Table 4.11 indicates that coal C had the highest micropore surface area of 155.56 m^2/g, while B1 had the lowest micropore surface area of 48 m^2/g. The percentage micro-porosity of coal C was 5.01% followed by coal B1 and B2 with slightly lower porosities of 4.2% and 4.04% respectively. Coal A and coal B3 contained the lowest micro-porosities of 2.06% and 2.93% correspondingly.

The relationship between the CO_2 BET surface area and the mineral matter content for each coal is depicted in Table 4.12.

Table 4.12: Minerals content vs. CO_2 BET surface area.

	A	B1	B2	B3	C
CO_2 BET surface area (m^2/g)	68.95	97.45	80.18	50.98	96.18
Minerals (wt. %)	59.9	18.8	38.8	78	38.5

The mineral matter content in each coal was determined by QEMSCAN analysis, presented in Table 4.5. One of the factors that influenced the gas adsorption behaviour of coals was mineral matter content (Rodrigues et al., 2008). From the results in Table 4.12 it can be seen that coal A and coal B3 contained the highest amount of minerals, 59.9% and 78% respectively. These coals also had the lowest CO_2 BET surface areas, 68.95 m^2/g and 50.98 m^2/g respectively. Coal B1 had the lowest minerals content, 18.8%, which corresponded to the highest CO_2 BET surface, 68.95 m^2/g. Rodrigues et al., (2008) reported that clean coal fractions with the lowest ash contents had the highest capacity to store gasses. They deduced that in the absence of minerals, especially those associated with the coal matrix, there are more voids and cavities allowing the gas to adsorb into any free space available. They found that the sink fractions, mostly composed of non-porous minerals, is the fraction with the lowest available free space and hence less space for gas to be adsorbed. This was also observed for coal B3 which contained the highest amount of minerals and the lowest CO_2 BET surface area.

When comparing the surface areas obtained from the CO_2 and N_2 BET analyses it is clear that the CO_2 surface areas are far larger than surface areas determined with N_2 BET analyses. A possible explanation is that some of the pores in the coals were closed to N_2 at 77K but accessible to CO_2 at 273K (Thomas & Damberger, 1976; Amarasekera et al., 1995). Gan et al., (1972) also observed this occurrence and reported that the areas determined by the CO_2 adsorption are considered to be the closest approximation to the total surface area of a specific coal. Therefore, the surface area obtained from CO_2 adsorption should give a good estimation of the surface area available for moisture adsorption. A summary of the N_2 BET results are displayed in Table 4.13.

Table 4.13: N_2 BET results.

	A	B1	B2	B3	C
Surface area					
Single point surface area (m^2/g)	2.25	4.40	4.58	4.68	10.83
BET surface area (m^2/g)	3.54	4.78	4.79	4.85	11.2
BJH Adsorption surface area of pores 17 Å <d_{pore}<3000 Å(m^2/g)	1.81	4.17	3.73	4.812	10.85
BJH Desorption surface are of pores 17 Å <d_{pore}<3000 Å(m^2/g)	2.65	6.92	4.79	5.61	13.72
Pore volume					
Single point adsorption total pore volume (cm^3/g)	0.005	0.011	0.014	0.019	0.032
BJH Adsorption pore volume 17 Å <d_{pore}<3000 Å (cm^3/g)	0.009	0.017	0.02	0.03	0.046
BJH Desorption pore volume 17 Å <d_{pore}<3000 Å (cm^3/g)	0.01	0.018	0.021	0.031	0.047
Pore size					
Adsorption Average pore width (Å)	342.28	337.1	399.4	416.8	343.35
BJH Adsorption average pore diameter (Å)	211.02	165.4	221.2	253.9	170.39
BJH Desorption average pore diameter (Å)	151.85	107.8	179.3	223.9	138.02
Porosity					
Porosity % 17 Å <d_{pore}<1500 Å	1.1	0.9	0.85	0.5	4.8

In the table above it is evident that coal C had the largest surface area which is consistent with the trend observed from the mercury porosimetry and CO_2 BET results. The nitrogen adsorption and desorption isotherms are illustrated in Figure 4.1. According to the BDDT classification system, described in Section 2.2, the adsorption isotherms are characterised as Type I isotherms, related to plateau behaviour, whereas the desorption isotherms are classified as Type IV isotherms associated with hysteresis. A noticeable amount of hysteresis was present in the desorption isotherm of coal C and to a lesser extent present in the other four coal samples. The presence of hysteresis can be attributed to the structural heterogeneity of coal and the fact that capillary condensation takes place at certain relative pressures (Gregg & Sing, 1982).

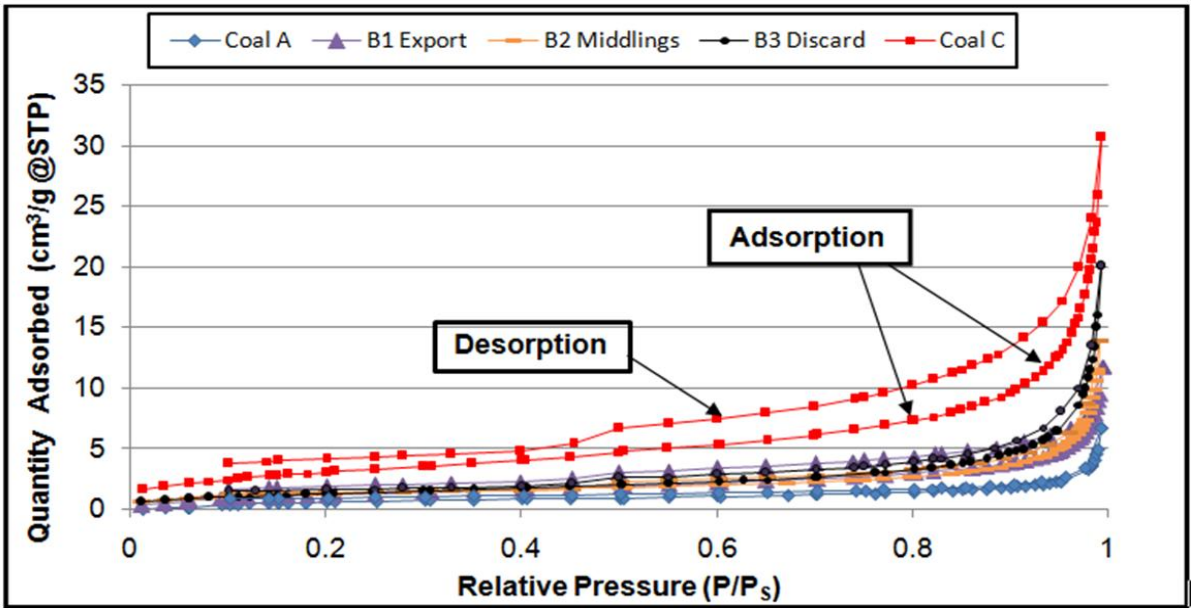

Figure 4.1: Nitrogen adsorption/desorption isotherms.

It can also be noted that there was very little hysteresis present in the vitrinite rich coal A, although it contained a significant amount of minerals.

4.5.4 SEM

Table 4.14 presents the elemental analysis of all five coal samples investigated in this study. The most prominent elements present in the coal samples were carbon, oxygen, aluminium, silicon, sulphur, iron and calcium.

Table 4.14: Elemental SEM analysis.

Element	A	B1	B2	B3	C
C	70.89	65.59	55.45	38.74	56.16
O	20.8	25.63	30.9	36.94	31.72
Mg	0.15	0.16	0.13	0.24	0.1
Al	2	1.82	3.59	4.28	3.68
Si	3.47	2.35	5.37	6.19	5.31
S	0.73	0.66	0.61	3.63	0.23
K	0.39	0	0.19	0.3	0.16
Ca	0.79	2.54	1.55	4.01	1.59
Ti	0.27	0.32	0.46	0.43	0.49
Fe	0.49	0.94	1.74	5.25	0.55
Total	100	100	100	100	100

(*Results reported in weight %, based on atomic %)

The results obtained from the elemental SEM analysis as exhibited in Table 4.14 were supported by the XRF analysis in Table 4.3. From the XRF analysis it could be inferred that the main minerals present were from the clay, quartz, pyrite and carbonate groups. Figure 4.2 illustrates visible layers found inside the coal particle according to SEM analysis.

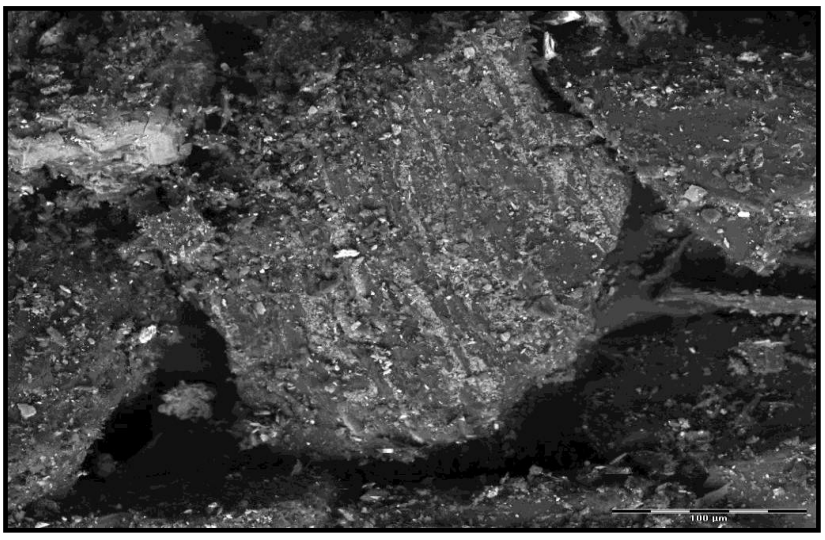

Figure 4.2: SEM photograph of coal B1 export.

At present large quantities of fine and ultra-fine coal are being discarded in South Africa due to the quality of the coal, more specific the heat value of the coal, it is too low to be included in the export product. In the past South Africa's export coal were mined from the No. 2 Seam where the fine coal fraction was relatively easy to beneficiate. In the future a large portion of coal will be produced from the No. 4 Seam where the fine coal fraction is difficult to beneficiate and low quality fines will be produced that cannot be included in the final export product (de Korte, 2002). If wet fine coal is added to the coarse coal product the heat value of the combined product decreases. To compensate for this, the coarse coal product must be produced at a higher heat value which in turn decreases the yield of the coarse product. Generally, the yield loss from the coarse coal are more than the gain by adding the fine coal, and it is therefore more economical to discard the fine coal (de Korte & Mangena, 2004). Thermal drying can reduce the moisture content to acceptable levels but there is a concern that fine coal can pick up moisture during transportation and stockpiling.

4.6 Summary

A summary of the characterisation analysis performed on all five coal samples is presented in Table 4.15.

Table 4.15: Summary of coal characterisation analyses on all five coal samples.

	A (ROM)	B1 (Export)	B2 (Middlings)	B3 (Discard)	C (ROM)
Chemical and mineral analysis					
Moisture content (wt.% ,air dried)	0.6	2.6	2.2	1.2	3.9
Ash content (wt.% air dried)	50.1	14.9	31.6	63.5	34.1
Volatile matter (wt.% air dried)	13.8	26.2	20.6	18.2	20.6
Fixed carbon (wt.% air dried)	35.5	56.3	45.6	17.1	41.4
Predominant species in the ash					
Al_2O_3	24.61	28.93	30.35	21.36	32.19
SiO_2	66.65	49.46	56.65	42.58	51.50
CaO	0.97	8.86	3.55	4.49	7.87
Fe_2O_3	2.71	1.81	2.61	22.38	2.37
SO_3	0.68	4.21	2.89	6.04	1.85
Petrographic analysis					
Vitrinite (vol. % m.m.b)	45.3	20.3	8.8	12.2	14.5
Liptinite (vol. % m.m.b)	0	4	1.2	0.2	1.5

Inertinite (vol. % m.m.b)	27.4	67.3	72.4	50.9	64.8
Structural analysis					
Macro pore area (m^2/g)	15.41	17.73	12.61	6.31	23.2
Micropore surface area (D-R) (m^2/g)	87.34	48.09	120.26	73.89	155.56
BET surface area, N_2 adsorption (m^2/g)	3.54	7.78	4.79	4.85	11.2
Total macro-porosity (Mercury porosimetry) %	6.2	5.9	5.4	3.9	10.7
Micro-porosity (CO_2 BET) %	2	4.2	4.04	2.93	5
Meso-porosity (N_2 BET) %	1.1	0.9	0.85	0.5	4.8

Proximate analysis revealed that coal C was enriched in moisture. Coal B3 contained the highest amount of ash followed by coal A C, B2 and coal B1 with the lowest ash content.

It could be concluded from the extensive mineral characterisation analysis conducted on the five coal samples that clay and quartz minerals were the predominant minerals present in all the coal samples. The variation in clay and quartz minerals in these coal samples will make it possible to see a trend regarding the influence of clay mineral matter on these specific coals in following chapters.

Coals B and C are characterised as bituminous, medium rank C coal and coal A as a bituminous, medium ranked B coal. Coals B and C were similar in rank, therefore coal rank was not expected to play a major role when comparing the moisture adoption/desorption properties of these coal samples. Important conclusions regarding the influence of coal rank on moisture adsorption/desorption can also be made when investigating the medium rank B coal A and comparing the results with the lower ranked bituminous coals B and C. Coals B and C are inertinite rich high ash coal and coal A is a vitrinite rich high ash coal.

A negative correlation was found between the CO_2 BET surface area and the amount of minerals present in each coal. The coals containing the highest amount of minerals (A and B3) had the lowest CO_2 BET surface areas whereas the coal with the lowest amount of

minerals (B1) had the highest CO_2 BET surface area. In the absence of minerals, especially those associated with the coal matrix, there are more voids and cavities allowing the gas to adsorb into any free space available.

A visual observation during the SEM analysis showed that coal particles contain finely dispersed bands of minerals associated with the coal matrix.

Chapter 5 establishes a link between the influences of all the parameters determined by the above- mentioned characterisation study and the moisture adsorption and desorption properties for each specific coal.

CHAPTER 5:

MOISTURE ADSORPTION AND DESORPTION

5.1 Introduction

This chapter presents the results regarding the effect of minerals and other coal properties on the moisture adsorption and desorption properties of South African fine coal. The results were prepared by exposing coal particles to varying climate conditions in a constant climate chamber. A detailed discussion on the experimental apparatus as well as the procedures followed to achieve the above- mentioned outcome is presented in Section 5.2. The adsorption/desorption results are discussed in Section 5.3. The results presented in this section not only focus on the influence of minerals on the adsorption/desorption properties of South African coal, but also include an elaboration on the influences of oxygen content and porosity, coal rank, coal petrology and temperature. Due to the heterogeneity of coal it is important to view the influence of these properties on moisture adsorption holistically, as they are intimately associated with the mineral matter included in these coal samples and consequently are expected to have an effect on the adsorption/desorption characteristics of each coal type. Chapter 5 concludes with a summary of the results and observations obtained from the moisture adsorption and desorption characteristics of South African fine coal.

5.2 Experimental

An assessment of the adsorption and desorption properties was conducted in a constant climate chamber. The climate chamber allowed for accurate control of the temperature as well as the relative humidity surrounding the coal samples. Section 5.2.1 addresses the experimental equipment, whereas Sections 5.2.2 and 5.2.3 present the experimental procedures and programme respectively.

5.2.1 Experimental apparatus

The climate chamber used to assess the moisture adsorption and desorption properties was supplied by Advanced Laboratory Solutions. This climate chamber controls and records the relative humidity as well as the temperature as a function of time. A schematic representation of the apparatus is depicted in Figure 5.1.

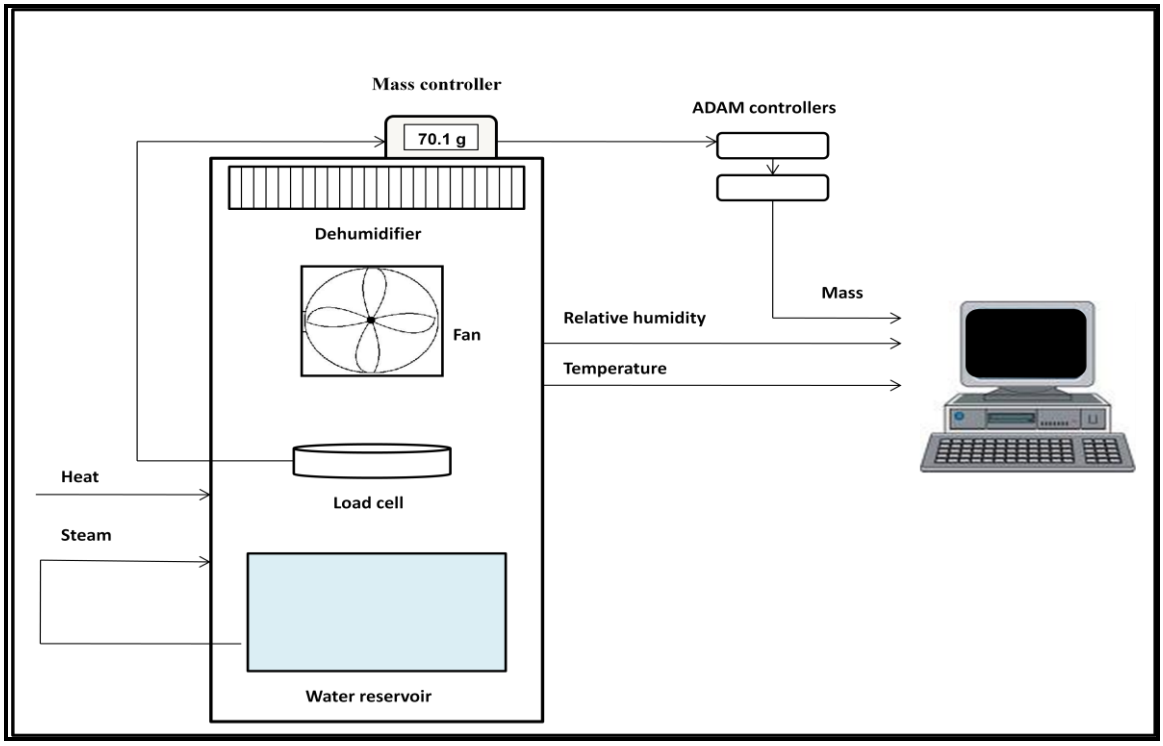

Figure 5.1: Schematic representation of climate chamber.

An analytical balance was installed inside the climate chamber to measure the increase in mass due to moisture adsorption and any decrease in mass due to moisture desorption under varying environmental conditions. The analog signal from the balance was sent to a mass controller, where it was converted to a mass reading. The signal was then sent to two ADAM controllers which made it possible to continuously log the mass on a computer. The mass, temperature and humidity data were logged every minute and exported to a Microsoft Excel spreadsheet for further interpretation. The mass logging program was implemented by using Microsoft Visual Basics. The experimental apparatus can be seen in Figure 5.2.

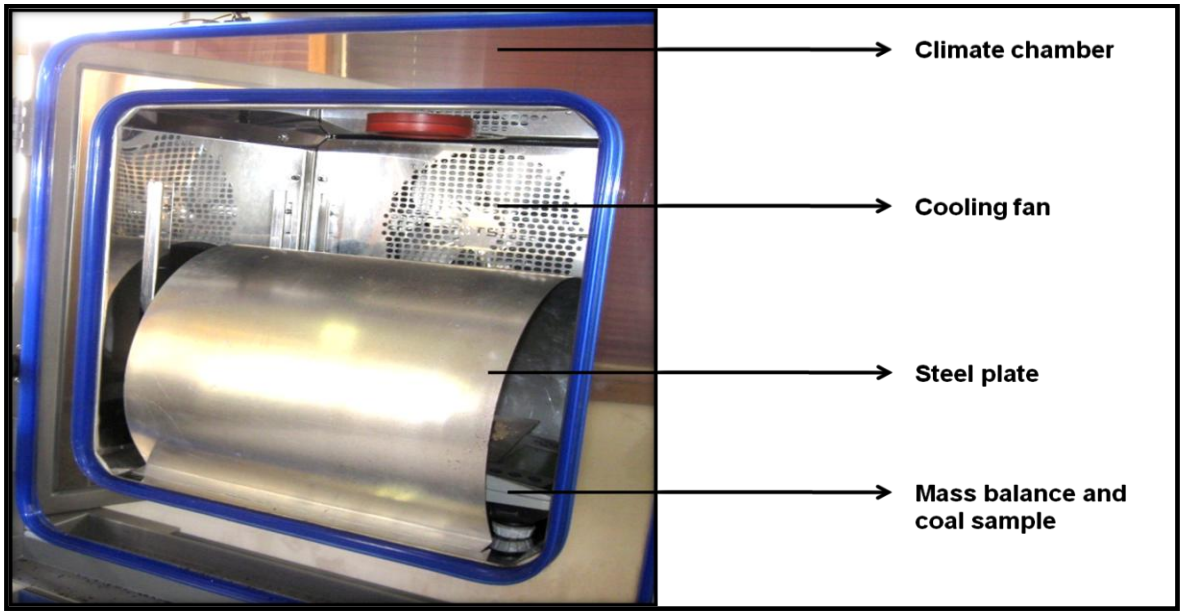

Figure 5.2: Experimental apparatus with steel plate.

A curved steel plate was installed in the chamber to cover the coal samples on the mass balance in order to prevent any disturbances from the cooling fan during the experiments. This ensured that the amount of noise present during the mass logging was kept to a minimum. An interior view of the climate chamber without the steel plate and containing a clay sample as depicted in Figure 5.3.

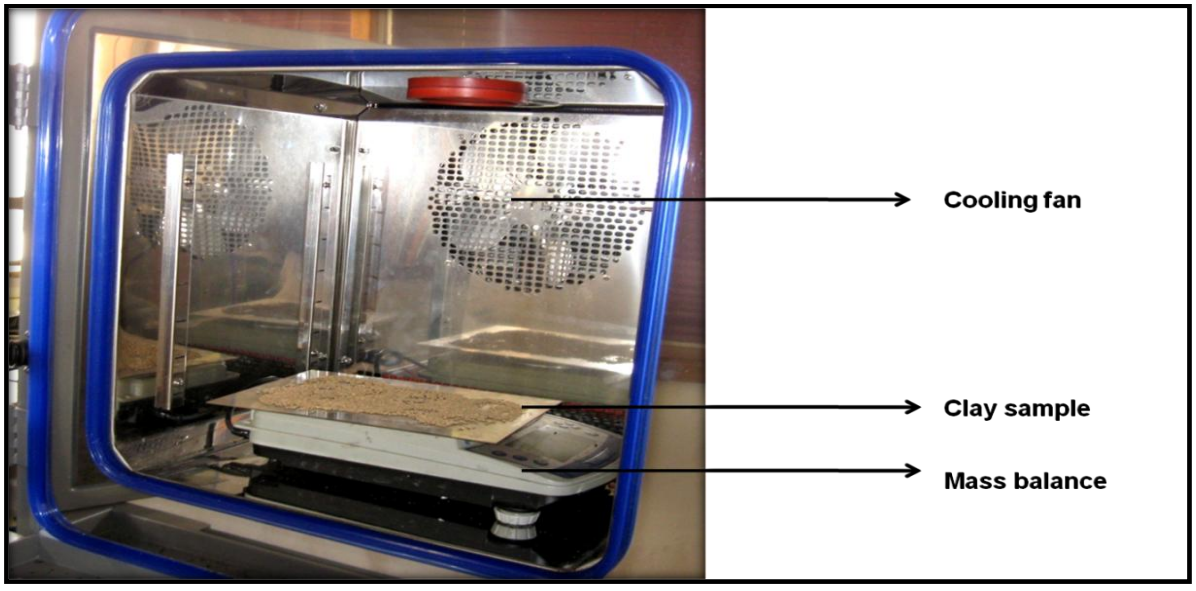

Figure 5.3: Illustration of the experimental setup inside the climate chamber.

The mass balance was able to measure a maximum of 300g with a sensitivity of 1mg which provided precise mass readings. The climate chamber is also equipped with a water reservoir that supplies the system with water for each experiment with changing conditions.

The system uses only distilled water and the water mixture must be drained and refilled every 200 hours.

5.2.2 Experimental procedures

The samples used for the adsorption/desorption experiments were prepared by crushing and dry sifting them into +1mm - 2mm size fractions. The main purpose of the milling was to reduce the particle size of the coal samples before sifting them. A jaw crusher was specifically used to ensure that the particles break along their inherent lines of weakness, exposing the finely dispersed mineral matter present in the coal particle (Schlitt et al., 1992).

The experimental procedure involved the selection of a 70 g coal sample between +1mm - 2mm. The sample was dried over night in a vacuum oven at 105°C to ensure that most of the moisture is excluded from the sample before each experiment. The sample was then placed into the climate chamber at a relative humidity (RH) of 20% at a specific temperature. The system was then allowed to reach equilibrium which was indicated by a constant mass reading. The humidity was then increased to 40%, 60% and 80% in turn, once again allowing each step to reach equilibrium. After a maximum of 80% RH was reached the humidity was decreased in the same sequence as for the adsorption steps, from 80% to 60%, 40% and 20% RH while the temperature was kept constant under atmospheric pressure conditions. The overall time required to complete an experiment was in the order of 70 hours to ensure that a constant mass was reached in each step. Directly after each experiment was completed the sample was weighed and placed immediately in a vacuum oven for several hours after which the sample was weighed once again to determine the final moisture content of the coal sample. This equilibrium mass data were used to calculate the mass of adsorbed moisture per unit mass of coal. The mentioned humidity sequence was investigated at temperatures of 15°C, 28°C and 35°C for only one coal sample to establish the effect of temperature on the adsorption/desorption properties. The remainder of the experiments were conducted isothermally at 28°C.

5.2.3 Experimental programme

A review of the moisture adsorption and desorption data obtained from the experiments conducted in the climate chamber is presented in this section. The experimental approach was to simulate an environment inside a climate chamber resembling typical South African weather conditions to which stored or transported coal would be exposed to. The results obtained from these experiments will provide relevant and valuable information regarding the

behaviour of coal in varying environmental conditions. A specific humidity sequence was chosen wherein 20% to 40% RH resembled a dry environment and 60% to 80% RH resembled environmental conditions nearing precipitation. This humidity range was studied at isothermal (28°C) and atmospheric conditions since that is similar to South African weather conditions. A temperature range between 15°C and 35°C was selected to study the influence of temperature on the adsorption and desorption characteristics, where 15°C represented winter temperatures and 35°C represented temperatures experienced during summer in South Africa. Table 5.1 gives an overview of the main experimental parameters and ranges investigated.

Table 5.1: Operating conditions for adsorption/desorption experiments.

Variables	Ranges
Temperature	15°C, 28°C, 35°C
Relative humidity	20 - 80%
Pressure	87.5 kPa
Coal samples	A, B1, B2, B3, C
Particle size	+1mm - 2mm

The effect of temperature on the adsorption/desorption properties were only investigated for a particular coal sample by varying the temperature according to the temperature range presented in the above- mentioned table. The temperature was kept constant for the remainder of the experiments at 28°C. Selected experiments were repeated to validate the repeatability of the experiments.

5.3 Moisture adsorption and desorption: Results and discussion

This section focuses on the results and observations obtained from the adsorption/desorption experiments conducted on five coal samples and a clay sample according to the procedures outlined in Section 5.2. This was done in order to evaluate the adsorption/desorption behaviour of South African coal and to link its behaviour to the mineral matter content and other intrinsic coal properties present in these coal types. Section 5.3.1 describes how the raw data were obtained and further calculations that were made in order to obtain isotherms for each coal investigated. Section 5.3.3 gives a detailed account of the

influence of minerals on the adsorption/desorption properties. The influence of oxygen content and porosity, together with coal rank and petrology, are evaluated in Section 5.1.2 and Section 5.1.3 accordingly. Section 5.1.4 describes the influence of temperature on the adsorption/desorption properties. Section 5.3 concludes with an investigation into the hysteresis behaviour present during moisture desorption.

5.3.1 Experimental results

Figure 5.4 illustrates a typical mass gain and loss curve obtained for coal C during varying relative humidity at a constant temperature of 28°C and pressure of 87.5 kPa.

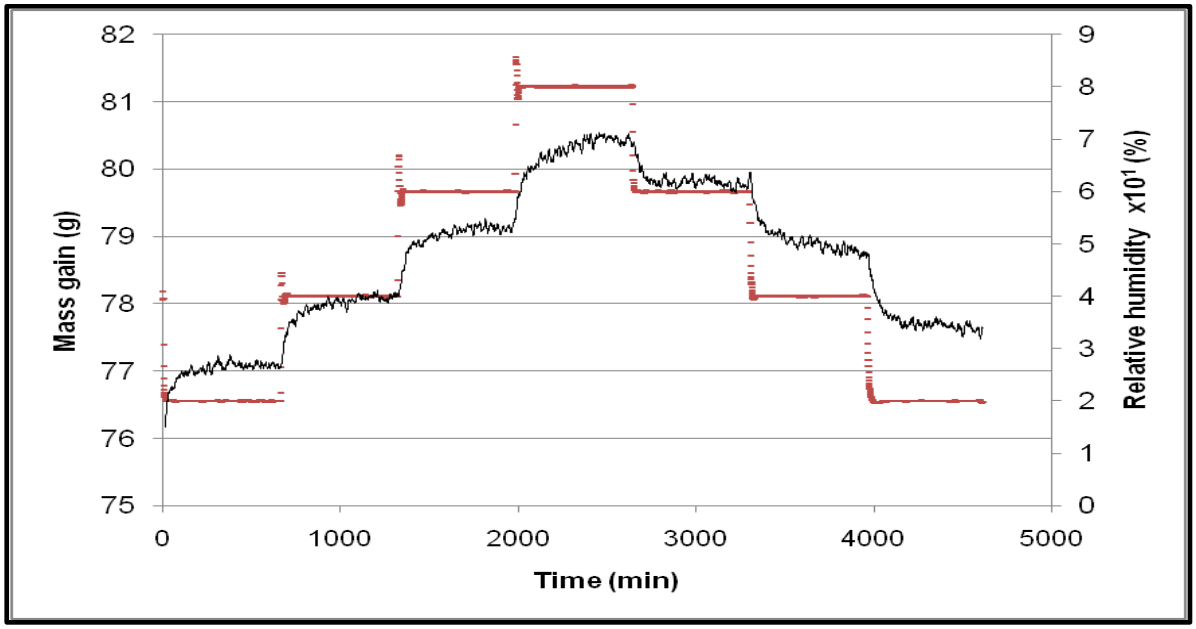

Figure 5.4: Typical mass gain and loss curve for moisture adsorption and desorption.

The relative humidity varied according to the sequence described in Section 5.2.2 which resulted in a variation in mass. A constant mass gain or loss indicated that equilibrium conditions were reached. It took on average 8 hours for the mass to reach equilibrium for each step in relative humidity, resulting in an overall average experimental time of 70 hours. A temperature of 28°C was selected for all the experiments, except where temperature effects were investigated, as this is representative of the environmental conditions that the coal would be exposed to in South Africa during summer.

The coal samples were dried in a vacuum oven prior to each experiment. In order to calculate the amount of moisture adsorbed per amount of dry coal. In Figure 5.4 it is evident that all the moisture adsorbed does not equal all the moisture desorbed. This is an early indication of adsorption/desorption hysteresis present during the experiment.

To calculate the percentage moisture adsorbed or desorbed Equation 5.1 was employed.

$$\text{Percentage moisture } (\%) = \left(\frac{M_1 - M_2}{M_2}\right) * 100 \qquad (5.1)$$

Where M_1 refers to the mass at the equilibrium points and M_2 refers to the mass recorded after drying in an oven. The amount of moisture per amount of dry coal could then be calculated and isotherms could be constructed. A typical isotherm constructed for Coal B1 at 28°C is presented in Figure 5.5. Isotherms for all five coal samples are presented in Section 5.3.3. Lines were added to the experimental data to allow for a better differentiation between the adsorption and desorption data with the adsorption isotherm highlighted in a bolder colour for better readability.

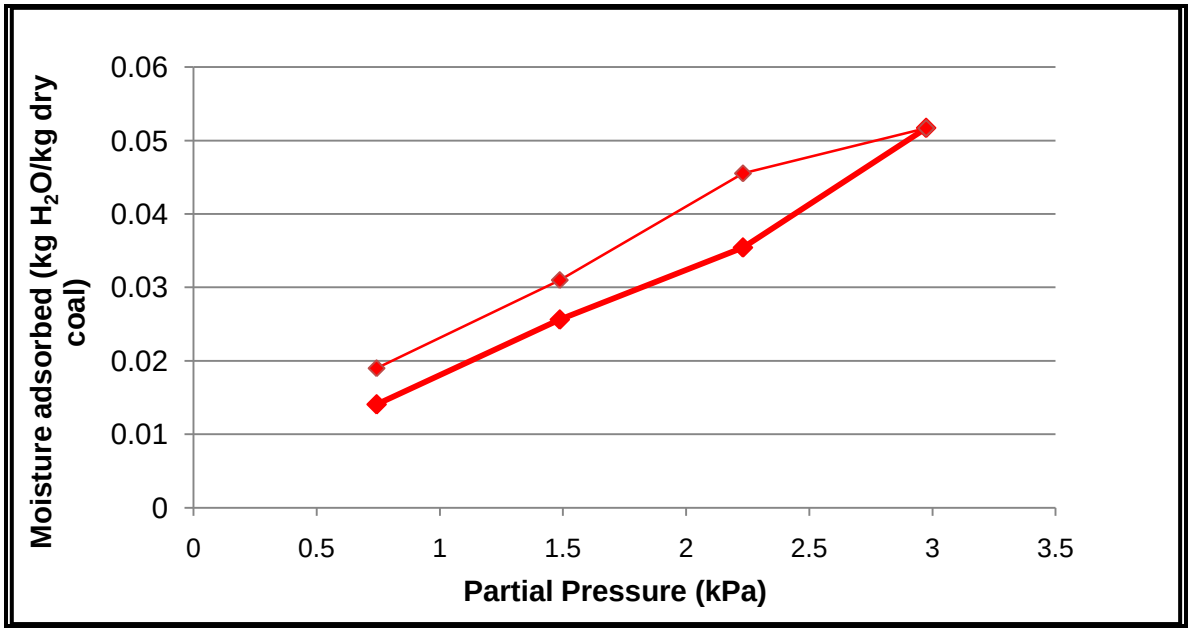

Figure 5.5: Adsorption and desorption isotherms for coal B1 at 28°C.

The partial pressure of water (P) as a function of relative humidity (RH) and temperature can be defined by the following equation;

$$P = \frac{RH}{100} * P_s \qquad (5.2)$$

The saturation pressure P_S of water was calculated, at a specific temperature, by using the Antoine equation (Koretsky, 2003).

$$\ln(P_s[\text{bar}]) = A - \frac{B}{T[K] + C} \quad (5.3)$$

where P_S is the saturation pressure in bar at a specific temperature measured in Kelvin.

5.3.2 Reproducibility of experimental results

The experimental error associated with the experimental results obtained for coal C can be seen in Table 5.2.

Table 5.2: Calculated experimental error for coal C at 28°C.

%RH	Experiment 1 (kg moisture/kg coal)	Experiment 2 (kg moisture/kg coal)	Standard deviation
20	0.018	0.019	± 0.0007
40	0.031	0.032	± 0.0007
60	0.045	0.046	± 0.0007
80	0.062	0.063	± 0.0007
60	0.054	0.055	± 0.0007
40	0.041	0.042	± 0.0007
20	0.026	0.027	± 0.0007

From Table 5.2 it was evident that the experiments were reproducible for coal C at the whole range of humidities investigated at 28C°. It was assumed that the experiments for remainder of the four coals would also be reproducible.

5.3.3 Effect of minerals

The main focus of this study was to investigate the influence of minerals on the moisture adsorption and desorption properties of South African coal. In order to do so, precise experiments were conducted according to the procedures explained in Section 5.2.2. The moisture data obtained for each coal sample were then converted into adsorption and desorption isotherms for the five coal samples including a kaolinite sample according to the steps discussed in Section 5.3.1. The moisture adsorption and desorption properties of a pure mineral (kaolinite) was studied in order to make semi- quantitative conclusions

regarding the influence of kaolinite on the moisture adsorption and desorption properties as well as the carbon content of the whole coal samples. The influence of the clay mineral illite present in the coal samples was also investigated since it is the second most abundant clay mineral present according to QEMSCAN analysis.

5.3.3.1 Effect of kaolinite

The adsorption and desorption isotherms are displayed in Figure 5.6 with coloured lines connecting the data points for the sake of better presentation making it easier to differentiate between the adsorption (highlighted in a bolder colour) and desorption isotherms.

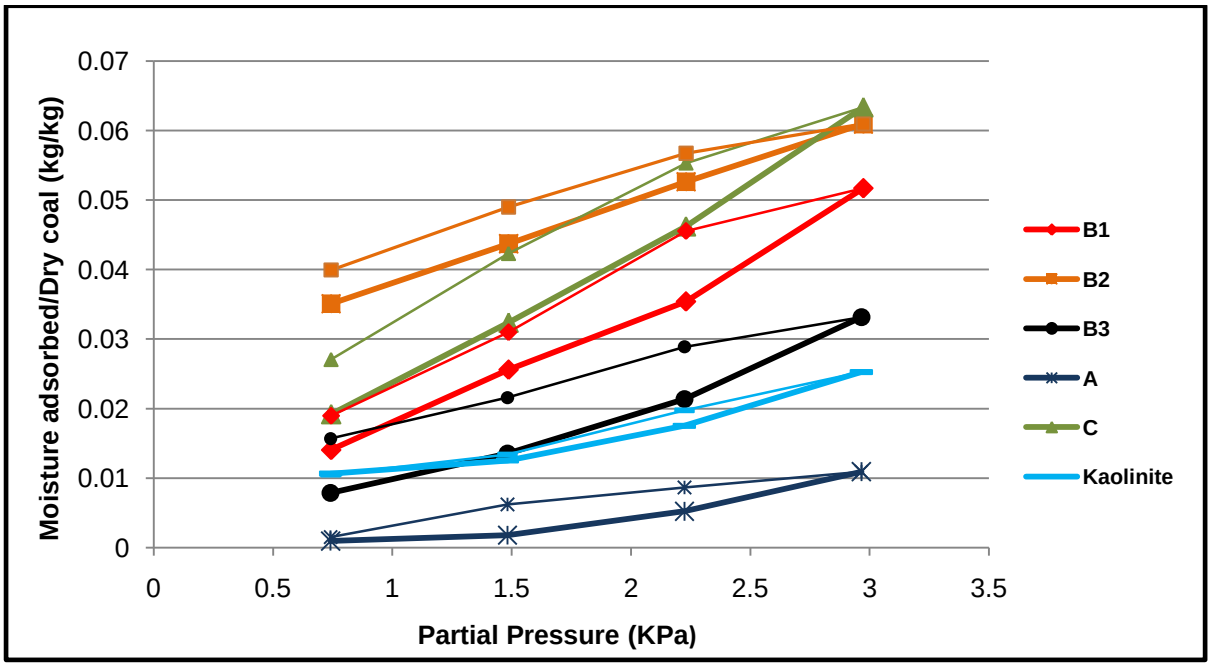

Figure 5.6: Adsorption and desorption isotherms at 28°C.

Figure 5.6 illustrates the adsorption and desorption isotherms for five coal samples and a pure mineral sample (kaolinite). The decision to use kaolinite as the pure mineral in the moisture adsorption experiments was based on the information obtained from the QEMSCAN analysis in Table 4.4, indicating that the predominant clay mineral present in each coal sample was kaolinite which is also typical of South African coals (Pinetown & Boer, 2006; Gaigher 1980). Literature also suggests that clay minerals influence moisture adsorption on coal more than other minerals do due to their structures and swelling characteristics in the presence of moisture (McCutcheon & Barton, 1999). The second largest mineral present in each coal was quartz and it was assumed that this mineral adsorbed no moisture. Different adsorption capacities, isotherm shapes and forms of hysteresis were observed for all the samples indicating different mechanisms present during adsorption and desorption. The water uptake of the pure kaolinite sample was less than the water up take for coals C, B1, B2 and B3.

In order to differentiate between the amount of moisture adsorbed in each coal sample due to the kaolinite and carbon constituents respectively, a mass balance was constructed around the experimental moisture adsorption data for both the raw coal and pure kaolinite samples. The subsequent calculation steps were followed;

- The quantitative amount of kaolinite in each coal was determined by QEMSCAN analysis.
- The amount of kaolinite present in the minerals of each coal sample, as determined by QEMSCAN analysis, was then calculated and subtracted from the amount of minerals, assuming that kaolinite was the only mineral significantly influencing the moisture adsorbed on each coal sample. This was a valid assumption since the bulk of the minerals consisted of kaolinite and no other mineral present influencing moisture adsorption could be identified in significant amounts, in the coal samples for this investigation.
- The amount of carbon was then determined by subtracting the amount of minerals as determined in the QEMSACN analysis from the mass of each coal sample.
- Total moisture adsorbed by the whole coal sample and the pure mineral (kg moisture/kg solids) was determined experimentally making it possible to calculate the moisture adsorbed by the carbon constituents in each coal sample by the difference.
- Consequently, the amount of moisture adsorbed by the carbon, kaolinite and whole coal sample (kg moisture/kg coal) could be calculated.

The total moisture adsorbed for the whole coal sample as well the moisture adsorbed by the kaolinite and carbon constituents in coal C can be viewed in Figure 5.7.

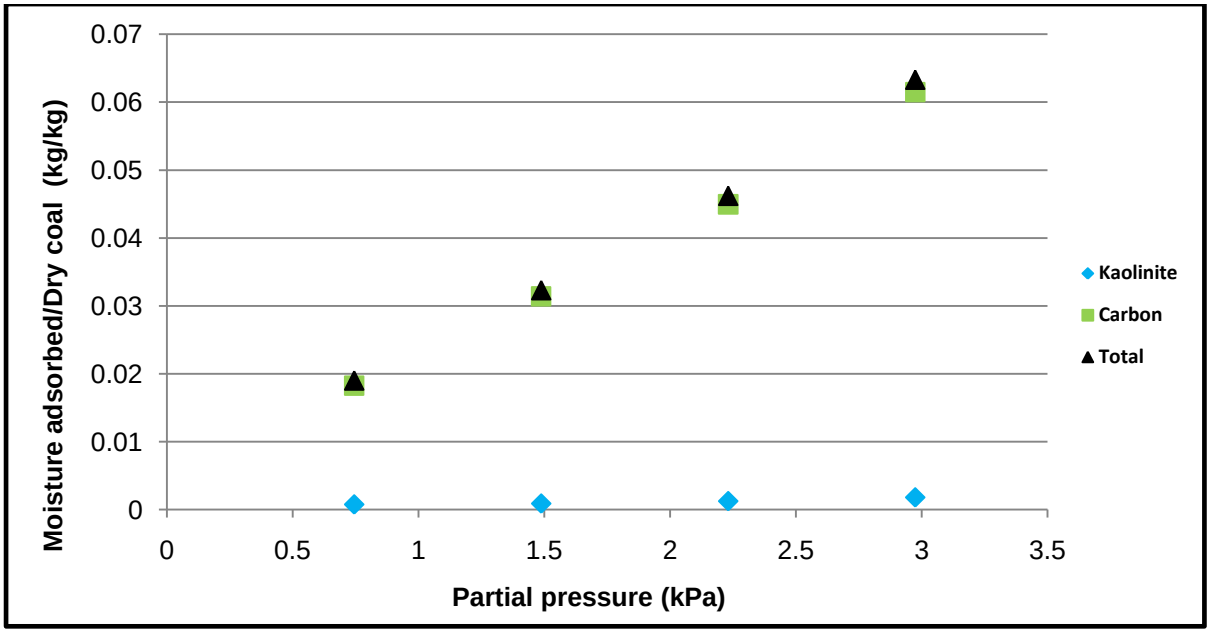

Figure 5.7: Total moisture adsorbed along with moisture adsorbed due to carbon and kaolinite content in coal C.

The results in Figure 5.7 show that the contribution of kaolinite content to the total amount of moisture adsorbed in coal C is minimal with the bulk of the moisture absorbed influenced by the carbon fraction of the coal. According to QEMSCAN analysis more than half of the minerals in coal C consist of kaolinite, 54.3 % (wt.). As a result the moisture adsorbed by kaolinite (non-swelling clay) for this South African medium rank C bituminous coal is minimal. A study by McCutcheon & Barton (1999) investigating the contribution of mineral matter to water associated with bituminous coals found that coal mineral matter containing montmorillonite (swelling type clay) had more than twice the water uptake than mineral matter containing clay minerals in the form of kaolinite.

The amount of moisture adsorbed due to the carbon and kaolinite constituents in coal A are illustrated in Figure 5.8 as well as the total amount of moisture adsorbed by the whole coal sample.

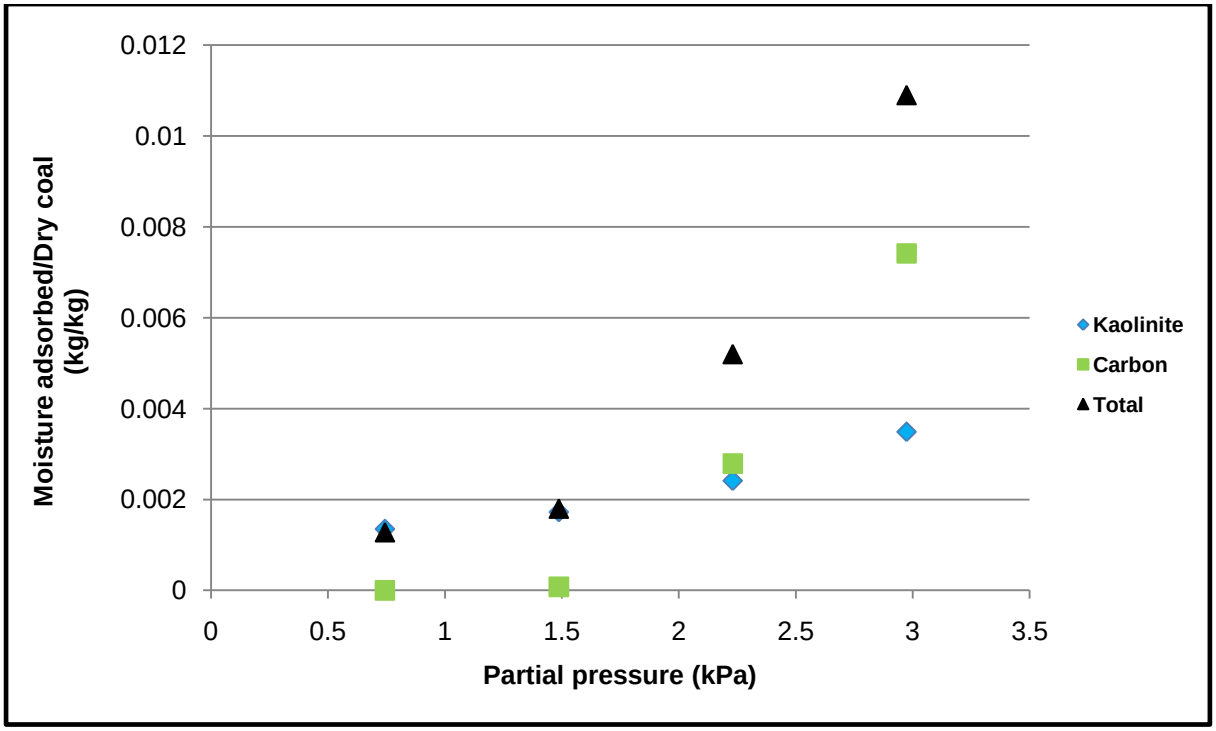

Figure 5.8: Total moisture adsorbed and moisture adsorbed due to the carbon and kaolinite content in coal A.

When comparing the total amount of moisture adsorbed by coal A and C, significant differences can be observed. The results from Figure 5.8 indicate that coal A adsorbed very little total moisture at every relative humidity level compared to coal C. However, the amount of moisture adsorbed due to the kaolinite fraction in coal A is more pronounced than that for coal C. At low relative pressures the bulk of the moisture in coal A was absorbed by kaolinite and only at higher relative pressures the amount of moisture adsorbed, influenced by the carbon content, became more significant. This was expected since the water uptake by the organic material of the higher ranked bituminous coal A is less in comparison to the lower ranked bituminous coal C (Day *et al*., 2008; Unsworth *et al*., 1988; McCutcheon & Barton, 1999). This could explain the small amount of moisture adsorbed by coal A despite the presence of high amounts of kaolinite.

The influence of kaolinite can therefore contribute to moisture adsorbed in South African coal but to a lesser extent than expected. It is consequently vital to identify the type of clay minerals present in a specific coal type and only then determine the adsorption behaviour of the specific coal since different minerals display different moisture adsorption capacities (McCutcheon & Barton, 1999). The contributions of kaolinite and carbon contents to moisture adsorption for the remainder of the coal samples (B1, B2 and B3) show similar trends to coal C and can be viewed in Appendix A.

A visual representation of the percentages of moisture adsorbed estimated for the carbon and kaolinite components in each coal sample are portrayed in Figure 5.9.

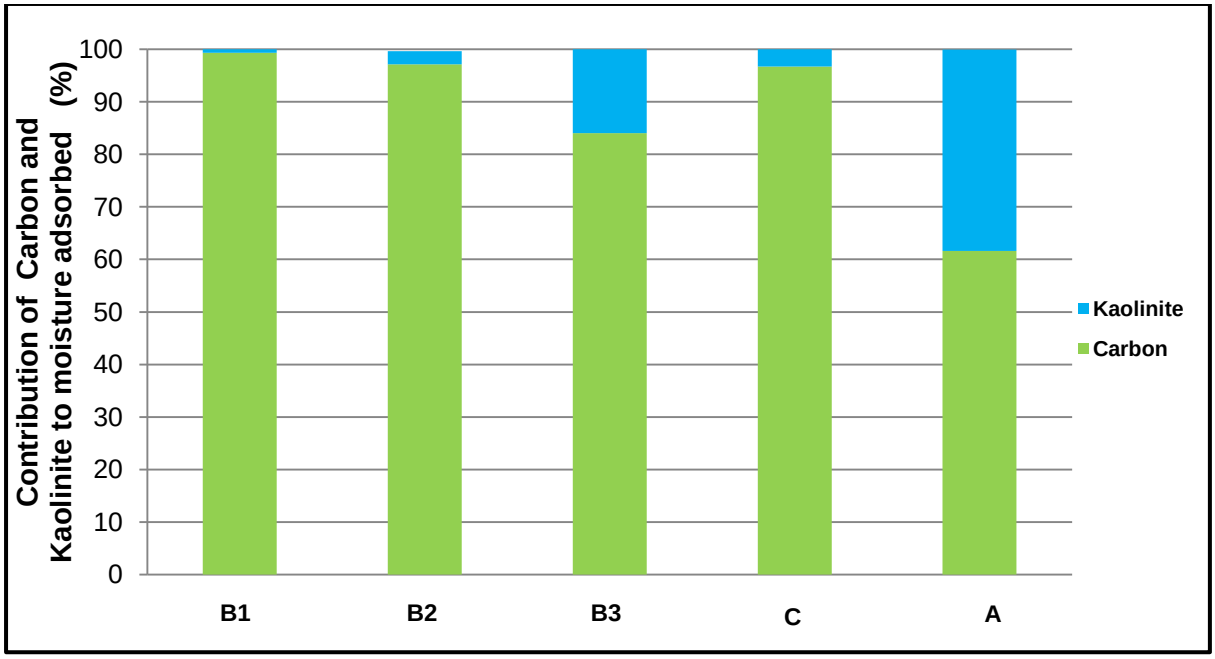

Figure 5.9: Percentage contribution of carbon and kaolinite to moisture adsorbed for each coal.

The data presented in the figure above indicates that the percentage of moisture adsorbed for the coal samples due to the presence of kaolinite varies between 0.7% (B1) and 38% (A). The moisture adsorbed by the carbon component varies between 99.3% (B1) and 62% (A). Moisture adsorbed by the carbon component in the higher ranked bituminous coal A is less pronounced than in the lower ranked bituminous coals B and C. Kaolinite influences moisture adsorption but to a lesser extent in lower ranked bituminous coal. The amount of moisture adsorbed by the kaolinite seems to be less for lower rank bituminous coals containing more oxygen (B1, B2 and C) and more for higher ranked coal containing less oxygen (A). It can thus be concluded that the amount of moisture adsorbed in coal is influenced by kaolinite but to a lesser extent for lower ranked bituminous coal, suggesting that coal rank and the oxygen containing functional groups related to coal rank influenced moisture adsorption on these coals to a certain degree (Day et al., 2008; Švábová et al., 2011; Charrière & Behra, 2010; Mahajan & Walker 1970; McCutcheon & Barton, 1999). This conclusion encouraged further investigation into the influence of oxygen, which could be an indication of the adsorption sites made available by surface oxygen containing functional groups, on moisture adsorption which is discussed in Section 5.1.2.

5.1.1.1 Influence of Illite

The influence of illite on the moisture adsorbed at 80% RH and 28°C is illustrated in Figure 5.10.

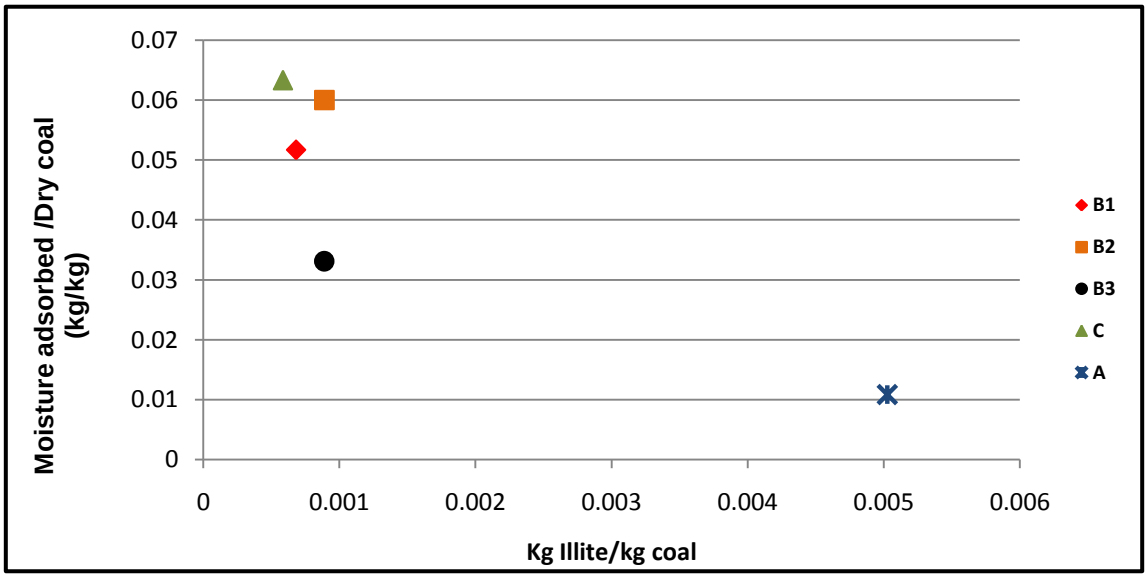

Figure 5.10: Influence of illite on the moisture adsorbed

It was evident from the figure above that coal A contained the largest amount of illite, 0.005 kg Illite/kg coal but adsorbed the least amount of moisture at 80%RH. For the lower ranked bituminous coals B1 and B2 (compared to the higher rank bituminous coal A) there was a positive correlation between the moisture adsorbed and amount of illite. Coal B1 contained 0.00068 kg Illite/kg coal and adsorbed 0.052 kg moisture/kg coal, whereas coal B2 contained 0.00089 kg Illite/kg coal and adsorbed 0.06 kg moisture/kg coal. According to Figure 2.6 illite adsorbed more water than kaolinite, but in all five coal samples in this study the bulk of the minerals consisted of kaolinite. The quantities of illite present in four of the five coals were very small and could therefore not have had a significant influence on the moisture adsorbed in comparison to kaolinite. Where illite was more significantly present (coal A) there seemed to be no considerable influence in moisture adsorption compared to the other four coals.

5.1.2 Effect of coal rank and surface oxygen

The influence of oxygen content on the moisture adsorbed at 80% RH is illustrated in Figure 5.11. The percentage oxygen in each coal sample was obtained, by difference from the ultimate analysis reported in Section 4.2 as weight percentage on a dry, ash free basis. It was evident from the results obtained in the previous section that mineral matter does not significantly influence the moisture adsorption of these five coals and therefore it was decided to report the oxygen content on ash free basis. This highlighted the influence of oxygen on the moisture adsorption, in the absence of ash content.

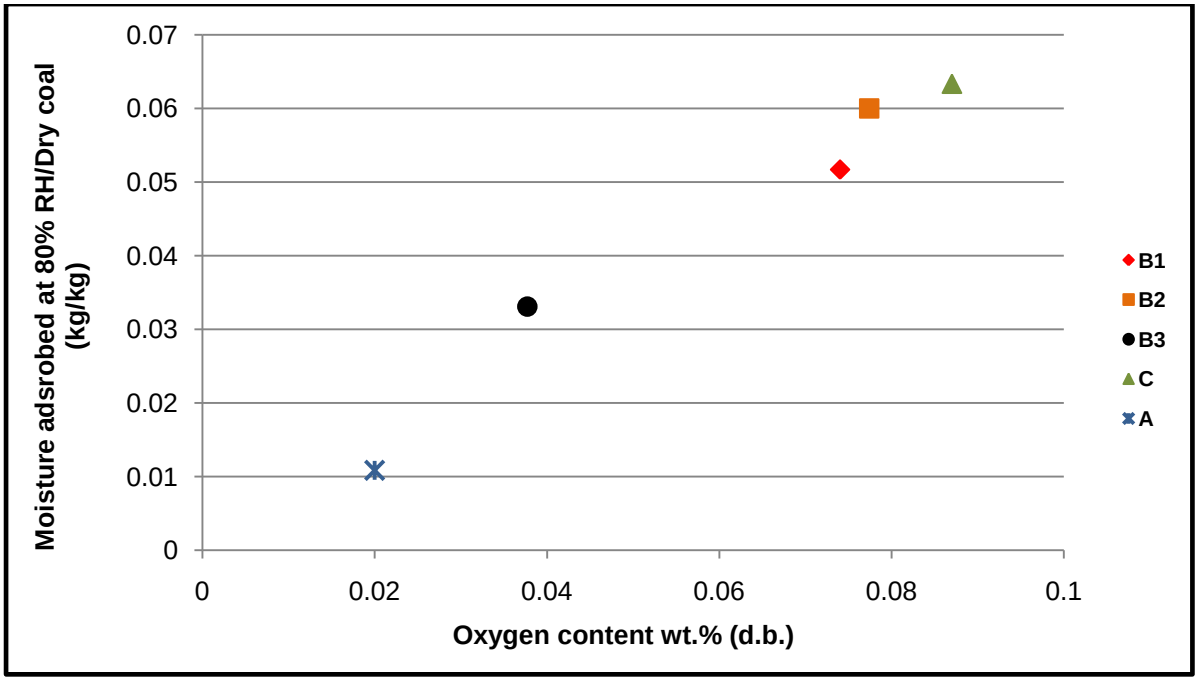

Figure 5.11: Influence of oxygen content on moisture adsorbed at 80%RH for all five coal samples.

It must be clearly emphasised that the oxygen content as determined in the ultimate analysis was calculated by difference and errors accumulate in this value. The oxygen value used in Figure 5.11 was only to indicate a trend and was not an attempt to quantify the influence of oxygen on moisture adsorption.

According to Figure 5.11 the amount of moisture adsorbed at 80% RH increased almost linearly with an increase in oxygen content for all the coal samples. Oxygen content is an important indicator of the primary sites available for moisture adsorption. Nishino (2000) found a positive correlation between the oxygen content and functional groups on the coal surface. Numerous studies have revealed that oxygen containing functional groups on the coal surface facilitate primary moisture adsorption prior to multilayer adsorption and capillary condensation (Day et al., 2008; Švábová et al., 2011; Charrière & Behra, 2010; Nishino, 2000). Day et al., (2008) established that the BET monolayer capacity correlates with the number of hydrophilic functional groups, suggesting that initial adsorption occurs at the surface via `hydrogen bonding. Further adsorption takes place by cluster forming or multilayer adsorption on top of the monolayer which finally leads to capillary condensation. This process highlights the importance of the hydrophilic surface sites present on the coal surface in order for moisture adsorption to occur. It is thus important to observe the correlation of moisture adsorption and surface oxygen content at low relative pressures before viewing the transition in adsorption from multilayer to capillary condensation which

generally occurs at higher relative pressures, since oxygen is an important indicator of the functional groups providing sites for moisture adsorption (Schafer, 1972).

Coal A had the lowest amount of oxygen available on the surface due to its higher rank in comparison to the other four coals and it was thus expected to absorb the least amount of moisture. As the coalification process progresses narrow pores and apertures in the coal structure are closed thereby forming closed pores preventing moisture vapour to penetrate the coal matrix, explaining the low moisture adsorbed in higher ranked coals (Day et al., 2008; McCutcheon *et al*., 2003).

5.1.3 Petrographic influence

The influence of inertinite content on the amount of moisture adsorbed at 80%RH is presented in Figure 5.12 with the inertinite content obtained from the maceral analysis that was performed in Section 4.4, reported a volume percentage on a mineral matter free basis (m.m.f.b.). This basis was chosen since previous findings revealed that moisture adsorbed on the five coal samples investigated in this study is not significantly influenced by the minerals present.

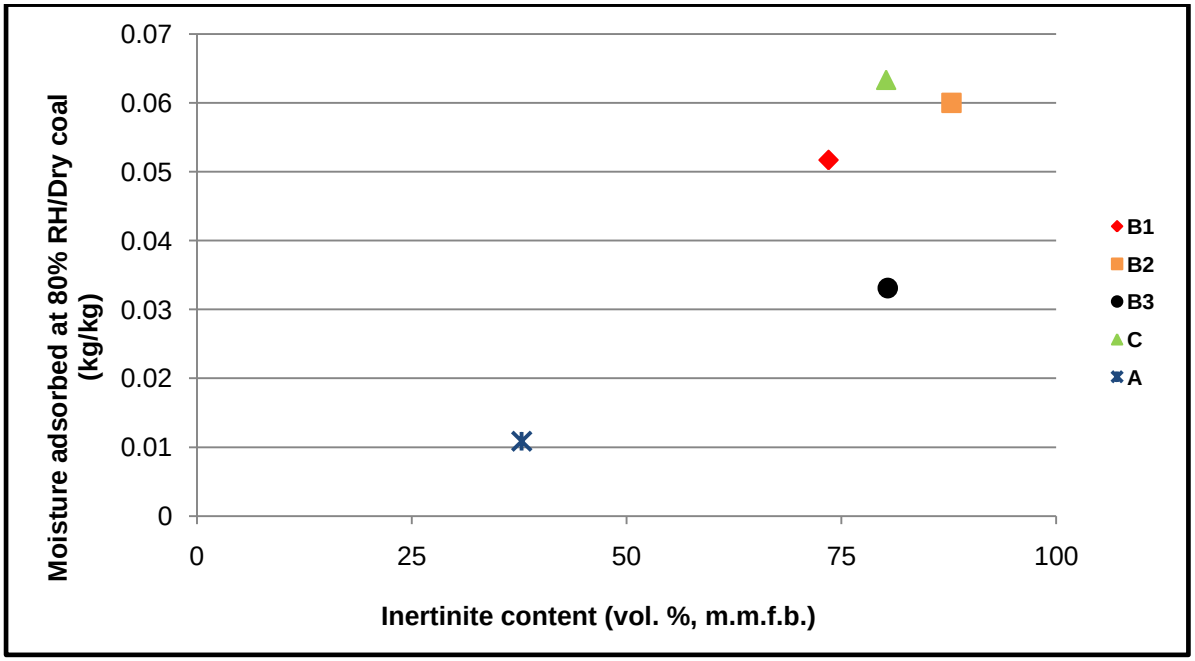

Figure 5.12: Inertinite influence on moisture adsorption for all five coal samples at 80% RH and 28°C.

Differences in the petrographic composition between southern and northern hemisphere coal types are mainly due to different climates and depositional environments resulting in southern hemisphere coal being inertinite rich and northern hemisphere coal being vitrinite

rich (Kershaw & Taylor, 1992). Almost all of the studies conducted on moisture adsorption on coal found in literature were for vitrinite rich northern hemisphere coal or vitrinite rich coal originating from other parts of the world (Charrière & Behra, 2010; Švábová et al., 2011; McCutcheon & Barton, 1999; Mahajan & Walker, 1970). By taking a closer look at the data presented in Figure 5.12 better insight can be gained into the moisture adsorption characteristics of inertinite rich South African coal. The results indicate a correlation between the inertinite content and the moisture adsorbed at 80% RH except in the case for coal B3. To eliminate the effect of coal rank on the adsorption properties, the data presented for coals B1 and B2 could be evaluated and compared. Coal B1 contained less inertinite than coal B2 and adsorbed less moisture than coal B2, indicating a positive relationship between moisture adsorbed and inertinite content. However, a slight difference in oxygen content between coals B1 and B2 was observed from data presented in Figure 5.11 which could also explain the difference in moisture adsorbed.

Literature states that the strong influence of coal rank can overshadow the influence of macerals on moisture adsorption especially if the main factor influencing moisture adsorption is the oxygen containing functional groups which are dependent on coal rank (Faiz et al., 1992).

5.1.4 Temperature effect

The adsorption/desorption isotherms for coal B1 can be seen in Figure 5.13 with lines connecting the data points only for the sake of clarity; with the darker bold shaded lines indicating adsorption and lighter shaded lines indicating desorption. Three different temperatures, 15°C, 28°C, and 35°C, were investigated.

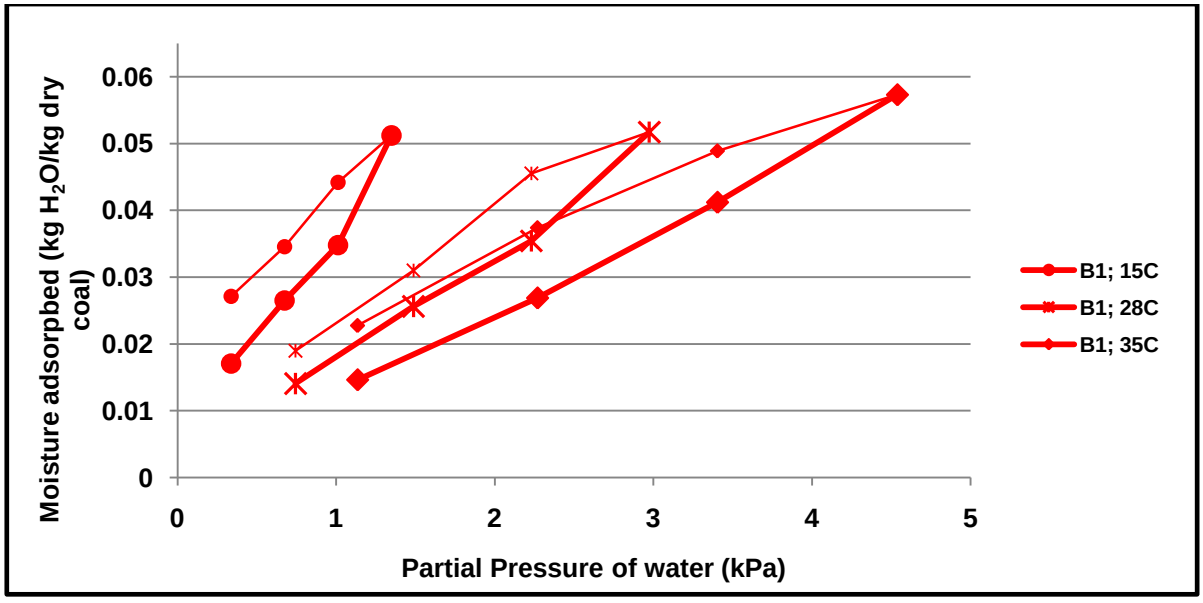

Figure 5.13: Influence of temperature on adsorption/desorption of coal B1 Export.

This specific temperature range was chosen as it resembles typical South African temperatures during the summer (28 ˚C and 35 ˚C) and winter (15 ˚C) months. It was also decided to investigate the influence of these temperatures on the B1 coal sample because this specific coal was more subjected to varying temperatures than the other coal samples, especially when transported to the Richard's Bay coal terminal. Figure 5.13 highlights the presence of hysteresis in coal B1 for each temperature at both low and high relative pressures. To ensure that hysteresis did not occur as a result of not reaching the required equilibrium, selected experiments were left at a specific relative humidity and temperature level for an additional period of time and no further mass loss or gain was noted which confirmed the presence of hysteresis.

It can also be noted that the effect of temperature at all the relative humidity levels seem to have had little effect on the moisture adsorbed. The amount of moisture desorbed however was not equal to the amount of moisture adsorbed. This means that even if the coal samples adsorbed the same amount of moisture at different temperatures, the same amount of moisture was not desorbed equally for the coals. Consequently, it is important to bear in mind that coal history plays an important role in the amount of moisture that is present in a specific coal. If for instance the coal is dewatered/dried prior to being transported from a climate high in relative humidity (where the moisture is adsorbed) to a climate low in relative humidity, the amount of moisture in the coal can be higher than anticipated due to hysteresis. This process can occur for example where the dewatered/dried coal transported from the mainland on a rainy day in summer, experiences lower humidity conditions over drier parts in the mainland and arrives at the coast where it is ,once again, exposed to

elevated relative humidity conditions. It is thus essential to not only study the adsorption process but also the desorption process to accurately predict the moisture presence in coal. Allardice and Evans (1971) concluded that thermally released water can be reabsorbed when exposed to moisture at lower temperatures and that this adsorbed water can only be released by raising the temperature again. This is not desirable since drying coal is a very costly process and it seems extremely ineffective if the moisture is simply reabsorbed when the coal is transported or stored on stockpiles.

In Figure 5.14 the effect of temperature variation on moisture content can be seen very clearly when comparing the maximum amount of moisture adsorbed at a relative humidity (RH) of 80% to varying temperatures.

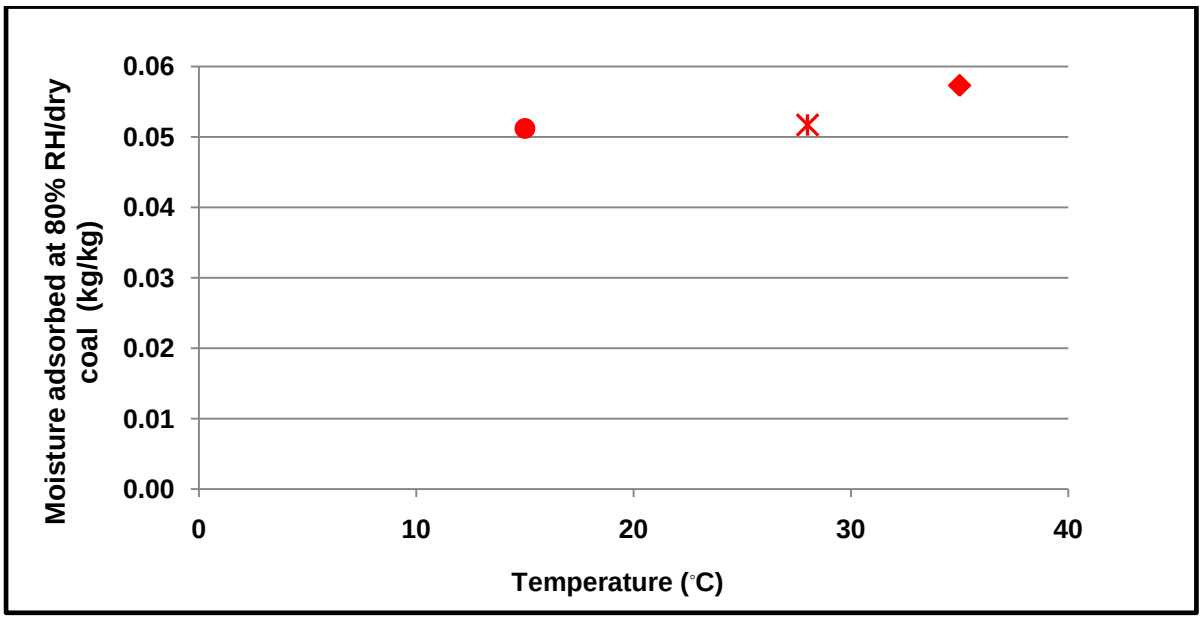

Figure 5.14: Influence of temperature on the moisture adsorbed at 80%RH.

According to the results presented in Figure 5.14 the effect of temperature on the maximum amount of moisture adsorbed seems to be minimal with only a slight increase in moisture content at 35°C (0.057 kg water/kg dry coal). A negligible difference in the amount of moisture adsorbed at 80% RH was found between 15 °C (0.051 kg water/kg dry coal) and 28°C (0.052 kg water/kg dry coal). Studies including an investigation on the adsorption properties of thermally dried South African fine coal concluded that temperature does not significantly influence moisture content (van der Merwe & Campbell, 2002; Monazam et al., 1998).

5.1.5 Adsorption/desorption hysteresis

The amount of moisture present in each coal typre is a function of relative pressure in the atmosphere to which it is exposed. Generally the approach to studying moisture in coal is to measure a water isotherm, where the moisture content is depicted as a function of relative humidity or else as relative vapour pressure. Figure 5.15 illustrates the water isotherms for the five coal samples and a pure mineral sample, kaolinite.

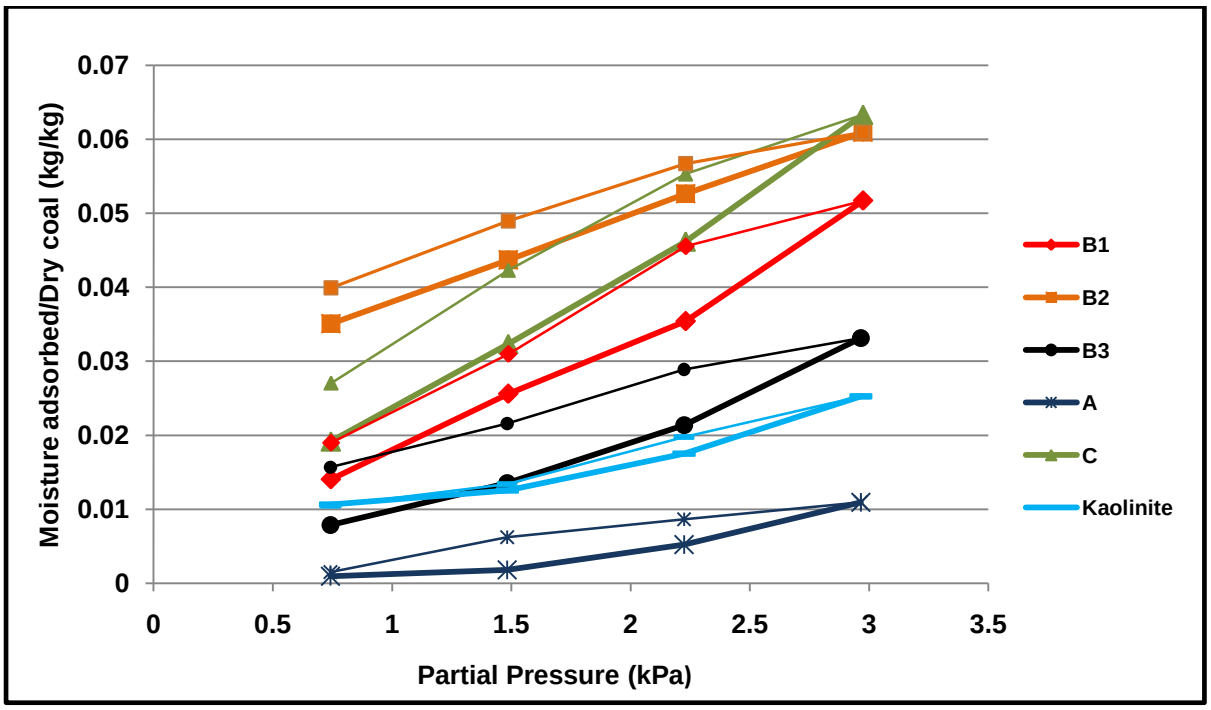

Figure 5.15: Illustration of hysteresis present during desorption

When considering the adsorption/desorption results obtained for the various samples presented in Figure 5.15, it is clear that the behaviour of water for the adsorption and desorption isotherms are different with marked hysteresis present for all the coal samples. Studies done on moisture adsorption on coal reported that the hysteresis loop often only closes when the relative pressure is reduced to zero (Mahajan & Walker, 1970). A certain amount of moisture is held tightly in the pore system of the coal or through hydrogen bonding. Adsorption or desorption of this strongly bound moisture will induce changes in the character of the solid during adsorption and desorption (Monazam et al., 1998). Marked hysteresis for the relative pressure range $0.3<P/P_S<0.8$ was also observed by Charrière & Behra (2010), who studied water sorption on coal. N_2 sorption analysis results in Section 4.5.3 also indicate hysteresis for all the coal samples, except for coal A, which is consistent with the results illustrated in Figure 5.15.

In the case of coal A and the pure kaolinite sample, the hysteresis loop closed at a low relative humidity level ong before the other coal samples. A smaller hysteresis loop was

also observed for these two samples. Kaolinite possesses a well defined crystalline structure which prevents the moisture from penetrating beyond the external structure (Johansen & Dunning, 1957; Ward, 2002). The moisture can therefore adsorb and desorb more easily from its surface, thus explaining the lack of significant hysteresis present compared to other clay minerals. Hysteresis at low relative pressures is commonly associated with a swelling of the coal matrix, since high ranked coals is less porous with more rigid structures it is less likely to swell with moisture adsorption explaining the absence of low pressure hysteresis present in coal A (McCutcheon *et al*., 2001).

5.2 Summary

An investigation into the influence of minerals and other intrinsic coal properties influencing the moisture adsorption and desorption properties of South African fine coal constitutes a unique study as there is currently no literature available regarding the influence of mineral matter content and type on the moisture adsorption and desorption properties of South African fine coal. In the beginning of this chapter the experimental apparatus used and procedures followed to achieve the above- mentioned outcome were discussed.

Moisture adsorption was not significantly influenced by the presence of the clay mineral, kaolinite, as determined by QEMSCAN analysis. The bulk of the adsorbed moisture was influenced by the carbon fraction of each coal. Kaolinite however, played a more significant role in the moisture adsorbed for the higher ranked bituminous coal A. A linear correlation was observed between the amount of moisture adsorbed at 80% RH and oxygen content.

Where illite was more significantly present (coal A) there seemed to be no considerable influence in moisture adsorbed compared to the other four coals. For the lower ranked bituminous coals B1 and B2 (compared to the higher rank bituminous coal A) there was a positive correlation between the moisture adsorbed and amount of illite. Coal B1 contained 0.00068 kg Illite/kg coal and adsorbed 0.052 kg moisture/kg coal, whereas coal B2 contained 0.00089 kg Illite/kg coal and adsorbed 0.06 kg moisture/kg coal.

Moisture adsorbed increased for a decrease in coal rank (Day *et al*., 2008). Inertinite content appeared to have little influence on the moisture adsorption characteristics.

The investigation into the effect of temperature on the adsorption and desorption properties revealed that for adsorption temperature variation had no significant influence but desorption was however affected.

A significant amount of hysteresis was present during the moisture desorption of the lower rank bituminous coal with less hysteresis observed for the higher rank bituminous coal. Kaolinite also showed little hysteresis due to its well defined crystalline structure, with the hysteresis loop closing at low relative pressures.

The following chapter further investigates the moisture adsorption mechanisms involved by matching appropriate models and interpreting the relevant parameters calculated to gain better insight into the moisture adsorption behaviour of South African fine coal.

CHAPTER 6:

MODELLING: RESULTS AND DISCUSSION

6.1 Introduction

Considering the results obtained from the previous chapter regarding the influence of minerals and oxygen content on the adsorption behaviour of all five coal samples it was decided that the BET and modified BET models would be appropriate to describe their moisture adsorption behaviour. The decision was also based on literature suggesting that moisture adsorption mainly occurs at the primary oxygen containing functional groups on the coal surface as opposed to capillary condensation which only takes place at higher relative pressures outside the scope of this investigation. The BET model is only applicable to a narrow range of relative pressures ($P/P_s<0.35$) but valuable information can be obtained from the relationship between the monolayer capacity and the oxygen content present in a specific coal. If a positive relationship is found then it indicates that initial adsorption took place at the surface oxygen containing functional groups, that is, if the oxygen content is an indication of the primary site available (Švábová et al., 2011; Charrière & Behra, 2010; McCutcheon et al., 2003; Nishino, 2000; Allardice & Evans 1971). The relative pressure range ($0.2<P/P_s<0.8$) used in this study would also fall well into the relative pressure range where the modified BET model is applicable ($P/P_s < 0.8$) (Do, 1998). Furthermore, the modified BET model, which takes into account the presence of secondary sites with lower energies than the primary sites, was successfully applied by various other authors to illustrate the moisture adsorption mechanism on coal (Švábová *et al*., 2011; Charrière & Behra, 2010). This chapter focuses on the application of the BET and the modified BET models on the experimental data and the subsequent evaluation of the parameters calculated and their relation to moisture adsorption.

6.1.1 BET model

The amount of moisture or vapour adsorbed is related to the saturation pressure and is expressed by Equation 2.2. To determine the monolayer coverage, Equation 2.2 can be written in its linear form which is depicted in Equation 6.1.

$$\frac{P}{n'_0(P_S - P)} = \frac{1}{n'_0 K} + \left(\frac{K-1}{n'_0 K}\right)\frac{P}{P_S} \qquad (6.1)$$

By plotting the left hand side of Equation 6.1 versus P/P_S in the relative pressure range where this equation is applicable ($0.05<P/P_s<0.35$), a straight line can be obtained (Allardice & Evans 1971; Do, 1998). The BET graph for coal C at 28°C is presented in Figure 6.1. The BET graphs for the remainder of the coal samples can be viewed in Appendix B.

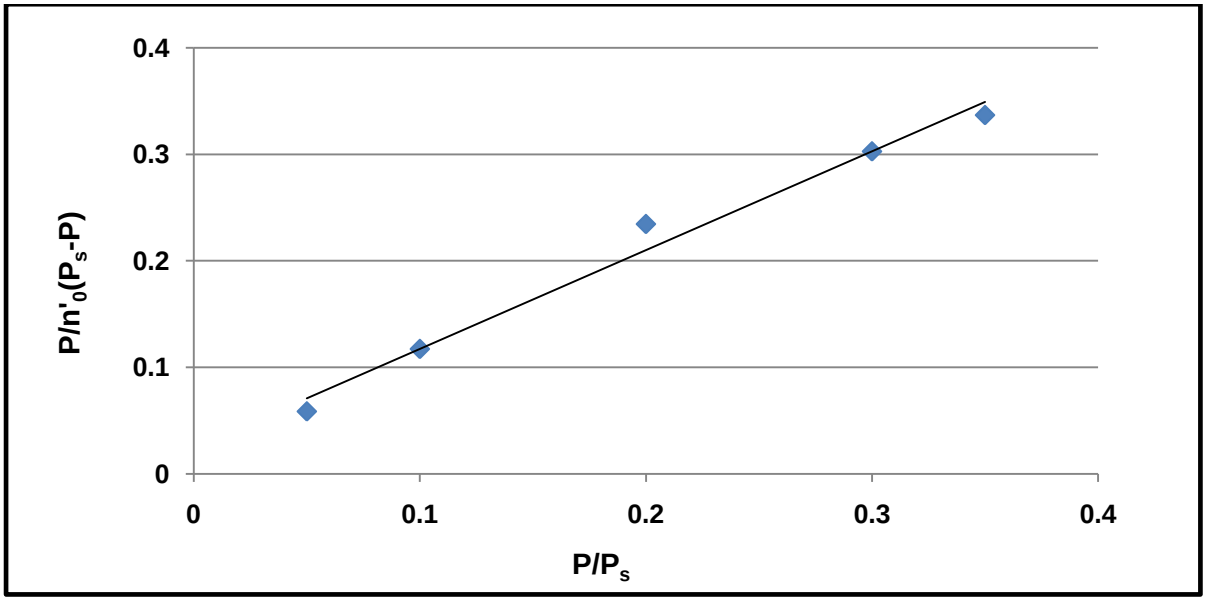

Figure 6.1: BET plot of the water adsorption isotherm for coal C at 28°C.

The two suitable parameters for the BET model can then be determined from the slope, Equation 6.2, and the intercept, Equation 6.3 obtained from the straight line graph depicted in Figure 6.1.

$$\left(\frac{K-1}{n_0' K}\right) \qquad (6.2)$$

$$\frac{1}{n_0' K} \qquad (6.3)$$

The constant K is related to the energy E (kJ/mol) of adsorption at the first layer; this is depicted by the following equation (Do, 1998; Charrière & Behra, 2010);

$$K = A^{\left(\frac{E-E_L}{RT}\right)} \qquad (6.4)$$

E_L is equal to the heat of water liquefaction which is about 43.99 kJ/mol at 298 K (Koretsky, 2003). Once the monolayer coverage n_0' (mmol/g) is determined from the equations cited above, the surface area (S) is calculated using equation (Do, 1998);

$$A = n'_0 N_A a_m \quad (6.5)$$

Where N_A is Avogadro's number (molecules/mole) and a_m (A^2/molecule) is the molecular area of water (Do, 1998). The surface areas of all the coal samples were calculated by using the approximated cross sectional area of a water molecule as 0.106 nm^2 (Mahajan & Walker, 1970). Table 6.1 summarises the calculated values obtained from the BET model.

Table 6.1: Parameters calculated with the BET model for moisture adsorption.

	BET model				
Coal	**n'$_o$ (mmol/g)**	**K (-)**	**R (-)**	**E (kJ/mol)**	**S (m^2/g)**
B1	1.00	10	0.99	50	63
B2	1.69	20	0.98	52	107
B3	0.44	36	0.99	53	27
C	1.05	19	0.97	53	67
A	0.07	25	0.98	52	7

The monolayer capacities calculated with the BET model varied between 1.69 mmol/g and 0.07 mmol/g for coals B2 and A respectively. There is a relationship between the BET specific surface areas and the monolayer capacity (Nishino, 2000). Coal B2 exhibited the highest BET surface area (107 m^2/g) which corresponded to the highest monolayer capacity (1.69 mmol/g). The water surface areas for the lower ranked coals B and C were greater than the surface areas calculated for the higher ranked coal A. This result was expected as lower ranked coal tends to have a larger proportion of surface polar sites which can facilitate moisture adsorption as opposed to higher ranked coal (Day et al., 2008).

Charrière & Behra (2010) reported values between 14 and 15 for the adsorption constant K which are in agreement with the parameters estimated and reported in Table 6.1. They also reported values for the BET surface area ranging between 68 m^2/g and 45 m^2/g, which support the values reported in the table above. The BET model provided a good fit for all

five coal samples and the capability of the model to fit the experimental data was evaluated by the following equation;

$$\%ARE = \left(\frac{100}{N}\right)\sum\left[\frac{(n_{cal} - n_{exp})}{n_{exp}}\right] \qquad (6.6)$$

The model was found to describe the experimental results well within the relative pressure range applicable for this model with an acceptable average relative error ranging between 3.2% and 8%.

The BET monolayer capacity gives a measure of the specific adsorption sites available for primary adsorption at the oxygen functional groups rather than the amount of adsorbate necessary for monolayer formation (Allardice & Evans, 1971; Mahajan & Walker, 1970). The monolayer capacity also corresponds to the point at which all of the polar sites are occupied by water (Day et al., 2008). The relationship between the BET monolayer capacity and the surface oxygen is illustrated in Figure 6.2.

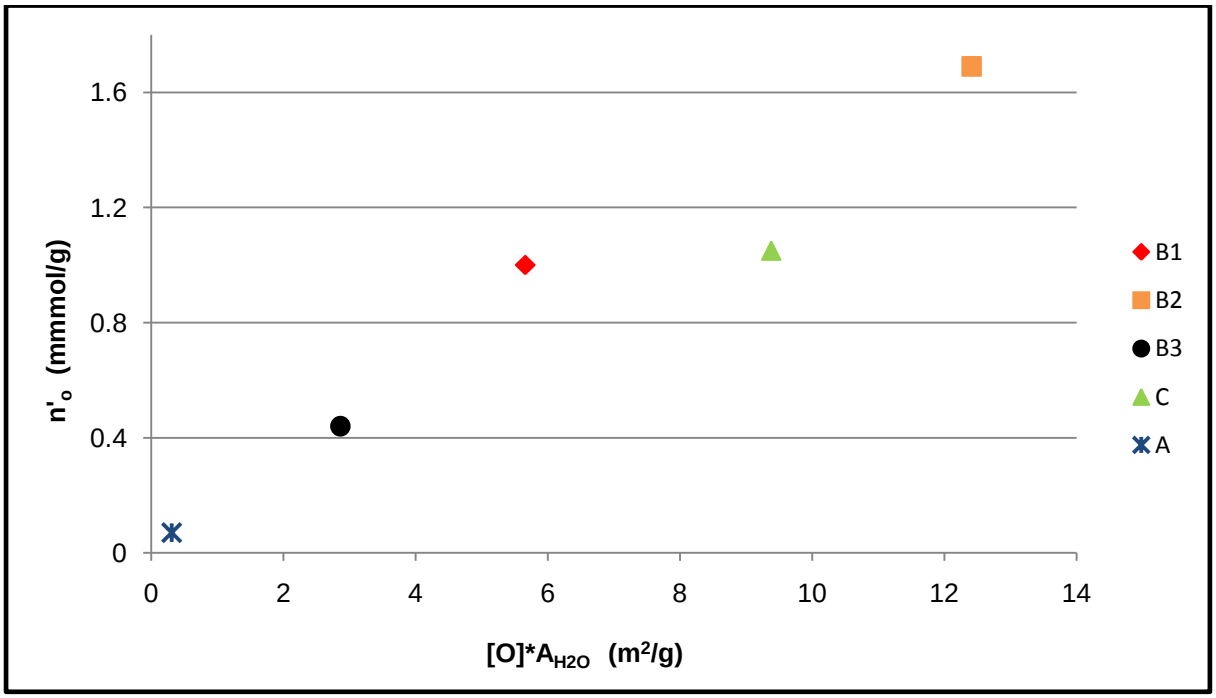

Figure 6.2: Relationship between BET monolayer coverage and surface oxygen.

The specific surface area (S) of water, presented in Table 6.1, was estimated with Equation 6.5 using the monolayer coverage calculated by the BET model which was then multiplied by the oxygen [O] content present in each coal sample to approximate the hydrophilic surface sites. A linear relationship between the approximated surface hydrophilic sites and the monolayer coverage as approximated by the BET model was observed in Figure 6.2. This

relationship suggests that water may be adsorbed at the hydrophilic sites present on the coal surface if the oxygen in each coal is related to the oxygen containing functional groups (McCutcheon et al., 2003; Mahajan & Walker, 1970). It was thus expected that coal C would have the highest monolayer capacity because of its substantial amount of oxygen present as indicated by the characterisation results. This was, however, not the case as can be seen from Figure 6.2; the monolayer capacity of coal C was less than that for coal B2.

The difference could be explained by the influence of the pore structure of coal C overshadowing the influence of the surface oxygen groups on the monolayer coverage. According to N_2 sorption results presented in Section 4.5.3 coal C contained a significant amount of mesopores which could only be filled at higher relative pressures where multilayer and ultimately capillary condensation generally take place. The increased amount of moisture adsorbed by coal C at the higher relative pressures as presented in Section 5.1.2 showed that the mesopores could only have been filled at these higher relative pressures. The lower surface area seen in coal C could also be due to the presence of a significant amount of closed pores.

6.1.2 Modified BET

Recognising the narrow range of validity for the BET model described in the previous section and the fact that the actual amount of moisture adsorbed was smaller than predicted by the BET model at higher relative pressures, it was decided to use the modified BET model to predict the moisture adsorption mechanism on the five coal samples investigated in this study. The three parameter model is described in Section 2.9.3 by Equation 2.3. The parameters were estimated according to the procedure described by Jonquières & Fane (1998). This procedure involved a nonlinear multiparameter regression method using the Microsoft Excel solver function©. The two- parameter BET model described in Section 6.1.1 provided the initial values for the two parameters n'_o and K allowing for faster convergence of the numerical computing. The constants K_1 and K_2 were estimated with Equation 2.4 and Equation 2.5 accordingly. The parameters estimated by this model are summarised in Table 6.2.

Table 6.2: Parameters calculated for moisture adsorption with the modified BET model.

	Modified BET model						
Coal	$n_o^{'}$ **(mmol/g)**	**K_1 (-)**	**K_2 (-)**	**R (-)**	**E_1 (kJ/mol)**	**E_2 (kJ/mol)**	**S (m^2/g)**
B1	0.83	12	0.94	0.96	50	44	53
B2	2.47	8	0.45	0.98	49	42	157
B3	0.90	3	0.71	0.99	47	43	57
C	1.51	8	0.75	0.99	49	43	96
A	0.33	1	0.76	0.97	44	43	19

Table 6.2 indicated that the highest monolayer coverage (2.47 mmol/g) and water surface area (157 m^2/g) was associated with coal B2. The lowest monolayer coverage (0.33 mmol/g) was observed for coal A which was also accompanied by the lowest surface area (19 m^2/g). The modified BET model distinguishes between the water adsorbed at primary and secondary sites. The contribution of the water adsorbed at the primary and secondary sites are described by Equations 2.4 and 2.5 respectively. The estimated values of K_1 and K_2 are related to the adsorption energies on the primary (E_1) and secondary sites (E_2). According to the modified BET model, the oxygen containing functional groups are considered as the primary site of adsorption and the secondary sites of adsorption are assumed to be the interaction between additional water molecules adsorbed through interactions between the previously adsorbed water on the primary sites through hydrogen bonding. The estimated values for K_1 and K_2 are in agreement with work done by McCutcheon et al., (2003) which reported values between 11 and 26 for the adsorption constant on primary sites (K_1) and values between 0.3 and 0.8 for the adsorption constant on secondary sites (K_2). In addition, Charrière & Behra (2010) reported values between 8 and 13 for K_1 and values between 0.6 and 0.7 for K_2 which further supports the above estimated further.

Research done by Day et al., (2008) on bituminous coals similar in rank to the coals studied in this dissertation obtained values varying between 24 and 45 for K_1 and 0.7 and 0.58 for K_2. The values of K_2 were in good agreement with the results obtained in Table 6.2. The K_1 values in this study were lower than the values presented by Day et al., (2008). K_1 values are associated with the interactions between the coal surface and the water molecules. The coals in this study contained a considerable higher amount of minerals than the coals in the study by Day et al., (2008). The elevated amount of minerals present in the coals used in this study could influence the interaction of the water molecules and the coal surface more so than the coals used in the study of Day et al., (2008).

The specific areas estimated with the modified BET model were higher than those estimated with the classical BET model due to the limited range of validity for the BET model. The energy of adsorption at the primary sites (E_1) was lower than the adsorption energies (E_2) at the secondary sites. This is consistent with the fact that the weak interactions between the water molecules and the coal surface requires more energy for adsorption at the primary sites than the energy needed for secondary adsorption where water-water molecules interacts through strong hydrogen bonding (Charrière & Behra, 2010). The primary and secondary moisture adsorbed as well as the monolayer capacity is illustrated in Figure 6.3.

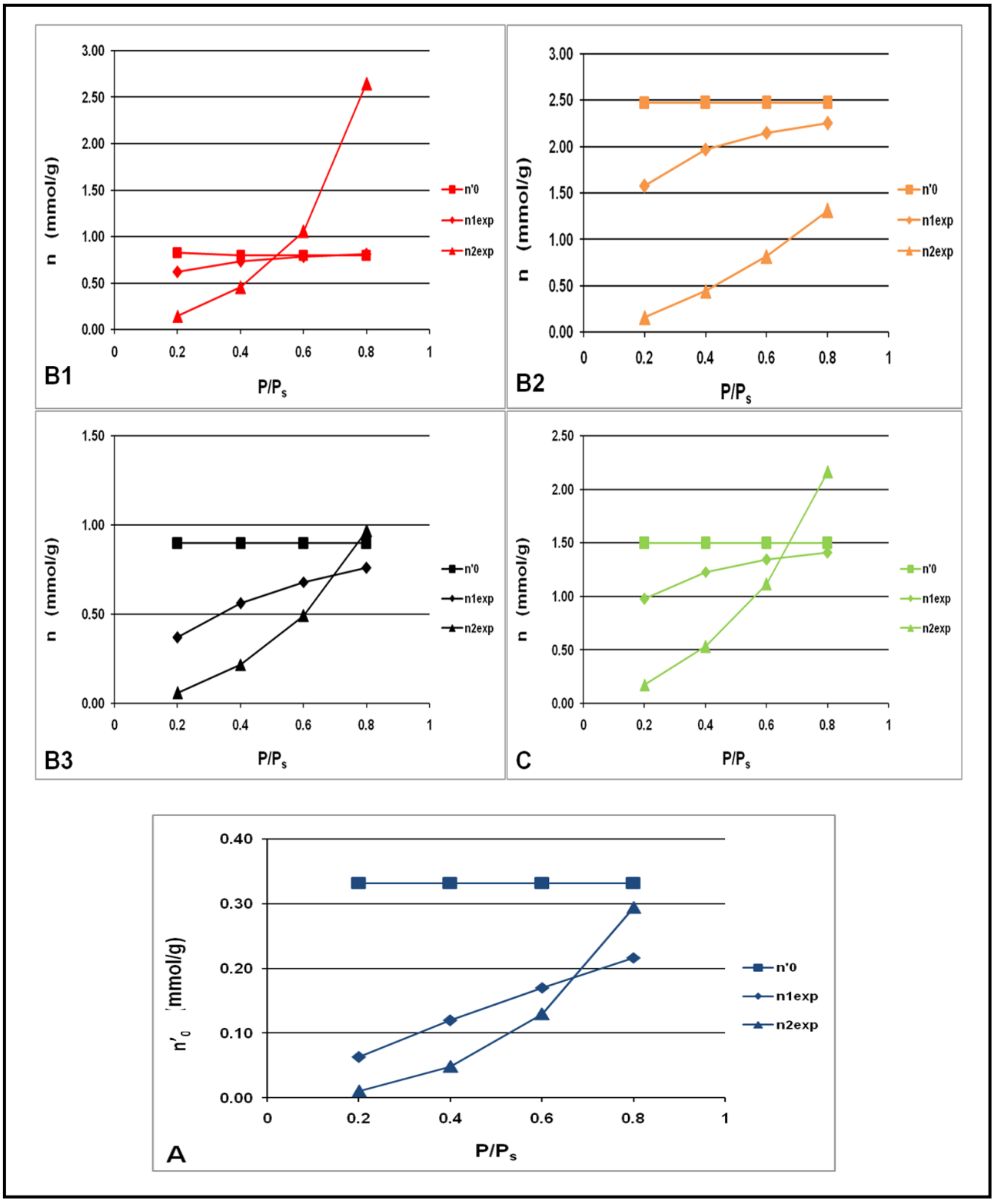

Figure 6.3: Primary and secondary moisture adsorbed on all five coals estimated by the modified BET model at 28°C.

A comparison between the primary and secondary site adsorption at 28°C for all five coal samples illustrated in Figure 6.3, demonstrates that the initial contribution of the primary sites (n_1^{exp}) to the moisture adsorbed dominates over secondary site adsorption (n_2^{exp}) at low relative pressures. The figure also illustrates that as the relative pressure increases, the

secondary site adsorption becomes more notable. According to the BET classification system (Gregg & Sing 1982), the primary adsorption isotherm (n_1^{exp}) corresponds to the type I isotherm which is characteristic of moisture adsorbed at the monolayer. The secondary site adsorption (n_2^{exp}) is similar to the Type III isotherm in the BET classification system and is characteristic of multilayer adsorption (Gregg & Sing 1982). For an increase in pressure the amount of water adsorbed at secondary sites increases and will eventually intercept with the primary site adsorption isotherm. This was true for all the coal samples except for coal B2. The horizontal line in each figure depicts the moisture content of a completely saturated monolayer n'_o which is a parameter calculated by the modified BET model. This value does not have to be reached since, even at saturation pressure, adsorption sites can remain vacant as seen in the case of coal B2. Adsorption on secondary sites began at low relative pressures for all the coal samples. For coal B1 adsorption on secondary sites became more pronounced than the primary adsorption at $P/P_s>0.5$. For coal B3, A and C the secondary site adsorption became more significant than the primary adsorption at $P/P_s>0.65$. It can is noteworthy that coal B1 had a significant amount of moisture associated with the secondary sites compared to coal B2.

Earlier results in Section 5.3, where Figure 5.15 showed that coal B2 had less hysteresis present than coal B1 for $0.2<P/P_s<0.8$, supports the results in

Figure 6.3. The larger amount of hysteresis for coal B1 can be associated with the large amount of moisture present due to secondary site adsorption and the subsequent difficulty associated with the desorption of this strongly bound water. On the other hand, coal B2 had less hysteresis present which can be attributed to the smaller amount of moisture contributed by secondary site adsorption. The high surface area of coal B2 could facilitate more moisture on the surface so much so that secondary adsorption and therefore cluster formation was minimal. Surface areas of 53 m^2/g and 96 m^2/g for coal B1 and C respectively, were far less than for coal B2, providing less space on the coal surface for moisture to be adsorbed and therefore secondary adsorption and cluster formation were more significant for these coal samples than for coal B2. The surface area for coal A was very low, 19 m^2/g, resulting in very little space available for water adsorption on the coal surface. Therefore, secondary adsorption started at very low relative pressures and exceeded the primary adsorption at relative pressures of $P/P_s >0.65$, signifying the possibility of cluster formation.

The model was found to describe the experimental results well within the relative pressure range applicable for this model with an acceptable average relative error, calculated by using Equation 6.6 and, ranging between 2% and 7%.

6.1.3 Comparison of surface areas determined by CO_2 adsorption and water adsorption

The different surface areas as determined by water and CO_2 adsorption are summarised in Table 6.3.

Table 6.3: Comparison of the surface areas determined by CO_2 and water adsorption

	A	B1	B2	B3	C
BET CO_2 surface area (m^2/g)	**68.95**	**97.45**	**80.18**	**50.98**	**96.18**
BET H_2O surface area (m^2/g)	**7**	**63**	**107**	**27**	**67**
Modified BET H_2O surface area (m^2/g)	**19**	**53**	**157**	**57**	**96**

The BET CO_2 surface areas for coal samples A (68.95 m^2/g), B1 (97.45 m^2/g), B3 (50.89 m^2/g) and C (96.18 m^2/g) were higher than the corresponding BET H_2O surface areas for coal A (7 m^2/g), B1 (63 m^2/g), B3 (27 m^2/g), C (67 m^2/g) as depicted in Table 6.3. This showed that only a small portion of the total surface area was accessed by water since the water molecules were restricted to the polar sites, whereas, CO_2 and CH_4 capacities were independent of the type of surface Day et al., (2008). The lower ranked bituminous coals contained a greater amount of polar sites and therefore their water surface areas were greater when compared to the higher ranked bituminous coal A (Day et al., 2008). The water and CO_2 surface areas reported in the study by (Day et al., 2008) was on a dry, ash free basis. The values reported in Table 6.3, included the minerals present in each coal. Rodrigues et al., (2008) reported that the amount of minerals present inhibit the gas storage capacity for a specific coal. The influence of minerals on the CO_2 BET surface area for the five coals in this study was investigated and the results were presented in Table 4.12. Coal A and coal B3 contained the highest amount of minerals, 59.9% and 78% respectively. These coals also had the lowest CO_2 BET surface areas of 68.95 m^2/g and 50.98 m^2/g respectively.

6.2 Summary

Water isotherms obeyed the BET model in the relative pressure range of $0.05<P/P_s<0.35$ and the values obtained for the monolayer capacity correlated very well with the

approximated surface oxygen for each coal sample. Therefore the monolayer capacity may be taken as an indication of the adsorption sites on the coal surface rather than the amount of adsorbate needed for monolayer coverage. The modified BET model provided a satisfactory description of water adsorption on all the coal samples. The contribution of water adsorbed due to primary and secondary sites were also estimated. Energies for the primary sites, ranging between 44 kJ/mol and 50 kJ/mol, were higher than energies for the secondary sites, varying between 42 KJ/mol and 43 KJ/mol. This indicated that water- coal interactions in the monolayer were weaker than water-water interactions in subsequent layers. The final chapter of this dissertation discusses the objectives that were reached as set at out the beginning of this study, as well as recommendations for possible future research.

CHAPTER 7:

CONCLUSIONS AND RECOMMENDATIONS

7.1 General conclusions

The moisture adsorption and desorption properties of five South African coal samples were evaluated in this dissertation. The chemical-, petrographical-, mineralogical and physical characteristics of the five South African coal samples and their influence on the moisture adsorption and desorption properties were also investigated. Appropriate models were matched to the experimental data in order to predict the moisture adsorption behaviour of these coal samples. The conclusions of this investigation are presented subsequently.

7.1.1 Coal characterisation

An extensive coal characterisation investigation revealed that four of the five coal samples in this study were high ash coals. Coals B and C were characterised as inertinite rich, bituminous, rank C coals while coal A was characterized as vitrinite rich, bituminous, rank B coal. There seems to be a good correlation between the oxygen content and coal rank, with the lower ranked coals B and C, containing more oxygen than the higher ranked coal A.

Elemental analysis indicated that a significant amount of aluminium and silicon were present in the ash of all the coal samples. QEMSCAN analysis determined that the bulk of the minerals of each coal consisted of the clay mineral, kaolinite, and quartz. Coal A was rich in illite and muscovite, coal C contained a significant amount of calcite, and elevated levels of pyrite was observed in coal B3.

Low pressure CO_2 and N_2 sorption analyses characterised the pore network of each coal and a significant amount of mesopores were found in coal C. A negative correlation was found between the CO_2 BET surface area and the amount of minerals present in each coal. The coals containing the highest amount of minerals (A and B3) had the lowest CO_2 BET surface areas whereas the coal with the lowest amount of minerals (B1) had the highest CO_2 BET surface area. In the absence of minerals, especially those associated with the coal matrix, there were more voids and cavities allowing the gas to adsorb into any free space available.

7.1.2 Moisture adsorption and desorption

The effect of minerals and other intrinsic coal properties on the moisture adsorption and desorption characteristics of South African coal was investigated under varying environmental conditions in a climate chamber using coal particles varying between 1mm and 2mm. The results indicated that moisture adsorbed was not significantly influenced by the presence of the clay mineral, kaolinite. The bulk of the moisture was influenced by the carbon fraction present in four of the five coal samples. Kaolinite played a more noteworthy role in the moisture adsorbed for the higher ranked coal A.

For the lower ranked bituminous coals B1 and B2 (compared to the higher ranked bituminous coal A) there was a positive correlation between the moisture adsorbed and amount of illite. The quantities of illite present in four of the five coals were very small and could therefore not have had a significant influence on the moisture adsorbed in comparison to moisture adsorbed by kaolinite. Where illite was more significantly present (coal A) there seemed to be no considerable influence in moisture adsorpted compared to the other four coals.

A linear correlation was observed between the amount of moisture adsorbed at 80%RH and oxygen content.

The investigation into the effect of temperature on the adsorption and desorption properties revealed that, for adsorption, temperature variation had no significant influence but desorption was, however, affected.

Hysteresis was present during moisture adsorption and desorption for the lower ranked coal samples with less hysteresis observed for the higher ranked coal A. Kaolinite also showed little hysteresis due to its well defined crystalline structure, with the hysteresis loop closing at low relative pressures.

7.1.3 Model evaluation

Water isotherms obeyed the BET model in the relative pressure range of $0.05<P/P_s<0.35$ and the values obtained for the monolayer capacity correlated very well with the approximated surface oxygen for specific each coal. Therefore, the monolayer capacity may be taken as an indication of the adsorption sites on the coal surface rather than the amount of adsorbate needed for monolayer coverage. The modified BET model provided a good description of water adsorption on all of the coal samples. Energies for the primary sites,

ranging between 44 kJ/mol and 50 kJ/mol, were higher than energies for the secondary sites, varying between 42 kJ/mol and 43 kJ/mol. This indicated that water- coal interactions in the monolayer were weaker than water-water interactions in subsequent layers.

7.2 Recommendations

Results from this study were interpreted and the following recommendations regarding future research on the moisture adsorption and desorption properties of South African coals could be made.

- It is strongly recommended to determine the equilibrium moisture according to ASTM D 1412 and make relevant conclusions regarding the relationship between this moisture and different coal properties for South African coals such as rank and minerals content.
- South African coal containing montmorillonite should be identified and the effect of such swelling type clays on moisture adsorption should be investigated and compared to the moisture adsorption results obtained for non- swelling clays such as kaolinite. Coal samples should also be demineralised, eliminating any influences from impurities on their adsorption behaviour.
- It can also be recommended to test the moisture adsorption/desorption behaviour of a pure illite sample and compare the moisture adsorbed with the moisture adsorbed due to the carbon fraction in the coal according to the procedure described in 5.3. According to Figure 2.6 illite adsorbed more water than kaolinite, but, in all five coal samples in this study the bulk of the minerals consisted of kaolinite. The quantities of illite present in four of the five coals were very small and could therefore not have had a significant influence on the moisture adsorbed in comparison to the moisture adsorbed by kaolinite. It would be interesting to investigate the adsorption behaviour of coals similar in rank, one with a significant amount of kaolinite and one with a significant amount of illite. The adsorption/ desorption behaviour for the two pure minerals could also be tested and compared.
- Results from this study indicated that there is some relationship between the moisture adsorbed and the oxygen content in each of the coal samples. An in-depth study regarding the influence of oxygen containing functional groups on moisture adsorption should be undertaken. Literature suggested that moisture is initially adsorbed at these hydrophilic sites and that carboxyl and hydroxyl groups are required for this process (Nishino, 2001). It would also be interesting to consider which of these two groups are most likely associated with the surface water

adsorbed. The relationship between hydroxyl and carboxyl groups with the oxygen content for a specific coal could also be investigated. The oxygen content in a specific coal could then be used as an early indicator to approximate what the adsorption behaviour would be for a specific coal without the need for expensive characterisation techniques.

- Kinetic data from this investigation could be used to obtain valuable information regarding the moisture adsorption and desorption characteristics of South African coal. Knowledge of both the rate and amount of moisture adsorbed is necessary in order to evaluate the influence of moisture on the self- heating of coal in storage (Monazam et al., 1998). The effect of varying humidity conditions, temperature particle size and minerals on the rate of moisture adsorption and desorption could also be investigated. The diffusion coefficients could be calculated from the kinetic data, allowing for a clear distinction between the different stages in moisture adsorption as the relative pressure increases (Charrière & Behra, 2010). Various models could also be investigated regarding the kinetic adsorption mechanisms present for each of the coal samples in this study.
- The net heat of adsorption could be calculated to determine the extent of interaction between the coal surface and the adsorbed water molecules as a function of their coverage (McCutcheon et al., 2003).

BIBLIOGRAPHY

ALLARDICE, D.J. & EVANS, D.G. 1971. The brown coal/water system: Part 2. Water sorption isotherms on bed-moist Yallourn brown coal. *Fuel*, 50 (3): 236-253.

AMARASEKERA, G., SCARLETT, M.J., MAINWARING, D.E. 1995. Micropore size distributions and specific interactions in coals. *Fuel*, 74 (1): 115-118.

ANDERSON, R.B. 1946. Modifications of the Brunauer, Emmett and Teller equation. *Journal of the American Chemical Society*, 68: 686-691.

ARNOLD, B.J. & APLAN, F.F. 1989. The hydrophobicity of coal macerals. *Fuel,* 68: 651-657.

ASTM. 2009-2012. [Web:] http://www.astm.org. [Date accessed: 08 April 2012]

ASTM D 4326 – 11. Standard test method for major and minor elements in coal and coke ash by x-ray fluorescence.

ASTM D 3174. Standard test method for ash in the analysis sample of coal and coke from coal.

ASTM D 3177. Standard test method for sulphur in the analysis sample of coal and coke.

ASTM D 388. Standard classification of coals by rank.

ASTM D 1412 - 07. Standard test method for equilibrium moisture of coal at 96-97 % relative humidity and 30°C.

AZMI, A.S., YUSUP, S., MUHAMAD, S. 2006. The influence of temperature on adsorption capacity of Malaysian coal. *Chemical Engineering and Processing,* 45: 392-396. Jul.

BP Statistical Review of World Energy. [Web:] http://www.bp.com/assets/bp_internet/globalbp/globalbp_uk_english/reports_and_publications/statistical_energy_review_2011/STAGING/local_assets/pdf/statistical_review_of_world_energy_full_report_2011.pdf [Date accessed: 08 April 2012]

BORREGO, A.G., ALVAREZ, D. & MENENDEZ, R. 1997. Effects of inertinite content in coal on char structure and combustion. *Energy and Fuels*, 43: 702-761.

BOURGEOIS, F., BARTON, W., BUCKLEY, A., MCCUTCHEON, A., CLARKSON, C., LYMON, G. 2000. Fundamentals of fine coal dewatering. http://www.acarp.com.au/reports.aspx?catId=3&subCatId=23 Date of access: 14 July 2010.

BRUNAUER, S., DEMING, L.S., DEMING, W.E., TELLER, E.J. 1938. Adsorption of gases in multimolecular layers. *Journal of the American Chemical Society*, 60: 309-319.

CAMPBELL, Q.P. 2006. Dewatering of fine coal with flowing air using low pressure drop systems, PhD Thesis, Potchefstroom: North-West University.

CHARRIÈRE, D. & BEHRA, P. 2010. Water sorption on coals. *Journal of Colloid and Interface Science*, 344:460-467.

CLARKSON, C.R. & BUSTIN, R.M. 1999. The effect of pore structure and gas pressure upon the transport properties of coal: a laboratory and modeling study. 1. Isotherms and pore volume distributions. *Fuel,* 79: 1333:1344.

CRESSWELL, G.M. 2006. Process design of the new Phola coal preparation plant. XVth International Coal Preparation Conference: Beijing.

DE KORTE, G.J. & MANGENA, S.J. 2004. Thermal Drying of Fine and Ultra-fine Coal. Report no. 2004-0255.

DE KORTE, G.J. 2002. Dense-medium beneficiation of fine coal revisited. *The Journal of The South African Institute of Mining and Metallurgy,* 393-396.

DE KORTE. G.J. 2000. Dewatering of Fine Coal Progress Report No. 2. Report for Coaltech 2020.

DEPARTMENT OF MINERLS AND ENERGY. 2007. South Africa's Mineral Industry 2007/2008. Directorate: Mineral Economics Report, Pretoria, South Africa.

DAY, S., SAKUROVS, R., WEIR, S. 2008. Supercritical gas adsorption on moist coals. *International Journal of Coal Geology*, 74: 203-214.

DO, D.D. 1998. Adsorption Analysis: Equilibria and Kinetics. Vol. 1. Imperial College Press. 913p.

EBERHARD, A. 2011. THE FUTURE OF SOUTH AFRICAN COAL; MARKET, INVESTMENT, AND POLICY CHALLENGES. http://iis-db.stanford.edu/pubs/23082/WP_100_Eberhard_Future_of_South_African_Coal.pdf. Date of access: 31 October 2011.

FAIZ, M.M., AZIZ, N., HUTTON, A.C., JONES, B.G. 1992. Porosity and gas sorption capacity of some eastern Australian coals in relation to coal rank and composition. (In Proceedings of the Coalbed Methane Symposium: Paper read at Townsville, USA on 19-21 November 1992.

FALCON, R.M.S., : Coal in South Africa- Part I: the Quality of South African Coal in Relation to its Uses and World Energy Resources, Minerals Sci. Engng, Vol. 9 (4)., Oct., 1977.

FALCON, R.M.S. & SNYMAN, C.P. 1986. An introduction to coal petrography: Atlas of petrographic constituents of the bituminous coals of Southern Africa. Johannesburg; The Geological Society of South Africa. 106p.

FALCON, R.M.S. 1986[a]. Classification of Coals in Southern Africa. Mineral Deposits of Southern Africa, pp 1899-1921.

FALCON, R.M.S. 1986[b]. Spontaneous combustion of the organic matter in discards from the Witbank coalfield. *Journal of the South African Institute of Mining and Metallurgy.* 86:243-250.

FALCON, R.M.S & HAM, A. 1988. The characteristics of Southern African coals. *Journal of the South African Institute of Mining and Metallurgy.* 88: 145-161.

GAIGHER, J.L. 1980. The mineral matter in some South African coal products, Report 45, Fuel Research institute of South Africa, University of Pretoria. (M.Sc.) 93p.

GAN, H., NANDI, S.P. & WALKER, P.L. 1972. Nature of porosity in American coals. *Fuel*, 51: 271-277.

GIL, A. & GRANGE, P. 1996. Application of the Dubinin-Radushkevich and Dubinin-Astakhov equations in the characterization of microporous solids. *In Colloids and Surfaces A: Physicochemical and Engineering aspects*, 113:39-50.

GREGG, S.J & SING, K.S.W. 1982. Adsorption Surface Area and Porosity. 2nd ed. New York: Academic Press. 303p.

HENSEN, E.M. & SMIT, B. 2002. Why clays swell. *Journal of Physical Chemistry*, 106 (49): 12664-12667.

IEA. 2011. Coal Information 2011 [Web]:
http://wds.iea.org/wds/pdf/documentation_for_coal_information_(2011_early_edition).pdf
Date of access: 31 October 2011.

INTERNATIONAL COMMITTEE FOR COAL AND ORGANIC PETROLOGY (ICCP). *2001.* The new inertinite classification (ICCP System 1994): *Fuel, 80: 459-471.*

INTERNATIONAL COMMITTEE FOR COAL AND ORGANIC PETROLOGY (ICCP). 1998. The new vitrinite classification (ICCP System 1994). *Fuel*, 77:349-58.

INTERNATIONAL UNION OF PURE AND APPLIED CHEMISTRY, *Pure Appl. Chem*, 1994: 66:1739.

ISO (International Organization for Standardization). 2011. ISO Standards. [Web:] http://www.iso.org/iso/iso_catalogue.htm. [Date accessed: 08 April]

ISO 1171 ; 1997 – Solid mineral fuels – Determination of ash

ISO 562 ; 1998 – Hard coal and coke – Determination of volatile matter

ISO 12902 ; 2001 – Solid mineral fuels – Determination of total carbon, hydrogen and nitrogen – Instrumental methods.

ISO 19579 ; 2006 – Solid mineral fuels – Determination of sulphur by IR spectrometry

ISO 7404-3 ; 1994 – Methods for the petrographic analysis of bituminous coal and anthracite – Part 3: Method of determining maceral group composition

ISO 7404-5 ; 1994 – Methods for the petrographic analysis of bituminous coal and anthracite – Part 5: Method of determining microscopically the reflectance of Vitrinite

ISO 11760 ; 2005 – Classification of coals

JASIŃSKA, I. 2011. Particle size and pore structure of nanomaterials. [Web]: http://www.co-nan.eu/pdf/ij.pdf. Date of access: 8 March 2012.

JEFRFEY, L.S. 2005. Characterization of the coal resources of South Africa. *The Journal of the South African Institute of Mining and Metallurgy.*

JOHANSEN, R.T. & DUNNING, H.N. 1957. Water vapour adsorption on clays. *Clays and Clay Minerals,* 6 (1): 249-258.

JONQUIÈRES, A. & FANE, A. 1998. Modified BET models for Modelling Water Vapour Sorption in Hydrophilic Glassy Polymers and Systems Deviating Strongly from Ideality. *Journal of Applied Polymer Science*, 67: 1415-1430.

KAJI, R., MURANAKA, Y., OTSUKA, K., HISHINUMA, Y. 1986. Water adsorption by coals: effects of pore structure and surface oxygen. *Fuel*, 65: 288-291.

KARTHIKEYAN, M & MUJUMDAR, A.S. 2007. M3TC Technical report: Factors influencing quality of dried low rank coals. [Web]: http://serve.me.nus.edu.sg/arun/file/m3tc/Coal%20Drying%20TN%2008-01.pdf Date of access: 7 September 2010.

KERSHAW, J.R. & TAYLOR, G.H. 1992. Properties of Gondwana coals with emphasis on the Permian coals Of Australia and South Africa. *Fuel Processing Technology*, 31: 127-168.

KORETSKY, M.D. 2003. Engineering and Chemical Thermodynamics. 1st Ed. Wiley. 580p.

LIU, Y., GUPTA, R., SHARMA, A., WALL, T., BUTCHER, A., MILLER, G., GOTTLIEB, P., FRENCH, D. 2005. Mineral matter–organic matter association characterisation by QEMSCAN and applications in coal utilisation. *Fuel*, 84: 1259-1267.

MAHAJAN, O.P. & WALKER, P.L. 1971. Water adsorption on coals. *Fuel*, 50: 308-317.

MANGENA, S.J. & DE KORTE, G.J. 2004. Thermal drying of fine and ultra-fine coal.

MATJIE, R.H. & VAN ALPEN, C. 2008. Mineralogical features of size and density fractions in Sasol coal gasification ash, South Africa and potential by- products. Fuel, 87:1439-1445.

MCCUTCHEON, A.L., BARTON, W.A., WILSON, M.A. 2003. Characterization of water adsorbed on Bituminous Coals. *Energy & Fuels*, 17:107-112.

MCCUTCHEON, A.L., BARTON, W.A., WILSON, M.A. 2001. Kinetics of Water Adsorption/Desorption on Bituminous Coals. *Energy & Fuels*, 15:1387-1395.

MCCUTCHEON, A.L. & BARTON, W.A. 1999. Contribution of mineral matter to water associated with bituminous coals. *Energy & Fuels*, 13:160-165.

MONAZAM, E.R., SHADLE, L.J., EVANS, R. and SCHROEDER, K. 1998. Water adsorption and desorption by coals and chars. *Journal of Energy & Fuels*, 12(6):1299–1304.

NISHINO, J. 2000. Adsorption of water and carbon dioxide at carboxylic functional groups on the surface of coal. *Fuel*, 80:747-764.

OSBORNE, D.G. 1988. Coal Preparation Technology: Volume 1. Graham & Trotman Limited. 600p.

PEATFIELD, D. 2003. Coal and Coal Preparation in South Africa – A 2002 Review. *The Journal of the South African Institute of Mining and Metallurgy*, 355-372.

PINETOWN, K.L. & BOER, R.H. A quantitative evaluation of the modal distribution of minerals in coal deposits in the Highveld area and the associated impact of the generation of acid and neutral mine drainage. 2006. Report to the Water Research Commission, Department of Geology, University of the Free State.

PINETOWN, K.L., WARD, C., VAN DER WESTHUIZEN. 2007. Quantitative evaluation of minerals in coal deposits in the Witbank and Highveld coalfields, and the potential impact on acid mine drainage. *International Journal of Coal Geology*, 70:166-183.

PRINZ, D. & LITTKE, R. 2005. Development of the micro- and ultra microporous structure of coals with rank as deduced from the accessibility to water. *Fuel*, 84:1645-1652.

PUSZ, S. 2002. Application of reflectance for the estimation of structural order. (Lecture presented on the 54th Annual Meeting of the International Committee for Coal and Organic Petrology (ICCP), 22-30 Sept. 2002). Pretoria, South Africa. 9p.

RAGLAND, K.W. & BAKER, A.J. 1987. Mineral matter in coal and wood-Replications for solid fuelled gas turbines. *Combustion fundamentals and applications: 1987 spring technical meeting of the central states section of the Combustion Institute:* 117-122.

ROUQUEROL, J., AVNIR, D., FAIRBRIDGE, C.W., EVERETT, D.H., HAYNES, J.H., PERNICONE, N., RAMSAY, J.D.F., SING, K.S.W., & UNGER, K.K. 1994. Recommendation for the characterization of porous solids. *Pure & Appl. Chem,* 66 (8): 1739-1758.

RUTHERFORD, S.W. & COONS, J.E. 2004. Equilibrium and Kinetics of Water Adsorption in Carbon Molecular Sieve: Theory and Experiment. *Langmuir*, 20: 8681-8687.

RUTHVEN, D.M. 1984. Principles of adsorption and adsorption processes. John Wiley & Sons. 426p.

RODRIGUES, C.F. & LEMOS DE SOUSA, M.J. 2002. The measurement of coal porosity with different gasses. *International Journal of Coal Geology*, 48: 245-251.

RODRIGUES, C.F., PINHEIRO, H.J., LEMOS DE SOUSA, M.J. 2008. Comparative study of the influence of minerals in gas adsorption isotherms of three coals of similar rank. *The Journal of The Southern African Institute of Mining and Metallurgy*, 108: 371-375.

SABS. 2008. SANS 5925. [Web:] http://www.sabs.co.za/webstore/standards/product.php?id=14016632. [Date accessed: 08 April 2012]

SAIKIA, B., & NINOMIYA, Y. 2011. An investigation on the heterogeneous nature of mineral matters in Assam (India) Coal by CCSEM technique. Fuel Processing Technology, 92:1068-1077.

SCHAFER, H.N.S. 1972. Factors affecting the equilibrium moisture contents of low-rank coals. *Fuel,* 51:4-7. Jan.

SCHLITT, W.J., CALLOW, M.I., KENYEN, V.P., PIZARRO, R.S. 1992. Mineral processing. (*In* Hartman, H.L., *ed*. SME Mining Engineering. Society for Mining Metallurgy & Exploration. p218-2205.)

SING, K.S.W., EVERETT, D.H., HAUL, R.A.W., MOSCOU, L., PIEROTTI, R.A., ROUQUEROL, L. & SIEMIENIEWSKA, T. 1985. Reporting physisorption data for gas/solid systems; with special reference to the determination of surface area and porosity. *Pure Applied Chemistry*, 57: 603-619.

SNYMAN, C.P., VAN VUUREN, M.J.C. AND BARNARD, J.M. 1983. Chemical and physical characteristics of South African coal and a suggested classification system. National Institute for Coal Research, C.S.I.R., Pretoria, Coal 8306, 110p.

SPEARS, D.A. 2000. Role of clay mineral in UK coal combustion. *Journal of Applied Clay Science*, 16: 87-95.

SPEIGHT, J.G. 1994. The chemistry and technology of coal. 2nd Ed. 642p.

SPEIGHT, J.G. 2005. Handbook of coal analysis. John Wiley & Sons. 214p.

STACH, E., MACKOWSKY., TEICHMÜLLER, M., TAYLOR, G.H., CHANDRA, D. AND TEICHMÜLLER, R. 1982. Stach's Textbook of Coal Petrology: 3rd ed., Gebr. Borntraeger, Berlin, 535p.

ŠVÁBONÁ, M., WEISHAUPTOVÁ, Z., & PŘIBYL, O. 2011. Water vapour adsorption on coal. *Fuel*, 90:1892-1899.

TODA, Y., HATAMI, M., TOYODA, S., YOSHIDA, Y., HONDA, H. 1971. Micropore structure of coal. *Fuel.* 50:187-200.

THOMAS, J. & DAMBERGER, H.H. 1976. Internal Surface Area, Moisture Content and Porosity of Illinois Coals: Variations with Coal Rank. [Web]: http://library.isgs.uiuc.edu/Pubs/pdfs/circulars/c493.pdf. Date of access: 16 November. 2011.

THOMAS, L. 2002. Coal Geology. John Wiley & Sons. England. 384p.

UNSWORTH, F., FOWLER, C.S., JONES, L.F. 1988. Moisture in coal. *Fuel*, 68:18-26.

VAN ALPHEN, C. 2005. Factors influencing fly ash formation and slag deposit formation (slagging) on combustion a South African pulverized fuel in a 200 MWe boiler, PhD Thesis, University of Witwatersrand.

VAN ALPHEN, C. 2007. Automated mineralogical analysis of coal and ash products-Challenges and requirements. *Minerals Engineering*, 20:496-505.

VAN DER MERWE, D., & CAMPBELL, Q.P. 2002. An investigation into the moisture adsorption properties of thermally dried South African fine coal. *The Journal of the South African Institute of Mining and Metallurgy*, 417-419.

VAN DYK, J.C., & KEYSER, M.J. 2005. Characterization of inorganic material in Secunda coal and the effect of washing on coal properties. *The Journal of the South African Institute of Mining and Metallurgy.*

WAANDERS, F.B., VINKEN, E., MANS, A., & MALABA-BAFUBIANDI, A.F. 2003. Iron Minerals in Coal, Weathered Coal and Coal Ash- SEM and Mössbauer results. *Hyperfine Interactions*, 148/149: 21-29.

WAGNER, J.N. & HLATSHWAYO, B. 2005. The occurrence of potentially hazardous trace elements in five Highveld coals, South Africa. *International Journal of Coal Geology.* 63: 228-246.

WANG, H. 2007. Kinetic analysis of dehydration of a bituminous coal using the TGA technique. *Energy & Fuels*, 21 (6):3070-3075.

WARD, R.C. 2002. Analysis and significance of mineral matter in coal seams. *International Journal of Coal Geology*. 50: 135-168.

WCA. 2010 [Web]: http://www.worldcoal.org/resources/coal-statistics/ecoal_aug11_final(23_08_2011).pdf. Date accessed 31 October 2011.

WCI. 2009. *Coal Facts: 2009 Edition with 2008 data*. [Web]: http://www.worldcoal.org/bin/pdf_original. Date accessed 31 October 2011.

YINGHUI, L., GUPTA, J., SHARMA, A., WALL, T., BUTCHER, A., MILLER, G., GOTTIEP, P., FRENCH, D. 2004. Mineral matter-organic matter association characterization by QEMSCAN and applications in coal utilization. *Fuel*, 84:1259-1267.

APPENDIX A:

EFFECT OF MINERALS

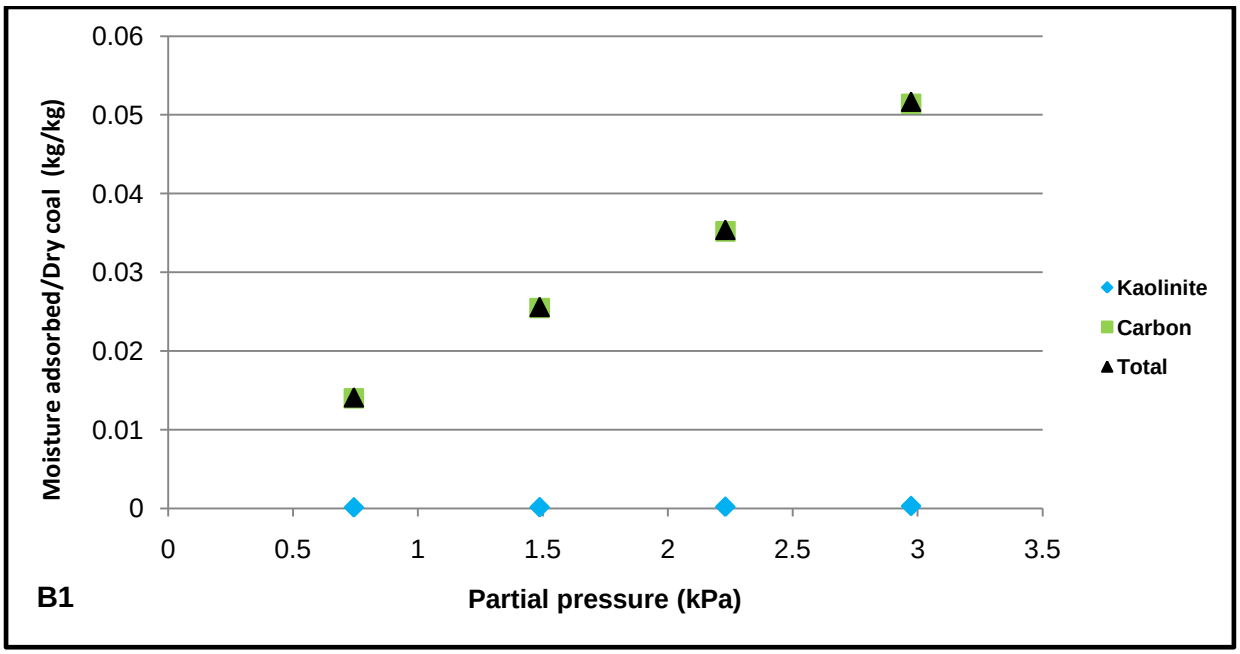

Figure A.1: Total moisture adsorbed and moisture adsorbed due to the carbon and kaolinite content in coal B1.

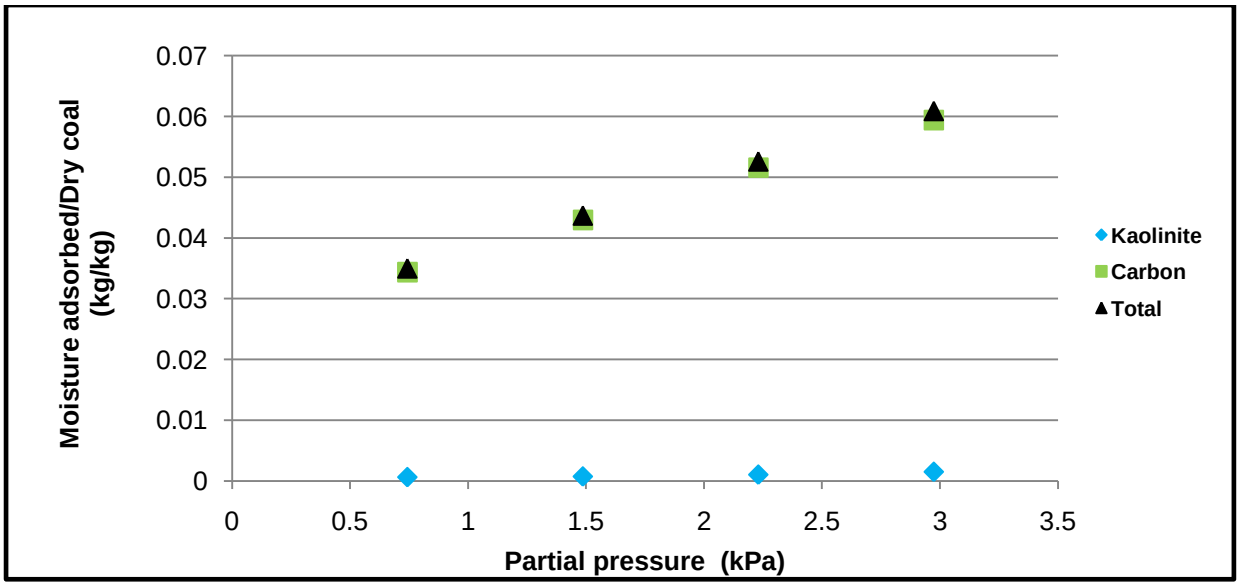

Figure A.2: Total moisture adsorbed and moisture adsorbed due to the carbon and kaolinite content in coal B2.

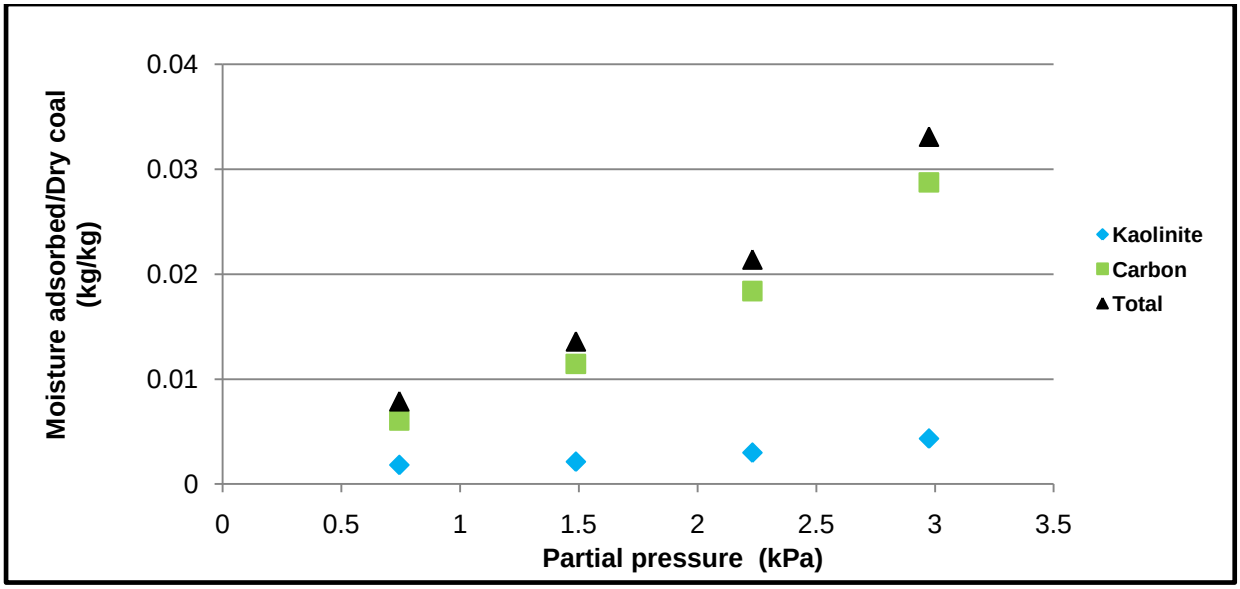

Figure A.3: Total moisture adsorbed and moisture adsorbed due to the carbon and kaolinite content in coal B3.

APPENDIX B:

BET GRAPHS

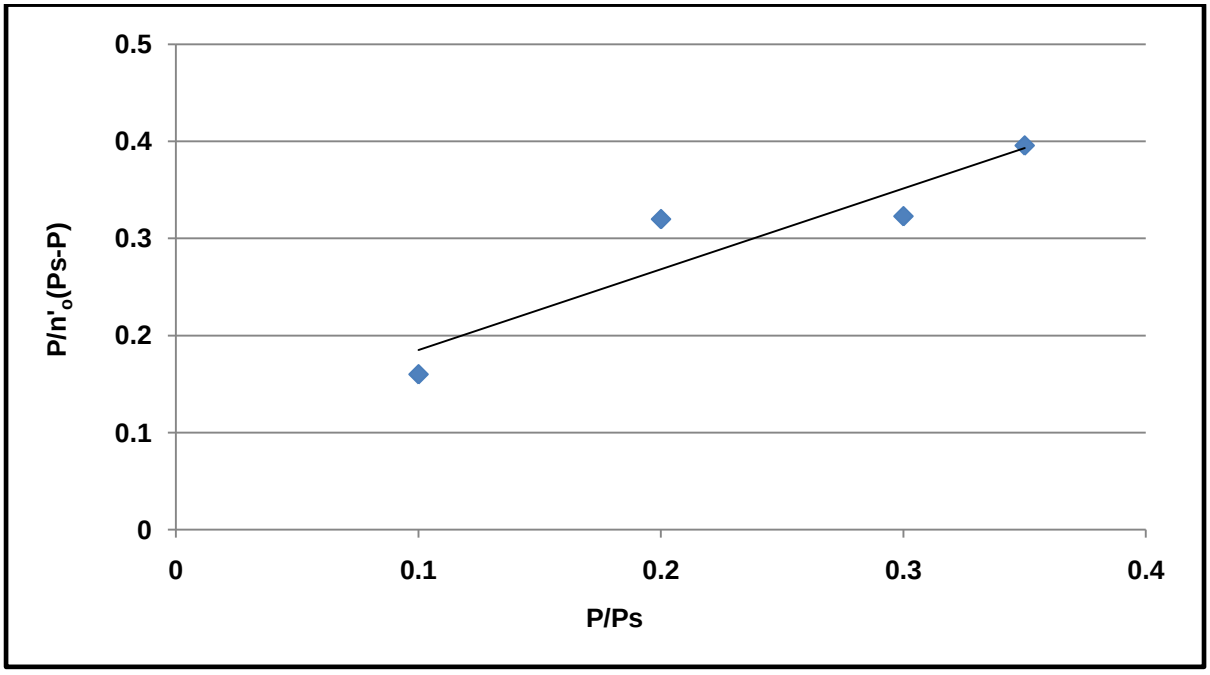

Figure B.1: BET plot of the water adsorption isotherm for coal B1 at 28°C.

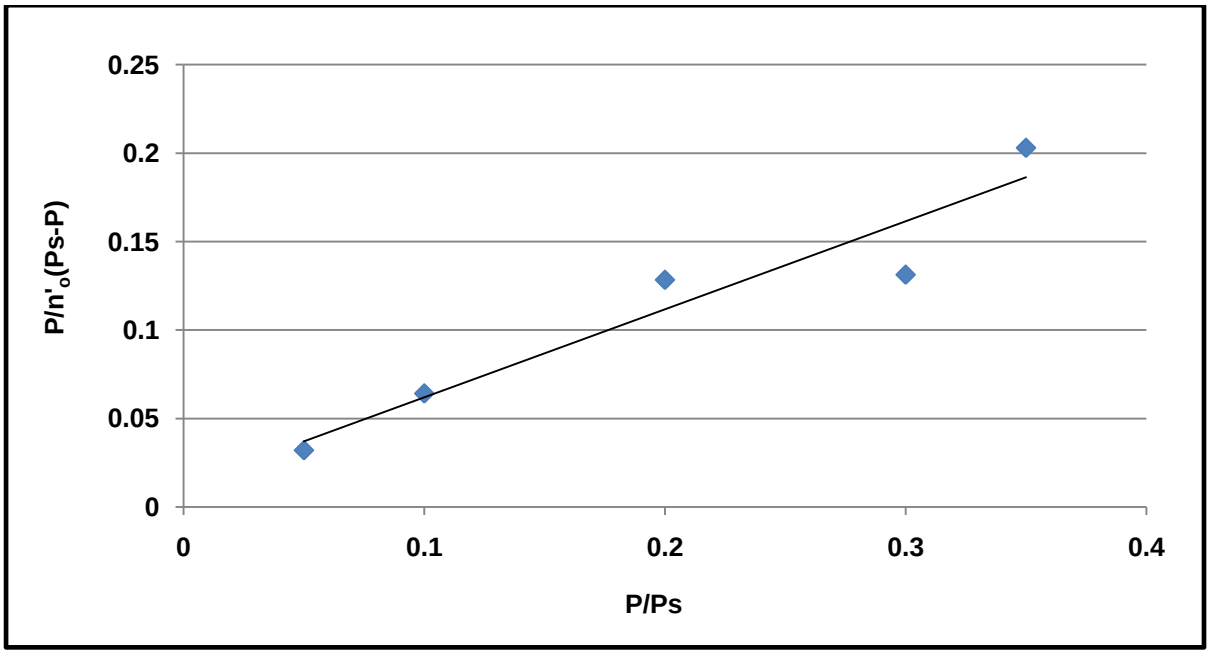

Figure B.2: BET plot of the water adsorption isotherm for coal B2 at 28°C.

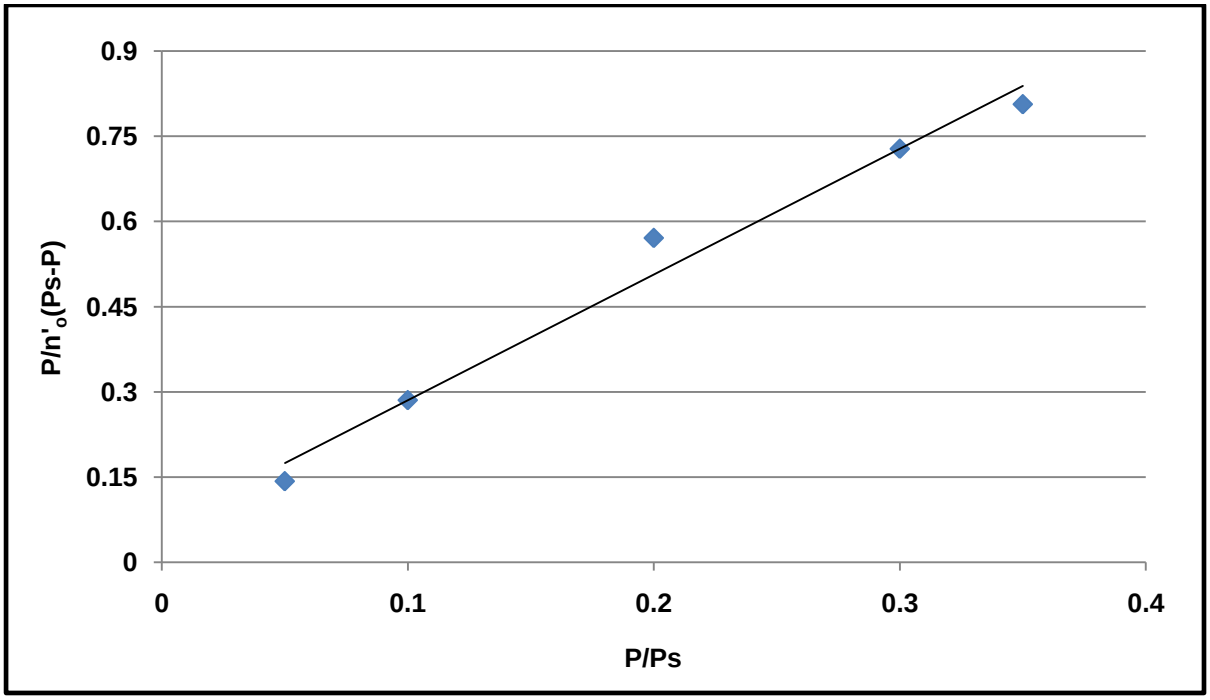

Figure B.3: BET plot of the water adsorption isotherm for coal B3 at 28°C.

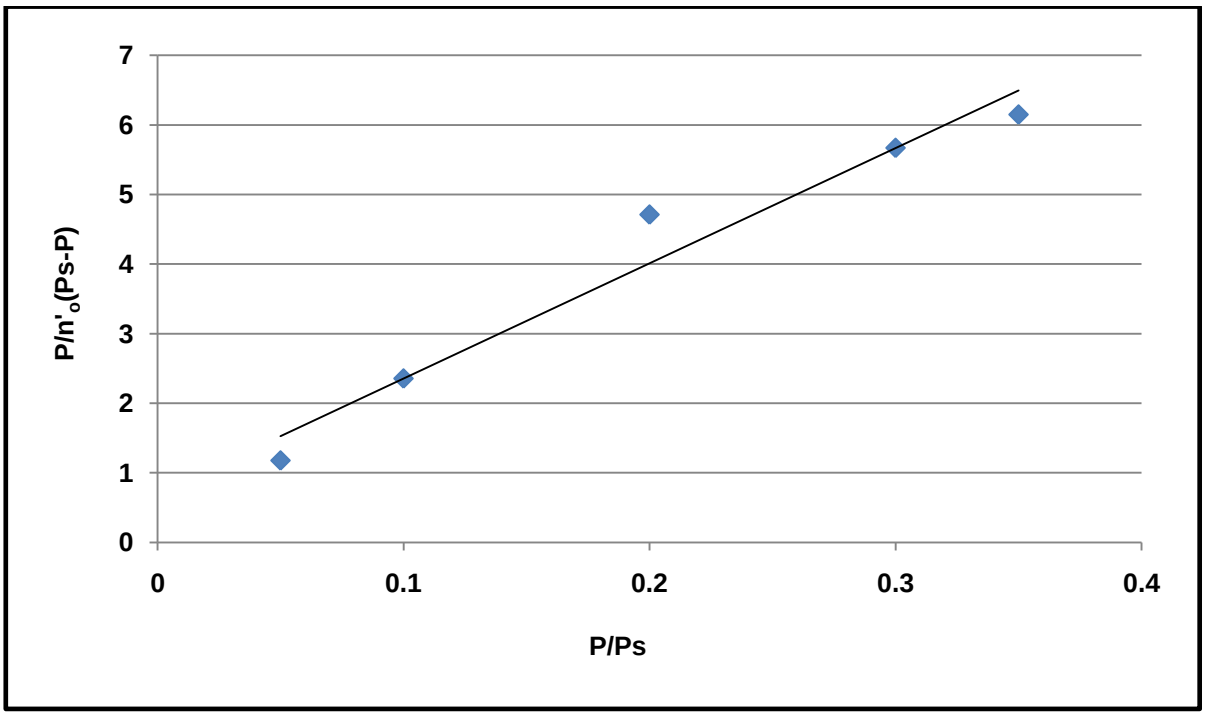

Figure B.4: BET plot of the water adsorption isotherm for coal A at 28°C.